Environment Canada

Environnement Canada

CANADA CENTRE FOR INLAND WATERS

CENTRE CANADIEN DES EAUX INTERIEURES

National Water Research Institute

Institut national de la recherche sur les eaux

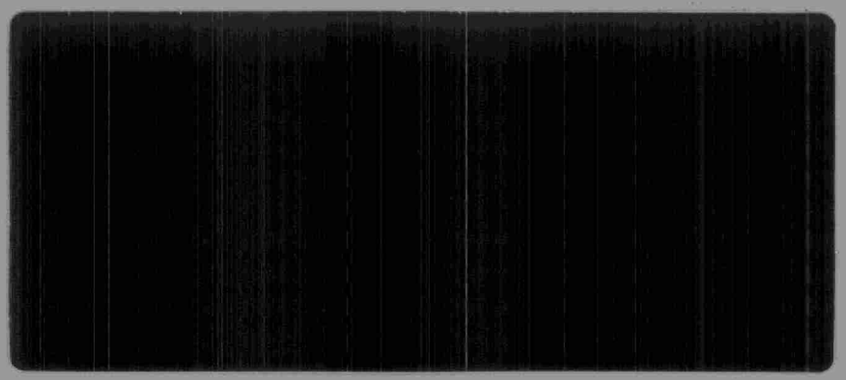

Canada

A COASTAL DISPERSION MODEL FOR EFFLUENT PLUMES

R.O.W. Kuehnel, C.R. Murthy, K.C. Miners
National Waters Research Institute
and
B. Kohli, Y. Hamdy
Ontario Ministry of the Environment

Project Leader: C.R. Murthy

Environment Canada Environnement Canada

Canada - Ontario Agreement on Great Lakes Water Quality

Ontario Ministry of the Environment

A COASTAL DISPERSION MODEL FOR EFFLUENT PLUMES

R.O.W. Kuehnel, C.R. Murthy and K.C. Miners
Aquatic Physics & Systems Division
National Water Research Institute
P.O. Box 5050
Burlington, Ontario
L7R 4A6

B. Kohli and Y. Hamdy
Great Lakes Section
Water Resources Branch
Ontario Ministry of the Environment
Toronto, Ontario
M4V 1P5

Project Leader: C.R. Murthy

September 1981

A COASTAL DISPERSION MODEL FOR EFFLUENT PLUMES

TABLE OF CONTENTS

		PAGE
	LIST OF TABLES	ii
	LIST OF FIGURES	iii
	ACKNOWLEDGEMENT	v
	SUMMARY	vi
1.	INTRODUCTION	1
2.	THE COASTAL ZONE	3
3.	COASTAL CLIMATOLOGY	4
4.	DIFFUSION AND THE GAUSSIAN PLUME	6
5.	THE GAUSSIAN PLUME MODEL	9
6.	EXTENDED GAUSSIAN PLUME MODEL	13
7.	MODEL PARAMETERS	15
7.1	The Decay Constant	16
7.2	The Diffusion Coefficient	17
7.3	The Diffuser Length	17
7.4	The Initial Dilution	17
7.4.1	Deep Water Models	19
7.4.2	Shallow Water Models	20
7.4.3	Diffusers in Ambient Cross Flow	20
8.	COMPUTER SIMULATION	21
9.	MODEL APPLICATIONS	24
9.1	Data Base and Procedure	24
9.2	Input Parameters	26
9.3	Estimate of Initial Dilution	27
9.4	Results and Discussions	28
10.	FUTURE DEVELOPMENTS	30
	REFERENCES	31
	APPENDIX	77

LIST OF TABLES

TABLE	TITLE	PAGE
1	A summary of the diffusion characteristics and lateral spreading of an effluent plume from a line source in steady current.	36
2	Current speed-direction summary, Pickering, Lake Ontario, 1980.	37
3	Current speed-direction histogram, Pickering, Lake Ontario, 1980.	38
4	Mean concentration field, Pickering, Lake Ontario 1980.	39
5	Location 043 Operating Log	40
6	Summary of current meter results in the vicinity of Lakeview WPCP Outfall.	41
7	Current speed-direction histogram (summer), Lakeview Lake Ontario, 1970.	42
8	Current speed-direction histogram (winter), Lakeview Lake Ontario, 1970-71.	43
9	Summer Current Episodes (Shore Parallel) Lakeview WPCP	44
10	Summer Current Episodes (Shore Antiparallel) Lakeview WPCP	45
11	Winter Current Episodes (Shore Parallel) Lakeview WPCP	46
12	Winter Current Episodes (Shore Antiparallel) Lakeview WPCP	47
13	Plume Dimensions at the Lakeview WPCP	48
14	Input Parameters for Effluent Plume Simulations	49
15	Alongshore current Frequency Table Lakeview WPCP	50

LIST OF FIGURES

FIGURE	TITLE	PAGE
1	Variation of Alongshore Mean Current with Distance from Shore	51
2	Monthly Vector Time-Series Plot, Pickering Lake Ontario, 1980	52
3	Vector Time-Series Plot, Douglas Point, Lake Huron, 1974	53
4	Vector Time-Series Plot, Lakeview, Lake Ontario, 1972	54
5	Schematic of a Continuous Plume Experiment	55
6	Crossplume Concentration Distribution-Relative	56
7	Crossplume Concentration Distribution-Absolute	56
8	Horizontal Eddy Diffusivity - Length Scale	57
9	Schematic of a Laterally Diffusing Effluent Field in a Steady Current	58
9A	Schematic of Plume Dispersal with Different Diffusion Mechanisms	59
10	Co-ordinate System for Gaussian Plume Calculations	60
11	Schematic of the Nearfield and Farfield Dilution	61
12	Nearfield Flow Stability	62
13	Diffuser Types	63
14	Dilution No Interference $\theta = 0^{o}$	64
15	Jet Width No Interference $\theta = 0^{o}$	65
16	Dilution No Interference $\theta = 20^{o}$	66
17	Jet Width No Interference $\theta = 20^{o}$	67
18	Dilution Factor for an Alternating Diffuser	68
19	Dilution Factor for a Staged Diffuser	69
20	Current Dilution	70

21	Schematic of the Average Concentration Field Obtained when Combining Plumes with Different Orientations	71
22	The Average Concentration Field of a Single Alongshore Current Episode	72
23	The Average Concentration Field of Shoreparallel and Antiparallel Current Episodes.	74
24	Lakeview WPCP Outfall Diffuser	76

ACKNOWLEDGEMENTS

The authors are indebted to F. M. Boyce of NWRI for discussions on some aspects of the model analysis. Critical review of the manuscript by D. Lam of NWRI and F.C. Fleischer, R.R. Weiler and J. Kinkead of MOE, is greatly appreciated.

The report was prepared jointly by NWRI and MOE under NWRI (study Number APSD 506) with additional support through the federal Great Lakes Water Quality Program on Limited Use Zone (Code 1104).

A COASTAL DISPERSION MODEL FOR EFFLUENT PLUMES

SUMMARY

A computer simulation model was developed to plot two dimensional dilution contours of an outfall discharging into the time variant coastal currents of a large lake. The computer model is based on an analytical steady state, depth integrated, two dimensional, Gaussian cross-plume model, which generates successive realizations of the farfield plume. The current speed and direction data (from the current meters) are used to map dilution/concentration contours in polar coordinates. The model assumes that:

- the effluent field moves with the prevailing currents without disturbing the existing flow pattern of the coastal zone.

- the diffusion in the flow direction is negligible compared to the advection.

- the lateral eddy diffusivity is a function of the initial plume width.

- the vertical diffusion is negligible and the effluent is uniformly distributed over the available water depths.

The following steps produce dilution contours from a diffuser outfall.

- determine the initial dilution due to the jet rise using the techniques discussed in this report;

- classify the current episodes according to the speed and the direction ranges;

- divide each episode into hourly speed and direction events;

- calculate the farfield dilution (or the total dilution including the initial dilution) for each hourly event at all points of a polar grid;

- repeat the procedure for other hourly events and then average the results over the whole episode.

These successive plumes provide statistical estimates of the plume transport under selected current regimes.

The model was applied to the Lakeview Water Pollution Control Plant (WPCP) diffuser outfall in Lake Ontario, using the 1970-72 current meter data, to predict dilution contours of a conservative pollutant. This method can also be applied to non-conservative pollutants, if their decay rates are known. The model can be applied to any diffuser outfall in a large lake, provided it is calibrated by collecting the current meter and plume tracking information, simultanously.

Present experience suggests two improvements to the computer model.

1. As the model was found to be more sensitive to the current direction than the current speed, the accuracy of diffusion field calculations can be improved by decreasing the current direction segments of the current episodes.

2. Short duration current episodes, where the plume length is limited by advection rather than diffusion, should be included in the analysis.

A COASTAL DISPERSION MODEL FOR EFFLUENT PLUMES

1. INTRODUCTION

One of the objectives of the Great Lakes Water Quality Agreement (International Joint Commission - IJC) of 1978, signed between Canada and the United States of America, is to achieve and maintain mutually acceptable water quality conditions in the Great Lakes. It was recognized at the time that it might not be economically or physically feasible to achieve the same water quality in the immediate vicinity of an effluent outfall as in the remainder of a lake. Consequently, in Annex 2 of the Agreement, the appropriate governing bodies were given the responsibility, with limiting guidelines, to define certain areas as limited use zones (LUZ). Within the LUZ, the water quality may not comply with the water quality objectives. However, before any water passes through a zone boundary, it must achieve the designated objective of the receiving lake. The purpose of this report, which is a joint effort by the National Water Research Institute (NWRI) and the Ontario Ministry of the Environment (MOE), is to describe how the coastal currents and dispersion characteristics derived from the existing climatological data bases of NWRI, MOE, and Ontario Hydro can assist in delineating the LUZ perimeter of an outfall discharging into a large lake.

Sewage outfalls and other discharge outlets are usually located at lake bottom within 2 km of the shoreline. These outfalls are generally multiport diffusers placed such that the diffuser jets are perpendicular to the predominant current direction. After the initial jet mixing, which takes place within a few minutes or a short distance, the effluents effectively form a line source at the surface. Further diffusion of this line source of effluents is governed by the prevailing coastal currents and their eddies. The dilution will depend upon the location of the effluent plume within the coastal zone, current transport and dispersion characteristics of the area.

The coastal currents and their dispersion characteristics can be

obtained by direct measurement or inferred from existing data bases after site specific validation. It is not yet possible to model all of the complex flows that have been observed in the coastal zones of the Great Lakes due to lack of knowledge of their interactions. Fortunately, the important and frequent case of longshore pollutant transport and dispersion by a nearly steady shore parallel current, can be predicted by the following combined statistical-analytic analysis. Similar shore parallel or antiparallel current episodes are selected from the climatological data base. (If a person stands on the lakeshore and looks towards the lake, his right hand direction is defined as 'shore parallel' and his left hand direction is defined as 'antiparallel'). These are used as the input data to a steady state, depth integrated, two-dimensional Gaussian cross-plume model which generates successive realizations of the effluent (farfield) plume. The minimum, mean, and maximum limits of the farfield plume, or a constant dilution contour within the plume, provide statistical estimates of the plume transport and dispersion under the selected current regime.

A computer program was developed to carry out the above procedure for conservative and nonconservative substances. This program of farfield dilution requires a value of nearfield or initial dilution as an input, which can be calculated separately or by means of a user subroutine. Providing the climatological data base and selected current regimes are representative of the site under investigation,a reasonable estimate may be made of the frequency, duration, and dimensions of future effluent plumes. The model can also be applied to conditions when the currents are in directions other than shore parallel or antiparallel, for example, offshore and onshore current directions.

2. THE COASTAL ZONE

It has been known for the last decade that at the edge of the Great Lakes there is a 5 - 10 km. coastal zone where the lakewide circulation adapts to the presence of the shore, i.e. the lake currents are influenced by bottom and the friction shore boundary (Csanady 1970, 1972a, 1972b). Thus, for our purposes, the coastal zone is defined as that area extending offshore over which bottom friction effects modify the lakewide circulation currents to the extent that the predominant local currents are shore-parallel and are increasingly dependent on local wind forcing (Bull and Murthy, 1978). During the summer months, when the lakes are strongly stratified, the coastal zone is narrower than during the winter months of weak stratification (Bull and Murthy, 1980). Extensive analysis of NWRI measurements suggests that the coastal zone can be divided into two distinct boundary layers, an inner or frictional boundary layer (FBL) dominated by shore and bottom friction and an outer boundary layer (OBL) of adjustment of the inertial component of midlake circulation (Murthy and Dunbar, 1977).

The above division is most easily illustrated at a given site by plotting the mean shore parallel currents versus distance from shore (Fig. 1) or by directly examining stick vector plots of the observed currents (Fig. 2). The plots indicate that the most efficient dispersal of pollutants, associated with the highest currents and turbulence, is obtained by locating the diffuser at the FBL-OBL interface 1-4 km. offshore. This is seldom cost effective but it should be kept in mind that as the diffuser approaches the FBL-OBL interface from the shore both the nearfield dilution, which usually depends on depth, and the farfield dilution, which depends on the current speed and turbulence, are likely to improve, all other factors being equal.

3. COASTAL CLIMATOLOGY

Field measurement programs designed to obtain time-series records of coastal currents and temperatures over periods of many months give a time history of the various flow regimes present in the coastal zone. Such records show an extremely complicated flow situation varying by season and from place to place that is often difficult to analyse. As yet, nearshore models are insufficiently comprehensive to be able to predict the complex array of flow regimes encountered in this area. Hence one is reduced to employing a statistical description of the measured flow properties. A climatology of the coastal zone is built up by cataloguing the relative frequency of occurrence and average duration of important flow regimes in an area. These are then used to estimate the flushing capability and dispersion of the local currents. It must be emphasized that some of the flow regimes which can be identified are not easily analysed with existing nearshore models, either because of the inherent complexity of the flow regime or due to insufficient information about the associated boundary conditions and forcing functions. Engineers and planners should always be aware that present dilution estimates are based on those subsets of the available current measurements which are sufficiently well behaved to be analysed with the existing nearshore models. Unusual and complex current episodes are nearly always excluded.

Over the past decade a large data base of coastal current measurements has been built up by researchers from NWRI, MOE, Ontario Hydro, and the University of Waterloo (Csanady and Pade, 1970, 1971, 1972; Kohli and Palmer, 1973; Kohli, 1976a, 1976b; Kohli and Farooqui, 1980; Bull and Farooqui, 1976; Jordan and Bull, 1977; Murthy and Dunbar, 1977; Kaiser and Bull, 1978a, 1978b; Bull and Kaiser, 1980; Bull, Kerman, and Lilly, 1980). An examination of these data sets indicates that strong shore-parallel currents dominate the organized flow patterns within the coastal zones of the Great Lakes. For the present calculations the current climatology is divided into two sets. The first contains all the quasi-steady shore parallel flow regimes persisting for a day or longer which are responsible for longshore pollutant transport.

The second or miscellaneous set contains the short term, irregular, and random flows which merely distribute the effluent in the immediate vicinity of an outfall. This division is necessary because the Gaussian plume model is only valid in quasi-stationary current regimes.

The longshore current flows are further subdivided into two directions (shore parallel and antiparallel) and three speed ranges (0-5, 5-15, >15 cm/s). The statistical behaviour of the effluent plume can now be modelled by calculating the farfield concentration occurring under these six flow regimes. The development of a persistent longshore current regime in any given direction invariably suggests a current reversal. However, there is usually a mass exchange between the coastal and offshore waters during current reversals (Csanady 1970). Hence the plume develops in clean water and the preceding flow field history is not required. Strong shore parallel currents usually persist from 1-7 days and follow the coastline. At an average speed of 10 cm/s a conservative effluent can easily be carried 25 km. or more from the source.

During the winter months the coastal currents exhibit a classic bi-modal character, flowing either parallel or antiparallel to the shore (Fig. 2). There may also be some asymmetry between the shore parallel and antiparallel episodes, the currents being stronger and of longer duration in one direction than the other (Fig. 3). The bi-modal character is less marked in the summer months when there is strong lake stratification. The longshore currents become weaker, less persistent, and are interspersed with weak or rapidly fluctuating current flows and other miscellaneous events (Fig. 4).

The following current regimes have been identified among the set of miscellaneous current events.

a) Short term shore parallel and antiparallel current episodes ($\sim$1 day).

b) Weak onshore and offshore current episodes.

c) Low speed current episodes with random speed and direction fluctuations.

d) Stagnation episodes.

These current flows are too complex and irregular to be analysed with our quasi-steady state model. Due to their low speed and short duration they do not disperse but merely pool the effluents near the source (Murthy and Kenney 1974). The resulting patch is not only undesirable from the viewpoint of effluent dispersal in the coastal zone, but under unfavourable conditions the pollutants may be transported toward and trapped near the shore (Murthy 1972). Such an incident is all the more likely because the mass exchange of coastal and offshore waters preceding the development of a persistent longshore current may not occur between successive low or random current episodes.

4. DIFFUSION AND THE GAUSSIAN PLUME

The spreading of a dye plume in a steady coastal current in the wake of a continous source exhibits two different scales of growth and diffusion (Fig. 5). The first is the lateral growth of the plume width relative to the instantaneous centre of gravity. This relative diffusion is caused by turbulent eddies comparable in size to the plume width (Csanady 1963, Murthy and Csanady 1971). The second is the meandering of the plume centre of gravity caused by turbulent eddies with length scales larger than the plume width (Murthy and Kenney 1974, Murthy and Miners 1980). Combining or superimposing these two statistically independent processes gives the net or absolute diffusion of the plume (Gifford 1959, Bowden et al. 1974).

It has long been recognized that at any instant the concentration field of an effluent plume is likely to be neither Gaussian nor symmetric. This is hardly surprising considering the complexity of the coastal flows, influenced as they are by wind and current

shear. The average plume concentration field, however, can be described by a symmetric cross plume Gaussian distribution. This is shown by figures 6 and 7, which diagram 48 successive crossings of a dye plume at a constant distance from the source (Murthy and Miners 1978, 1980). They show that the relative cross plume concentration distribution is nearly Gaussian and symmetric (Fig. 6), however, the absolute cross plume concentration distribution is flatter and has a sharper cutoff than a Gaussian distribution (Fig. 7).

This suggests the following strategy when utilizing time series current meter data to model the average concentration field of an effluent plume. An analytic cross plume Gaussian model is used to calculate the concentration field relative to the plume centre of gravity for each different speed and direction event of a shore parallel episode. These realizations are then weighted and averaged together according to their frequency of occurence during the current episode. The final numeric - analytic estimate of the average concentration field developed by the selected flow regimes thus includes, in an approximate manner, the combined effects of relative diffusion, current speed fluctuation, and plume meandering.

Having discussed the formulations of the advective flow field for the model, attention is now directed to the diffusion formulations. Three different diffusion models are generally considered (Murthy 1976). There is Fickian diffusion where the eddy diffusivity is constant, shear diffusion where the eddy diffusivity grows linearly with the scale of the diffusion field, and inertial subrange diffusion where the eddy diffusivity has a 4/3 power dependence on the scale of the diffusion field. Their properties are summarized in Table 1. Now the scale and intensity of the turbulent eddies inside the coastal zone depend not only on the local wind and current flows but also on the history of past lakewide wind and current events. The difficulty is to decide which diffusion mechanism or combination of diffusion mechanisms is operative at any time at a given site.

The following conclusions can be drawn from past coastal zone experiments. The vertical diffusivity is at least one to two orders

of magnitude less than the horizontal diffusivity and can be neglected in most plume spreading calculations (Csanady 1970, Murthy 1974). The difference in magnitude is attributed to stratification effects and the difference between the horizontal and vertical scales of motion in the coastal zone. It has also been observed that in a steady coastal current the width of an effluent plume increases according to the 4/3 power law in the immediate vicinity of a point source outfall (Csanady 1970, Murthy and Csanady 1971), however, the mechanisms of plume growth are less clear at distances far from the source. The centreline concentration has been observed to fall off as $x^{-1/2}$ (Csanady 1970, Murthy and Csanady 1971), and x^{-2} (Murthy 1972, 1974), indicating that Fickian and vertical and horizontal shear diffusion processes are present. Investigations by Murthy and Miners (1978), Lam and Murthy (1978) suggest that the horizontal eddy diffusivity of the coastal zone can be described by the empirical relationship shown in Figure 8, however, with suitable coefficients the standard diffusion models are equally applicable.

In summary, the ability to model the dispersion of effluents in the coastal zone is directly related to our knowledge and understanding of coastal zone diffusion processes. The average concentration field of an effluent plume can be modelled with reasonable accuracy if site specific measurements of the eddy diffusivity under different flow regimes are available. Such concentration estimates are less accurate if the strength and character of local diffusion mechanisms must be inferred from the data of similar, but not necessarily equivalent coastal sites, or from diffusion diagrams. (Okubo, 1971 and 1976)

Kohli (1981) reviewed the farfield dilution methods with steady current and presented a simple and quick method of estimating the two-dimensional dilution field. This method may be used for quick and rough estimates of dilution ratios at different distances from the sources under steady current regime.

5. THE GAUSSIAN PLUME MODEL

The analytic equations describing the diffusion mechanisms and average concentration field of an effluent plume in a steady current in the wake of a line source diffuser are readily available in the literature (Fisher et al 1979, Hinze 1959). The equations and their derivations are repeated here for completeness following the analysis of Brooks (1960). The advection - diffusion equation of a non-conservative tracer with an exponential decay rate in a field of homogeneous turbulence is

$$\frac{\partial c}{\partial t}+u\frac{\partial c}{\partial x}+v\frac{\partial c}{\partial y}+w\frac{\partial c}{\partial z}=\frac{\partial}{\partial x}\left(K_x\frac{\partial c}{\partial x}\right)+\frac{\partial}{\partial y}\left(K_y\frac{\partial c}{\partial y}\right)+\frac{\partial}{\partial z}\left(K_z\frac{\partial c}{\partial z}\right)-\lambda c \quad \text{..... (1)}$$

where $c(x,y,z)$ is the tracer concentration, (u,v,w) are the velocities in the $(x,y\,z)$ directions, (K_x, K_y, K_z) are the corresponding eddy diffusivities, and λ is the decay lifetime or dieoff constant of the tracer. Consider now a steady and continuous effluent line source of length b kept perpendicular to a uniform and steady shore parallel current of speed U as shown in figure 9. To allow for initial jet mixing it is assumed that the effluent has been diluted to concentration c_o prior to release from the ideal line source. Under these conditions equation (1) reduces to

$$u\frac{\partial c}{\partial x}=\frac{\partial}{\partial x}\left(K_x\frac{\partial c}{\partial x}\right)+\frac{\partial}{\partial y}\left(K_y\frac{\partial c}{\partial y}\right)+\frac{\partial}{\partial z}\left(K_z\frac{\partial c}{\partial z}\right)-\lambda c \quad \text{..... (2)}$$

The following assumptions further simplify the analysis:

1) It is assumed that the effluent field formed by the line source moves downstream in the x-direction at the same rate as the prevailing current and without disturbing the existing flow pattern of the coastal zone.

2) The diffusion in the flow direction is negligible in comparison to the advection ($K_x \sim 0$). The assumption is

justified by the fact that the concentration gradients in the x-direction are very small compared to the lateral direction because of the advection in the x-direction.

3) Vertical diffusion is negligible compared to the lateral horizontal diffusion ($K_y >> K_z \sim 0$). As described in the preceding section this is due to the difference between the width and depth scales of the coastal zone.

4) The effluent is distributed uniformly over the available depth, which is assumed to be constant, so that the mixing can be described by a two-dimensional depth integrated analysis. The available depth may be a section of the water column, the distance from the thermocline to the bottom, a surface layer, or the total height of the water column, depending on the diffuser characteristics and climatological conditions.

5) The lateral eddy diffusivity K_y is assumed to be a function of L, the plume width, which with the preceding assumptions is only a function of x, the distance from the source, and not of y. The assumption implies that

$$K_y / K = g[L(x)] / g(b) = f(x)$$

so that if an eddy diffusivity $K = g(b)$ is associated with the length b of the diffuser then

$$K_y = g[L(x)] = f(x)$$

where $L(x)$, $g(x)$, and $f(x)$ are functional relationships.

6) The outfall is located sufficiently far offshore that the spread of effluent in the coastal zone is not restricted by the shore boundary.

With the above assumptions the advection - diffusion equation reduces to

$$\frac{\partial c}{\partial x} - K_y \frac{\partial^2 c}{\partial y^2} + \lambda c = 0 \quad \text{..... (3)}$$

Equation (3) can be solved in the half plane $x \geq o$ the boundary conditions of x = o being

$$c \begin{cases} c = c_o & \text{for } |y| \leq b/2 \\ c = 0 & \text{for } |y| > b/2 \end{cases} \quad \ldots\ldots\ldots\ldots\ldots\ldots\ldots\ldots\ldots\ldots\ldots\ldots\ldots\ldots\ldots\ldots\ldots\ldots \quad (4)$$

The dieoff term is eliminated by the variable change

$$c = Ce^{-\lambda x/u} \quad \ldots\ldots\ldots\ldots\ldots\ldots\ldots\ldots\ldots\ldots\ldots\ldots\ldots\ldots\ldots\ldots\ldots\ldots\ldots\ldots\ldots\ldots\ldots\ldots\ldots\ldots\ldots\ldots\ldots\ldots \quad (5)$$

which simplifies equation (3) to the form

$$K_y \frac{\partial^2 C}{\partial y^2} = u \frac{\partial C}{\partial x} \quad \ldots\ldots\ldots\ldots\ldots\ldots\ldots\ldots\ldots\ldots\ldots\ldots\ldots\ldots\ldots\ldots\ldots\ldots\ldots\ldots\ldots\ldots\ldots\ldots\ldots\ldots\ldots\ldots\ldots\ldots \quad (6)$$

where C(x,y) is the concentration with no dieoff and x/u is the travel time to any distance x. Thus the diffusion problem can be solved without dieoff and then multiplied by the decay factor $e^{-\lambda x/u}$. The spatial dependence of the eddy diffusivity is eliminated by the transformation (assumption 5 above)

$$\frac{dX}{dx} = \frac{K_y}{K} = \frac{g(L)}{g(b)} = f(x) \quad \ldots\ldots\ldots\ldots\ldots\ldots\ldots\ldots\ldots\ldots\ldots\ldots\ldots\ldots\ldots\ldots\ldots\ldots\ldots\ldots\ldots\ldots\ldots\ldots\ldots\ldots\ldots\ldots\ldots\ldots \quad (7)$$

which reduces equation (6) to the form

$$K \frac{\partial^2 C}{\partial y^2} = u \frac{\partial C}{\partial X} \quad \ldots\ldots\ldots\ldots\ldots\ldots\ldots\ldots\ldots\ldots\ldots\ldots\ldots\ldots\ldots\ldots\ldots\ldots\ldots\ldots\ldots\ldots\ldots\ldots\ldots\ldots\ldots\ldots\ldots\ldots \quad (8)$$

The solution of this equation with standard integral techniques (Hildebrand 1965) is found to be

$$c(x,y) = C(x,y)\, e^{-\lambda x/u} = C(X,y)\, e^{-\lambda x/u} \quad \ldots\ldots\ldots\ldots\ldots\ldots\ldots\ldots\ldots\ldots\ldots\ldots\ldots\ldots\ldots\ldots\ldots\ldots\ldots\ldots\ldots\ldots\ldots\ldots\ldots\ldots\ldots\ldots\ldots\ldots \quad (9a)$$

$$= \frac{c_o e^{-\lambda x/u}}{\sqrt{4\pi KX/u}} \int_{-b/2}^{b/2} \exp\left\{-(y-\beta)^2/4KX/u\right\} d\beta \quad \ldots\ldots\ldots\ldots\ldots\ldots\ldots\ldots\ldots\ldots\ldots\ldots\ldots\ldots\ldots\ldots\ldots\ldots\ldots\ldots\ldots\ldots\ldots\ldots\ldots\ldots\ldots\ldots\ldots\ldots \quad (9b)$$

$$= \frac{1}{2} c_o e^{-\lambda x/u} \left\{ \operatorname{erf}\left[\frac{(y+b/2)}{\sqrt{4KX/u}}\right] - \operatorname{erf}\left[\frac{(y-b/2)}{\sqrt{4KX/u}}\right] \right\} \quad \ldots\ldots\ldots\ldots\ldots\ldots\ldots\ldots\ldots\ldots\ldots\ldots\ldots\ldots\ldots\ldots\ldots\ldots\ldots\ldots\ldots\ldots\ldots\ldots\ldots\ldots\ldots\ldots\ldots\ldots \quad (9c)$$

where

$$\operatorname{erf}(z) = \frac{2}{\sqrt{\pi}} \int_0^z e^{-\alpha^2} d\alpha = \frac{1}{\sqrt{\pi}} \int_{-z}^{z} e^{-\alpha^2} d\alpha \quad \ldots\ldots\ldots\ldots\ldots\ldots\ldots\ldots\ldots\ldots\ldots\ldots\ldots\ldots\ldots\ldots\ldots\ldots\ldots\ldots\ldots\ldots\ldots\ldots\ldots\ldots\ldots\ldots\ldots\ldots \quad (10)$$

Before equation (9) can be utilized the functional relationship between X and x must be specified (equation 7). This is accomplished as follows. Set

$$L = 2\sqrt{3} \cdot \sigma \quad \text{..... (11)}$$

where σ is the standard deviation of the cross plume distribution function, i.e.

$$\sigma^2 = \frac{1}{C_o b}\int_{-\infty}^{\infty} y^2 C(x,y)\, dy = \frac{1}{C_o b}\int_{-\infty}^{\infty} y^2 C(X,y)\, dy \quad \text{..... (12)}$$

With these definitions L=b at x=0 and equation (12) can be integrated to yield

$$\left(\frac{L}{b}\right)^2 = 3\left(\frac{2\sigma}{b}\right)^2 = \left[1 + \left(\frac{4KX}{u}\right)\frac{6}{b^2}\right] \quad \text{..... (13)}$$

Now from the preceding section the standard diffusion mechanisms relating the lateral eddy diffusivity K_y to the scale or width L of the effluent plume are:

1) Fickian diffusion $\quad K_y = \text{const} \quad f(x) = 1$ ..... (14a)

2) Shear diffusion $\quad K_y \alpha L \quad f(x) = L/b$ ..... (14b)

3) Inertial sub-range diffusion $\quad K_y \alpha L^{4/3} \quad f(x) = (L/b)^{4/3}$ ..... (14c)

Substitute equation (13) and any one of the functional relationships of equation (14) into equation (7). Integrating and rearranging the result then gives

$$\frac{4KX}{u} = \frac{b^2}{6}\left\{\left[1 + \frac{1}{n}\left(\frac{4Kx}{u}\right)\frac{6}{b^2}\right]^n - 1\right\} \quad \text{..... (15)}$$

where the diffusion model index n = 1,2,3 for Fickian, lateral shear, and inertial sub-range diffusion respectively. The results are summarized in Table 1 and Figure 9A.

The most useful form of equation (9c) is to refer all concentrations to the effluent concentration c_s before release from the diffuser. Introducing the dilution factors

$$\eta = \frac{c}{c_s} = \text{effluent field to source dilution factor}$$

$$\eta_{so} = \frac{c_o}{c_s} = \text{jet or nearfield to source dilution factor}$$

allows equation (9c) to be written

$$\eta_{(x,y)} = \frac{1}{2}\eta_{so}\, e^{-\lambda x/u}\left\{\text{erf}\left[\frac{(y+b/2)}{\sqrt{4KX/u}}\right] - \text{erf}\left[\frac{(y-b/2)}{\sqrt{4KX/u}}\right]\right\} \quad \ldots\ldots (16)$$

In the extreme farfield, the line source approaches a point source and the limit of equation (16) reduces to

$$\eta_{(x,y)} = \eta_{so} \cdot e^{-\lambda x/u} \frac{b}{\sqrt{4\pi KX/u}} \cdot e^{-y^2/(4KX/u)} \quad \ldots\ldots\ldots\ldots (17)$$

Equations (15)-(17) are the basic equations describing the average concentration field of an effluent plume in a steady current in the wake of a line source diffuser.

6. EXTENDED GAUSSIAN PLUME MODEL

The Gaussian plume model can be extended to include the effects of current speed fluctuations and plume meandering in the final estimate of the average effluent field concentrations. The method is to calculate the equilibrium or steady state concentration field produced by all the unique speed and direction events of a shore parallel episode. These realizations are then weighted and averaged together according to the frequency of occurrence of each generating speed-direction event. Such a procedure presumes that the average distribution of concentrations in a quasi steady current can be approximated by the weighted average of successive steady state solutions. The approximation would be reasonably accurate if there were only speed and no direction changes. This is because the above weighted average does not take into account the fact that the fluctuations in the flow direction of a meandering plume tend to alternate so that the flow remains close to the mean current direction (Fig.5). Consequently, the model overestimates the average plume width and underestimates the concentrations near the

centreline. However, it has been observed that during the meandering of a plume there is accelerated mixing due to shear diffusion (Murthy 1972, Murthy and Kenney 1974). This tends to compensate the limitations in the averaging procedure so that the calculated concentrations are likely to be better estimates of the average field concentrations than originally expected.

The averaging procedure is applied to the Gaussian plume model as follows. Consider a polar coordinate grid (r,θ) centred on the effluent source with the principal axis parallel to the shore (Fig. 10). Let there be a current u passing over the source making an angle ϕ with the shoreline. The current defines the x-y coordinate system of the Gaussian plume model described in the preceding section.

Noting that

$$x = r\,\mathrm{Cos}(\theta - \phi) \qquad y = r\,\mathrm{Sin}(\theta - \phi) \quad \ldots\ldots\ldots\ldots (18)$$

and the restriction

$$|\theta - \phi| < \pi/2 \quad \ldots\ldots\ldots\ldots (19)$$

the dilution factor $\eta(x,y)$ of equation (16) can be written

$$\eta_{(x,y)} = \eta_{(r,\theta,U,\phi)} \quad \ldots\ldots\ldots\ldots (20)$$

where the dependence of the dilution factor on the speed and current direction has been explicitly included.

Next divide the time series data (U, ϕ) of a shore parallel current episode into Q segments so that the speed and direction (U_q, ϕ_q) may be considered constant during the segment q, say hourly averages. Define the speed-direction frequency distribution f_{mn} of the current episode by sorting the speed-direction segments (U_q, ϕ_q) into the M*N bins of a speed-direction histogram and then dividing by Q so that

$$\sum_{mn} f_{mn} = 1 \quad \ldots\ldots\ldots\ldots (21)$$

This establishes the statistics of climatology of the current episode. For the Great Lakes a convenient selection of histogram intervals is 1 cm/s for speed and 5-45^{o} for direction.

Based on the described speed-direction histogram and equations (15) - (21) the average dilution factor at any (r, θ) is

$$\eta_{(r,\theta)} = \sum_{mn} f_{mn}\, \eta_{(r,\theta,U_m,\phi_n)} \qquad \text{.....(22)}$$

An alternate method of calculating the average dilution factor at (r, θ) is to first calculate the average sector velocity $\bar{U}_n$ using the equations

$$f_n = \sum_{m} f_{mn} \qquad \text{.....(23)}$$

$$\bar{U}_n = \sum_{m} f_{mn}\, U_m / f_m \qquad \text{.....(24)}$$

and then substituting the result in equation (15) - (21) to obtain

$$\eta_{(r,\theta)} = \sum_{n} f_n\, \eta_{(r,\theta,\bar{U}_n,\phi_n)} \qquad \text{.....(25)}$$

For well behaved current episodes the difference between the results of equations (22) and (25) is usually not significant.

The preceding analysis deals with a single current episode of an identifiable flow regime, say a shore parallel, medium speed flow. If there is sufficient data then it is possible to obtain further climatological information about the dispersion and mixing properties of the selected flow regime by calculating the average concentration field of each current episode belonging to the flow regime and then performing the relevant statistics on the ensemble of average concentrations.

7. MODEL PARAMETERS

The input parameters of the extended Gaussian plume model are those of an ideal line source of fixed strength lying perpendicular to a steady current in a homogeneous field of turbulence. The relationship between

these idealizations and their physically observable equivalents is shown in Figure 11. It shows that the calculated average dilution field of a line source diffuser can be divided into a nearfield and a farfield solution. The nearfield or initial dilution, which is assumed to occur in the immediate vicinity of the diffuser, is due to the kinetic and buoyant potential energy of the diffuser jet discharge. This energy is dissipated in the turbulent mixing of the jet with the surrounding lake water. The degree of mixing is a function of the effluent properties, water depth, diffuser design and discharge flow characteristics. After the initial jet mixing the effluent field stabilizes and moves with the speed of the ambient field. The parameters that define the effluent field or nearfield solution at this juncture are the ones used as input parameters to the farfield or Gaussian plume calculations. They are discussed below along with the assumptions and simplifications required to estimate their values.

7.1 The Decay Constant or Decay Lifetime ($\tau = 1/\lambda$)

The inverse of the decay constant, or decay lifetime, is the time required for the concentration of a non-conservative tracer, obeying an exponential decay law, to decrease to e^{-1} of the initial value. The decay constant can be obtained from laboratory measurements if the decay rate of the tracer is approximately independent of the ambient conditions as is the case for radionuclides. The experiments are more complex for those chemical and biological tracers (e.g. chlorine, coliform bacteria, etc.) where the decay rate depends on ambient conditions like temperature, mortality, flocculation, and sedimentation. In such cases, if the responsible regulatory agency has not set the decay rates, it may be necessary to augment laboratory results with on site measurements at different seasons.

The importance of the decay lifetime (τ) in effluent dilution depends upon its magnitude relative to the time (t) required to achieve dilution by diffusion alone. If $\tau \gg t$ then the first exponential term in equations (16) and (17) is nearly unity and can be omitted, i.e. $e^{-\lambda x/u} \approx 1$ and the effluent can be treated as a conservative substance for the time scale of the calculations. For other cases the

complete formulae must be used. However, if $\tau \ll t$ a quick estimate of the radial extension of the plume for a desired dilution can be obtained from the formula.

$$\eta = \eta_{so}\, e^{-\lambda x/u} \qquad \text{(26)}$$

7.2 The Diffusion Coefficient (K)

The selection of the initial value and growth law of the diffusion coefficient in the coastal zone was discussed in Section 4. If on site measurements are available, or if the eddy diffusivity can be inferred from the measurements at similar sites with similar growth laws, then these results should be used. Otherwise, the best estimate of the diffusion coefficient in the coastal zone can be obtained from the empirical growth law of Figure 8 or something similar.

7.3 The Diffuser Length (b)

The length of the ideal line source which initiates the farfield calculations is the width of the effluent field after the initial dilution (Fig. 11). At this point the effluent field moves with the prevailing current, so that the effective line source is perpendicular to the current, regardless of the original diffuser, - current orientation. If the current is roughly perpendicular to the diffuser, then the length of the effective line source is about the same as that of the diffuser projected perpendicular to the current direction. This approximation clearly fails when the current is parallel to the diffuser and a more in depth analysis is then required (e.g. Roberts 1977). It is also assumed that the distance downstream from the diffuser to the effective line source is small and can be ignored in comparison to the distances of the farfield calculations.

7.4 The Initial Dilution (η_{so})

By using multiport diffusers it is possible to improve the dispersive efficiency of the outfall considerably.

The initial mixing is caused by turbulent jet diffusion, a flow phenomenon that is governed by the source inputs and the receiving water characteristics. A clear understanding of physical processes associated with diffuser outfall discharges is needed so that an estimate of initial dilution and a reliable assessment of the impact of wastewater discharges on the environment can be made.

Hamdy (1981) reviewed the analyses of predictive models and their applicability to different types of submerged diffuser outfalls in stagnant receiving waters.

In general, for the purpose of initial dilution predictions from submerged sources, a distinction has to be made between "deep" and "shallow" receiving water.

Submerged discharges into deep receiving waters generally exhibit stable conditions that is, upon impingement on the free surface, the discharge spreads laterally in the form of a stable density current. These stable conditions create a stratified near-field flow regime which allows fresh ambient waters to entrain with the jet flow (Fig. 12). The vertical distance below the water surface up to which effective entrainment occurs is dependent on the thickness of the surface impingement zone. The diffusion layer thickness is the depth over which the sewage field is uniformly distributed which will be subjected to advection and dispersion. The diffusion layer thickness may vary from 8% to 30% of the total water depth (Abraham 1963). In shallow receiving waters, entrainment into the jet is limited and the jet impingement at the water surface usually results in a complete vertical mixing which is called unstable near-field (Fig. 13).

Criteria to this extent have been developed by Jirka and Harleman (1973), Almquist and Stolzenbach (1976) and Lee, Jirka and Harleman (1977).

For alternating diffusers (Fig. 14), the near-field flow regime is unstable if:

$$H/D < 1.7\ F^{4/3}\ (\ell/D)^{-1/3} \quad \text{.....(27)}$$

For staged or unidirectional diffusers (Fig. 13), the near-field flow is unstable if:

$$H/D < 0.46\ F^{4/3}\ (\ \ell/D)^{-1/3} \quad \text{..... (28)}$$

The above criteria are used regardless of the jet angle θ between the jet and the horizontal plane.

where

H = water depth above diffuser

D = port diameter

F = densimetric Froude Number = $V/\sqrt{g'D}$

$g' = g\frac{\Delta\rho}{\rho_a}$

V = jet velocity

$\Delta\rho$ = the density difference between receiving water and effluent

ρ_a = the receiving water density

g = acceleration due to gravity

ℓ = port spacing (between two consecutive ports)

7.4.1 Deep Water Models

All deep water models are based on an integral type analysis the principle of which are documented by Abraham (1963), Fan (1967) Cederwall (1971), and Fan and Brooks (1969).

Hamdy (1981) showed that these models may be limited to cases of jets with no jet interference and with low discharge densimetric Froude numbers ($F \ll 50$). The above limitation is valid for the shallow coastal zone of the Great Lakes.

Nomograms shown in Figures 14 - 17 can be used to estimate initial dilution ratios and the jet width for horizontal and inclined discharges.

It should be pointed out that these nomograms predict centreline ratios. To obtain the average dilution, multiply the centreline ratio by 1.35 (Brooks 1973). Also, the effective water depth which is about 70% - 80% of the total water depth should be used (Abraham 1963).

7.4.2 Shallow Water Models

Models for different diffuser types in stagnant shallow receiving waters predict average initial dilution in the nearfield taking into consideration the re-entrainment effects.

Estimates of average initial dilution ratios for alternating and staged diffusers can be stated as follows after Jirka and Harleman (1973) and Almquist and Stolzenbach (1976) respectively.

$$\eta_{so}(\text{alternating}) = .52 \left(\ell / DF \right)^{2/3} (H / D) \quad \ldots\ldots\ldots\ldots (29)$$

$$\eta_{so}(\text{staged}) = 0.61 \left(\ell H / D^2 \right)^{1/2} \quad \ldots\ldots\ldots\ldots\ldots\ldots (30)$$

Nomograms shown in Figures 18 and 19, can be used to easily determine average initial dilution ratios for alternating and stages diffusers.

7.4.3 Diffusers in Ambient Cross Flow

Roberts (1977, 1979 and 1980) has reported an interesting study that reveals important three dimensional properties of line diffusers for buoyant discharges. Roberts' experimental study and dimensional analysis for currents perpendicular and parallel to the diffuser are summarized in Figure 20.

The estimates are valid for a range of Froude number (F) from 0.1 to 100, and applicable for stable near-field flow regimes. For sewage outfalls with negligable density differences, the near-field instabilities and associated mixing generated by the momentum flux tend to inhibit any formation of a stably stratified zone and create a uniformly mixed downstream.

Thus, in the case of unstable near-field, the dilution ratio under cross flow will amount to the volume of flux ratio (UHL/Q).

8. COMPUTER SIMULATION

A computer package based on the extended Gaussian plume model was developed. It has a section for calculating the coastal climatology, the average concentration field, and provisions have been made for users to read in the results of section 7.4 or to incorporate their own initial dilution programs. The climatology section sorts hourly average wind and current meter data into speed-direction histograms, prints, plots, and stores the results for later retrieval or immediate use. The speed-direction histograms are used in the diffusion section to calculate, print, plot, and store the average concentration fields generated during shore parallel current episodes. The stored concentration fields of several shore parallel episodes can be retrieved and combined to obtain the average, minimum, and maximum concentrations associated with these current episodes.

It should be noted that what is desired when applying the above computer model is not the average concentration field calculated from a continuous time series of speed and direction events but rather the average concentration fields associated with all the individual shore parallel and antiparallel current episodes occurring within the time series. The concentration fields of the individual current episodes can then, under suitable conditions, be averaged or combined together. The necessity for this approach is illustrated schematically in figures 21a-e.

Figure 21 shows the effluent plume, as defined by a dilution contour, of two different shore parallel current episodes. The current speed is the same for each episode but their directions may differ. In Figure 21a the current directions are the same so that the individual plumes and their average are the same. In Figure 21b the directions of the two plumes differ slightly, as might occur when a plume meanders. The average plume is slightly shorter and broader than each individual plume. In Figure 21c the angle between the flow directions of the two episodes has become so large that their average concentration field is only half as long but somewhat wider than the original plumes. In Figures 21d and 21e it is clear that the outer perimeter of the two plumes (i.e. the concentration field obtained by overlapping the two plumes and retaining the maximum value) is a better estimate of the combined concentration field for our purposes. This is perhaps the main difficulty in using the extended Gaussian plume model, namely deciding how different concentration fields should be usefully combined.

The preceding remarks apply in a somewhat inverse manner to the hourly average speed and direction events of a current histogram. Suppose a histogram is obtained from two current measurements having the same speed but different directions. If the angular bin width of the histogram is very coarse then both measurements are likely to fall in the same direction sector leading to the result of Figure 21a. Two situations can occur when the angular grid is refined. If the angular width of the histogram bins or the angle between the two currents directions is small compared to the angular plume width, then the average concentration field will be little changed as shown in Figure 21b. However, if the angular difference is significant, then the average concentration field will be reduced as shown in Figure 21c. This indicates that the original sector angle was too large. It should be decreased until the sector size no longer affects the calculation, i.e. until the diffusion fields of adjacent current sectors overlap as shown in Figure 21b. Unfortunately, this condition cannot always be achieved owing to computer memory limitations.

The four January current episodes of Figure 2 are now analysed as an example. It will be shown how the average concentration field of a single current episode is calculated and then how similar episodes occurring at different times can be combined to give an estimate of the typical dilution field. The results of a single current episode are summarized in Tables 4-6 and in Figure 22. Figure 22 shows the plot output of the January 18-29 shore antiparallel episode with the 100:1 dilution contour drawn for reference. The input parameters for this simulation were the diffusivity (1000 cm^2/s), source dilution (10:1), diffuser width (200 m), shoreline angle (250^o), the diffusivity increasing as the 4/3 power of the scale of the diffusion field, the outer radius (10 km) and grid sector angle (5^o). The output parameters are the average current speed (11.8 cm/s) and the diffusion layer thickness (1.1 m), which is less than the diffuser depth if the initial dilution estimates are reasonable. The remaining parameters are of an informative nature and not used in the calculations.

The current advection diagram shows that the current carries the effluent to the edge of the polar grid, as it must if steady state calculations are to apply inside this region. The current histogram or rosette shows that the angular resolution was fine enough to include a $\sim 15^o$ plume meander in the calculations. The speed-direction histograms of Tables 2 and 3 show that this episode consists of 276 hourly average events, that there is a plume meander of $\sim 15^o$ about the mean current direction, and lists a maximum observed speed of 26 cm/s. The diffusion field of Figure 22 is repeated in Table 4 which lists the average concentration field of this episode and the diffusion field overlap between adjacent current histogram sectors. It shows that the diffusion fields of adjacent current sectors do not overlap after the first 3 km. Consequently, the sector angles should be decreased. Since this is not possible due to computer memory limitations the calculation will proceed with the understanding that the present calculation will overestimate the plume length.

The calculations were carried out for all four January episodes. The concentration fields of the two shore parallel episodes were

averaged together, as were those of the two shore antiparallel episodes. These results were then overlapped and combined in Figure 23, along with the average position and maximum and minimum ranges of the 100:1 dilution contour.

The average concentration field in Figure 23 exhibits a bifurcate behaviour both in the shore parallel and antiparallel direction. This may be characteristic of the location or due to using only the four January episodes instead of averaging over more winter episodes. Note that because the directions were different it was not really correct to average either the shore parallel or the antiparallel episodes together. This is clearly obvious from the maximum limits of the 100:1 dilution contour.

9. MODEL APPLICATIONS

Between 1970-72 the Ontario Ministry of the Environment gathered extensive time series current and temperature measurements in the vicinity of the Lakeview Water Pollution Control Plant. The data were used to assess the impact on adjacent municipal water intakes of different Lakeview WPCP outfall locations (Kohli and Palmer 1973). The purpose of this section is, to illustrate how the methodology of this report using the same data can assist in determining dilution contours associated with this outfall. The procedure is to calculate the average dilution field of a particular effluent from several realizations of a given current regime. The location of the Lakeview WPCP and current meter location 043 are shown in Figure 24. The shore parallel direction is taken to be SW or 225 degrees from true north.

9.1 Data Base and Procedure

The current meter operating log at the outfall site (043) is presented in Table 5; the drogues checked reasonably well with the current meter recordings. The data are the pre-whitened hourly average current speed and direction measurements obtained from current meter location 043 (Kohli and Palmer 1973).

The prewhitened data were subjected to statistical analysis and the summary is presented in Table 6. The currents were essentially bi-modal in character, as may be seen from the histograms of Tables 7 and 8. The time series data was divided into a summer (May 1 - Oct. 31) and a winter period (Nov. 1 - April 30). Such division showed that there were significant differences in the dimensions of the summer and winter effluent plumes. Current episodes were selected from time series speed and direction plots and stick vector diagrams for each of the two seasons. These were grouped into 6 current regimes according to three speeds (0-5, 5-15, >>15 cm/s) and two directions (shore parallel and antiparallel). There was some subjectiveness in grouping the episodes. For example the current speed of an episode might build up slowly, then shoot up rapidly to 12 cm/s and remain there a while before returning to zero, the average speed over the episode being 4.9 cm/s. The grouping of this episode then depends upon the relative importance of the 0-5 and 5-15 cm/s contributions of the episode. With minor exceptions, the average current speed of an episode fell within the range of the current regime to which it was assigned. (Tables 9 to 12) Episodes of less than a day were rejected in order to insure that there was a well developed alongshore current. The analysis is thus restricted to long term shore parallel transport. The effect of short term or non shore parallel events on the size of limited use zones must be obtained by other methods.

The time-average dilution field was calculated for every episode of a selected current regime. These realizations were then combined to produce an ensemble minimum, mean and maximum dilution field. The resulting dilution fields were then contoured. For a given current regime this procedure not only provides the dimensions of the average dilution contour but also an estimate of its range of variation.

The results of the average dilution contour plots are summarized in Table 13. The number of contour plots was kept at a tractable level by presenting only two plots for each current regime, i.e. the mean contours and the minimum-mean-maximum limits of a selected contour.

9.2 Input Parameters

The input parameters used for the computer simulations are listed in Table 14. The effective length of the diffuser, i.e. the length projected perpendicular to the direction of current flow, was set at 200m. This was based on the observation that the average angle between the normal to the diffuser axis and the direction of current flow was about 5^{o} - 10^{o} for well developed alongshore currents (Tables 7 and 8), accompanied by 5^{o} - 15^{o} fluctuations about the direction of mean current flow (Rosette diagrams of Figures 1.01 - 1.20). Thus, the projected diffuser length ranges from 190-210 m or is about 200 m on average.

The selection of a representative diffusion mechanism for computer simulations is somewhat arbitrary in view of the widely differing diffusion process known to occur in the coastal zone (Section 4). An inertial-subrange diffusion model, where the eddy diffusivity increases as a function of the initial plume width (Table 1), was adopted because this type of plume dispersion has been observed to occur near coastal zone outfalls (Csanady 1970, Murthy and Csanady 1971). The predictions from such a model may be somewhat optimistic at distances far from the source where the plume width becomes comparable to the offshore distance, thereby limiting the size of the dispersing eddies. The diffusion coefficient associated with the initial plume or effective diffuser width was therefore chosen very conservatively. The diffusion coefficient was obtained from Figure 8, divided it by two, and rounded to the nearest 100 cm^2/s. Remembering that Figure 8 was drawn with the convention $L = 3\sigma$, where σ is the standard deviation of the cross plume distribution function, while our model uses the relationship $L = 2\sqrt{3}\cdot\sigma$ (equation 11), the equation providing a conservative estimate of the eddy diffusivity near the line source becomes

$$K = 0.01(\sqrt{3}/2 \cdot L)^{1.2}$$

$$= 0.01\,(\sqrt{3}/2 \times 20000)^{1.2} \quad \text{where} \quad L = 200 \text{ m}$$

$$= 1200 \ cm^2/s$$

9.3 Estimate of Initial Dilution

The following outlines physical and governing parameters for the Lakeview sewage treatment plant outfall

Discharge Rate (a)	Water Depth	Port Diam.	Port Spacing	# ports	Jet vel.	ℓ/D	H/D
m^3/s	H(m)	D(m)	ℓ(m)		m/s		
2.1	9.5	0.4	12	35	0.48	30	24

The discharge densimetric Froude number is expressed as:

$$F = V/(g'D)^{1/2}$$

$$\text{where } g' = g\frac{\Delta\rho}{\rho_a}$$

For an effluent temperature of 22^{o} and the receiving water temperature of 14^{o} typical temperatures during the summer, g'= 0.0146 and F = 6.3.

As the port's diameter is less than that of the diffuser outfall, the effective Froude number of the jet is usually increased by a factor of about 1.8 (Effect of contraction which mainly increases the jet velocity). Thus, the effective densimetric Froude number is 11.34.

Since the diffuser can be regarded as an alternating diffuser, the near-field flow stability is examined according to equation (27) i.e. $H/D < 1.7\ F^{4/3}\ (\ \ell/D)^{-1/3}$.

The right hand of the above equation is 13.4 which is less than H/D indicating a stable near-field flow.

During winter conditions, when the ambient receiving water of $5^{o}C$ and an effluent temperature of $15^{o}c$ may prevail, the effective densimetric Froude number is about 20. The near-field flow regime in this case may be considered weakly stable.

For stable near-field condition, centreline dilution estimated from nomogram (Figure 14) is 13:1 (an effective relative water depth of $0.8 \times 24 \approx 20$ is considered) The average dilution is $13 \times 1.35 =$ 18.

For the weakly stable condition, it is appropriate to use nomogram to estimate the average initial dilution ratio which will amount to 16:1.

The above estimates are for stagnant or calm conditions.

Under cross flow currents the initial dilution may be estimated according to Roberts' (1979) for the case of a stable nearfield.

Based on a current speed of 10 cm/s perpendicular to the diffuser axis, an initial dilution 55:1 is achieved. As the current magnitude increases, the initial dilution may reach 100:1 or more.

For the weakly stable case, the initial dilution is equivalent to the volume flux ratio, i.e. (UHL/Q) for a current speed of 10 cm/s, a ratio of 95:1 is expected.

The calulations in this appendix use an initial dilution of 13:1 for all current flows. This conservative estimate was obtained by considering the stable nearfield centreline dilution under stagnant conditions.

9.4 Results and Discussions

The results of computer simulations based on the extended Gaussian plume model are presented in Tables 7 - 13 and the contour plots

1.01 - 1.20 as described in Section 9.1. Tables 7 and 8 summarize the summer and winter coastal current climatology near the Lakeview WPCP in the form of a current speed-direction histogram. During both seasons the currents are either mainly shore parallel (233 deg. true) or shore antiparallel (38 deg. true). The alongshore current events persisting for about a day or more and used in the analysis are listed in Tables 9 - 12 together with their duration, average velocity, and frequency of occurence, the latter being summarized in Table 15. The frequency Table 15 shows that the present analysis encompasses 42.2% of the summer and 77.1% of the winter current measurements. These figures would be even higher had alongshore current events persisting for less than a day been regularly included. The present analysis is, therefore, probably valid during most of the winter and much of the summer, however, there will be some current flows, especially during the summer, that will disperse the effluents outside the limits predicted by the present analysis.

For each current regime the reliability of the dilution contours depends upon the number of episodes used to calculate them and their variability. Thus the four current episodes of the 0-5 cm/s speed regime are likely to produce a rougher estimate of the average dilution field than the eight episodes of the 5 - 15 cm/s speed regime. In such cases it is useful to combine the episodes to find the maximum and minimum limits of the average dilution field (see Table 3). On the other hand the very high current episodes are often so similar to each other that the concentration calculated with any one or all of them is about the same (e.g. conservative effluent, winter, shore parallel, speed $\geq$ 15 cm/s).

One of the conclusions that emerges from an examination of the results is that there is a significant difference between the summer and winter current flows. This difference manifests itself in several ways. The summer and winter speed-direction histograms (Tables 7 and 8) indicate that current speeds are smaller and current direction fluctuations larger in the summer than in the winter. There are persistent alongshore currents lasting longer than a day 42.2% of the time in the summer but 77.1% of the time in the winter (Table 15). There are no persistent current episodes

with speeds ≥ 15 cm/s in the summer (Tables 9 - 12). Finally dilution is achieved closer to the source in summer than in winter, possibly because the current meanders more in the summer.

There does not appear to be a significant difference between the dilution characteristics of shore parallel and antiparallel flows. In the summer dilution is achieved slightly closer to the source by shore parallel than by shore antiparallel currents belonging to the same speed range, however, the converse applies to the winter flows (Table 13). For a given speed range the plume size, i.e. the dimensions of an average concentration contour, depends more on the season than the current direction.

10. FUTURE DEVELOPMENTS

This background report has described the coastal zone, some of the simpler and frequently occurring flow regimes, and their dispersion properties. A complete description of the coastal currents, their sources and driving mechanisms, is not yet possible but investigations are continuing at NWRI towards this objective. A computer package and methodology based on the extended Gaussian plume model has been presented. The model package using a limited number of time series current meter measurements or current climatology data, provides an approximate but rapid estimate of the alongshore effluent transport. Present experience suggests two improvements to the computer model.

1) The model is more sensitive to the current direction than the current speed. The accuracy of diffusion field calculations can therefore be improved by resolving the current directions to the nearest 1-2 degrees and the current speeds to the nearest 5 cm/s, i.e. the reverse of present practice.

2) Short duration current episodes, where the plume length is limited by advection rather than diffusion, should be included in the analysis. This can be accomplished by terminating the diffusion field calculation of these episodes at their advective transport limit.

REFERENCES

1. Abraham, G. (1963). Jet Diffusion in Stagnant Ambient Fluid. Delft Hydraulics Laboratory Publ. No. 29.

2. Almquist, C.W., and Stolzenbach, K.D. 1976 Staged Diffusers in Shallow Waters, Technical Report No. 213, R.M. Parsons laboratory for Water Resources and Hydrodynamics, Department of Civil Engineering, Massachusetts of Technology, Cambridge, Mass.

3. Bowden, K. F., D.P. Krauel, and R.E. Lewis (1974). Some Features of Turbulent Diffusion from a continuous source at Sea. Advan. Geophys. 18A, pp 315-329.

4. Brooks, N.H. (1960). Diffusion of Sewage Effluent in an Ocean-Current. Proceedings of the First International Conference on Waste Disposal in the Marine Environment, U.C. at Berkeley, July 22-25, 1959. Edited by E. A. Pearson. Pergamon Press.

5. Brooks, N.H. (1973). Dispersion in Hydraulic and Coastal Environments, Report No. 66013-73-010, U.S. Environmental Protection Agency.

6. Bull, J.A. and R. Farooqui (1976). Coastal Zone Limnological Observations at Bruce Nuclear Power Development. May - Nov. 1974, Joint CCIW/Ontario Hydro Report, CCIW Paper No. 17.

7. Bull, J.A. and D.E. Kaiser (1980). Coastal Zone Limnological Observations in Lake Ontario near Oshawa. May - Nov. 1972 and Dec. 1973 - March, 1974, NWRI Report.

8. Bull, J.A., M. Kerman and O. Lilly (1980). Coastal Current Climatology Summary, Pickering Generating Station, Lake Ontario. NWRI Report.

9. Bull, J.A. and C.R. Murthy (1978). Coastal Zone Climatology of the Great Lakes. Presented at Annual Meeting of the Coastal Society, Great Lakes Basin Committee, 26-27 September, 1978.

10. Bull, J.A. and C.R. Murthy (1980). Climatology and Structure of Coastal Currents in Lake Ontario during Winter Season. NWRI Report.

11. Cederwall, K. (1971). Buoyant Slot Jets into Stagnant or Flowing Environments, Report No. KH-R-25, W. M. Keck Laboratory, California Institute of Technology.

12. Csanady, G.T. (1963). Turbulent Diffusion in Lake Huron. J. Fluid Mech. 17, pp 360-384.

13. Csanady, G.T. (1970). Dispersal of Effluents in the Great Lakes. Water Research. 4, pp 79-114.

14. Csanady, G.T. (1972a). The Coastal Boundary Layer in Lake Ontario. Part 1: The Spring Regime. J. Phys. Oceanogr. 2, pp 41-53.

15. Csanady, G.T. (1972b). The Coastal Boundary Layer in Lake Ontario. Part II: The Summer - Fall Regime. J. Phys. Oceanogr. 2, pp 168-176.

16. Csanady, G.T. and B.H-G. Pade (1970). The Coastal Jet Project-Annual Report 1970. Contract Report to C.C.I.W.

17. Csanady, G.T. and B.H-G. Pade (1971). The Coastal Jet Project - Annual Report 1971. Contract Report to C.C.I.W.

18. Csanady, G.T. and B.H-G. Pade (1972). The Coastal Jet Project - Annual Report 1972. IFYGL Project No. 40 WM.

19. Fan, L.-N. (1967). Turbulent Buoyant Jets into Stratified or Flowing Ambient Fluids. W.M. Keck Laboratory Report KH-R-15, California Institute of Technology, Pasadena, California.

20. Fan, L.-N. and N.H. Brooks (1969). Numerical Solutions of Turbulent Buoyant Jet Problems. W.M. Keck Laboratory Report KH-R-18, California Institute of Technology, Pasadena, California.

21. Fischer, H.B., E.J. List, R.C.Y. Koh, J. Imberger, and N.H. Brooks (1979). Mixing in Inland and Coastal Waters. Academic Press.

22. Gifford, F. (1959). Statistical Properties of a Fluctuating Plume Dispersion Model. Advan. Geophys. 6, 117-137.

23. Hamdy, Y.S. (1981). Initial Mixing Processes state-of-the- Art and Applications to Diffuser Outfall Design. Proc. Can. Society of Civil Eng., Dept. of Civil Eng., Univ. of Windsor, Ontario, 24 Apr. 1981.

24. Hildebrand, F.B. (1965). Methods of Applied Mathematics. Prentice - Hall.

25. Hinze, J.O. (1959). Turbulence, An Introduction to Its Mechanism and Theory. McGraw-Hill.

26. Jirka, G., and Harleman, D.R.F. (1973). The Mechanics of Submerged Multiport Diffusers for Buoyant Discharges in Shallow Water, Technical Report No. 169, R.M. Parsons Laboratory for Water Resources and Hydrodynamics, Department of Civil Engineering, Massachusetts Institute of Technology, Cambridge, Mass.

27. Jordan, D.E. and J.A. Bull (1977). Coastal Zone Limnological Observations in Lake Ontario at Bronte. June 1973 - March 1974, CCIW Paper No. 18.

28. Kaiser, D.E. and J.A. Bull (1978a). Coastal Zone Limnological Observations in Georgian Bay near Byng Inlet, Nov. 1975 - Nov. 1976, CCIW Paper No. 19.

29. Kaiser, D.E. and J.A. Bull (1978b). Coastal Zone Limnological Observations in Lake Ontario at Oshawa. CCIW Paper No. 20.

30. Kohli, B.S. and M.D. Palmer (1973). Assessment of a Waste Outfall Location 1970-72. Proc. 16th Conf. Great Lakes Res, pp 754-773. Internat, Assoc. Great Lakes Res.

31. Kohli, B. (1976a). Water Movements in Thunder Bay 1970-73. Ontario Ministry of the Environment, Toronto, Ontario. 27 p.

32. Kohli, B. (1976b). Assessment of the Proposed Lorne Park Intake and Clarkson Outfall Lake Ontario, 1974. Ontario Ministry of the Environment, Toronto, Ontario, 29 p.

33. Kohli, B. (1981). Dispersion of Effluent Plumes from Diffusers on Near-Shore Regions of the Great Lakes, Vol. II, Surface Dilution. Ontario Ministry of the Environment, Toronto, Ontario. 21 p.

34. Kohli, B. and R. Farooqui, 1980. Nanticoke Water Movements 1967-1978. Ontario Ministry of the Environment, Toronto, Ontario, 69 p.

35. Lam, D.C. and R.C. Murthy (1978). Outfall Diffusion Models for the Coastal Zone. Proc. of the 16th Coastal Engineering Conference. ASCE. Chapter 156, pp 2584-2597.

36. Lee, J.H., Jirka, G.H., and Harleman, D.R.F. 1977, Modelling of Unidirectional Thermal Diffusers in Shallow Water, Report No. MIT-EL-77-016, U.S. Department of Commerce National Technical Information Service.

37. Murthy, C.R. and G.T. Csanady (1971). Experimental Studies of Relative Diffusion in Lake Huron. J. Phys. Oceanogo. 1, pp 17-24.

38. Murthy, C.R. (1972). Complex Diffusion Processes in Coastal Currents of a Lake. J. Phys. Oceanogr., Vol. 2, pp 80-90.

39. Murthy, C.R. (1974). Simulated Outfall Diffusion Experiments in Coastal Currents of a Lake. Water Research, 8, pp 961-967.

40. Murthy, C.R. (1976). Horizontal Diffusion Characteristics in Lake Ontario. J. Phys. Oceanogr. 6, pp 76-84.

41. Murthy, C.R. and B.C. Kenney (1974). Diffusion in Coastal Currents of Large Lakes. Rapp. P.-V. Reun. Cons. Int. Explor. Mer, 167, pp 111-120.

42. Murthy, C.R. and D.S. Dunbar (1977). Coastal Boundary Layer Characteristics at Douglas Point, Lake Huron. CCIW Unpublished Manuscript.

43. Murthy, C.R. and K.C. Miners (1978). Turbulent Diffusion Processes in the Great Lakes. Inland Waters Diectorate Scientific Series No. 83.

44. Murthy, C.R. and K.C. Miners (1980). Meandering effects on the Diffusion of Continuous Dye Plumes in Coastal Currents. J. Great Lakes Res. 6(1), pp 88-93.

45. Okubo, A. (1971). Oceanic Diffusion Diagrams. Deep-Sea Research, 18, pp 789-802.

46. Okubo, A. (1976). Remarks on the use of 'Diffusion Diagrams' in Modelling Scale-Dependent Diffusion. Deep Sea Research, 23, pp 1213-1214.

47. Roberts, P.J.W. (1977). Dispersion of Buoyant Waste Water Discharged from Outfall Diffusers of Finite Length. W.M. Keck Laboratory Report KH-R-35, California Institute of Technology Pasadena, California.

48. Roberts, P.J.W. (1979). Line Plume and Ocean Outfall Dispersion. Journal of the Hydraulics Division, ASCE, 105(HY4), pp 313-331.

49. Roberts, P.J.W. (1980). Ocean Outfall Dilution: Effects of Currents. Journal of the Hydraulics Division, ASCE, 106(HY5), pp 769-782.

TABLE 1

A summary of the diffusion characteristics and lateral spreading of an effluent plume from a line source in a steady current.

Diffusion Model	Diffusion Law	Diffusion Parameters	Plume Width	Centreline Concentration
Fickian	K = constant	constant diffusivity	$\frac{L}{b} = \left(1+\frac{\gamma x}{b}\right)^{1/2} \sim x^{1/2}$	$\frac{L}{b} = \text{erf}\sqrt{\frac{3/2}{\left(1+\frac{\gamma x}{b}\right) - 1}} \sim x^{-1/2}$
Shear	$K = U^* L$	L = length scale U^* = diffusion velocity	$\frac{L}{b} = \left(1+\frac{\gamma x}{2b}\right) \sim x$	$\frac{L}{b} = \text{erf}\sqrt{\frac{3/2}{\left(1+\frac{\gamma x}{2b}\right)^2 - 1}} \sim x^{-1}$
Inertial subrange	$K = L^{4/3} \cdot \epsilon^{1/3}$	L = length scale ϵ = energy dissipation parameter	$\frac{L}{b} = \left(1+\frac{\gamma x}{3b}\right)^{3/2} \sim x^{3/2}$	$\frac{L}{b} = \text{erf}\sqrt{\frac{3/2}{\left(1+\frac{\gamma x}{3b}\right)^3 - 1}} \sim x^{-3/2}$

L = width of effluent plume

x = distance downstream from line source

u = current speed

b = width or length of line source

K_o = diffusion coefficient associated with b

$\gamma = \frac{24K_o}{ub}$

TABLE 2

CONSERVED (WINTER). LAKE ONTARIO DATA. PICKERING. SHORE ANTIPARALLEL CURRENT.

FIRST DAY 80/ 1/18 MOORING: 79-00C-06S
FINAL DAY 80/ 1/29 DEPTH: 12 M.

SHORELINE ORIENTATION IN DEGREES TRUE SPECIFIED AS 250

DIRECTION FLOW TOWARD		PERCENT OBSERVED				MAXIMUM CURRENT	MEAN DURATION	MEAN EXCURSION	MEAN CURRENT	MEAN TEMP	
WRT SHORE	DEG TRUE	TOTAL	LIGHT	MEDIUM	HIGH	CM/S	HOURS	KM	CM/S	DEG C	
0.0	250.0	0.0	0.0	0.0	0.0	0.0	0.0	0.0	0.0	0.0	PARALLEL
5.0	245.0	0.0	0.0	0.0	0.0	0.0	0.0	0.0	0.0	0.0	
10.0	240.0	0.0	0.0	0.0	0.0	0.0	0.0	0.0	0.0	0.0	
15.0	235.0	0.0	0.0	0.0	0.0	0.0	0.0	0.0	0.0	0.0	
20.0	230.0	0.0	0.0	0.0	0.0	0.0	0.0	0.0	0.0	0.0	
25.0	225.0	0.0	0.0	0.0	0.0	0.0	0.0	0.0	0.0	0.0	
30.0	220.0	0.0	0.0	0.0	0.0	0.0	0.0	0.0	0.0	0.0	
35.0	215.0	0.0	0.0	0.0	0.0	0.0	0.0	0.0	0.0	0.0	
40.0	210.0	0.0	0.0	0.0	0.0	0.0	0.0	0.0	0.0	0.0	
45.0	205.0	0.0	0.0	0.0	0.0	0.0	0.0	0.0	0.0	0.0	
50.0	200.0	.4	0.0	.4	0.0	10.1	1.0	.4	10.1	0.0	
55.0	195.0	0.0	0.0	0.0	0.0	0.0	0.0	0.0	0.0	0.0	
60.0	190.0	0.0	0.0	0.0	0.0	0.0	0.0	0.0	0.0	0.0	
65.0	185.0	0.0	0.0	0.0	0.0	0.0	0.0	0.0	0.0	0.0	
70.0	180.0	0.0	0.0	0.0	0.0	0.0	0.0	0.0	0.0	0.0	
75.0	175.0	0.0	0.0	0.0	0.0	0.0	0.0	0.0	0.0	0.0	
80.0	170.0	.4	.4	0.0	0.0	1.7	1.0	.1	1.7	0.0	
85.0	165.0	0.0	0.0	0.0	0.0	0.0	0.0	0.0	0.0	0.0	
90.0	160.0	.4	.4	0.0	0.0	2.0	1.0	.1	2.0	0.0	OFFSHORE
95.0	155.0	0.0	0.0	0.0	0.0	0.0	0.0	0.0	0.0	0.0	
100.0	150.0	0.0	0.0	0.0	0.0	0.0	0.0	0.0	0.0	0.0	
105.0	145.0	1.1	.7	.4	0.0	9.8	1.5	.3	5.6	0.0	
110.0	140.0	1.1	.7	0.0	.4	15.9	1.5	.4	8.0	0.0	
115.0	135.0	1.1	.7	.4	0.0	5.8	1.0	.1	4.0	0.0	
120.0	130.0	0.0	0.0	0.0	0.0	0.0	0.0	0.0	0.0	0.0	
125.0	125.0	2.9	.4	.4	2.2	21.3	1.1	.6	15.1	0.0	
130.0	120.0	13.0	0.0	4.0	9.1	23.4	1.6	1.0	16.4	0.0	
135.0	115.0	18.8	.7	10.9	7.2	24.9	2.3	1.2	14.8	0.0	
140.0	110.0	15.9	1.1	12.0	2.9	22.0	1.4	.6	12.7	0.0	
145.0	105.0	10.1	0.0	10.1	0.0	14.1	1.8	.7	10.4	0.0	
150.0	100.0	10.9	.7	10.1	0.0	14.6	1.6	.5	8.2	0.0	
155.0	95.0	7.6	.4	5.4	1.8	16.4	1.6	.7	11.4	0.0	
160.0	90.0	5.8	.4	4.7	.7	16.4	2.0	.7	9.2	0.0	
165.0	85.0	4.0	.4	3.6	0.0	9.6	1.6	.4	6.8	0.0	
170.0	80.0	3.6	0.0	3.6	0.0	10.5	1.4	.4	7.5	0.0	
175.0	75.0	1.4	0.0	1.4	0.0	10.1	1.3	.4	8.7	0.0	
180.0	70.0	0.0	0.0	0.0	0.0	0.0	0.0	0.0	0.0	0.0	ANTIPARA
185.0	65.0	0.0	0.0	0.0	0.0	0.0	0.0	0.0	0.0	0.0	
190.0	60.0	0.0	0.0	0.0	0.0	0.0	0.0	0.0	0.0	0.0	
195.0	55.0	0.0	0.0	0.0	0.0	0.0	0.0	0.0	0.0	0.0	
200.0	50.0	.4	0.0	0.0	.4	15.5	1.0	.6	15.5	0.0	
205.0	45.0	0.0	0.0	0.0	0.0	0.0	0.0	0.0	0.0	0.0	
210.0	40.0	0.0	0.0	0.0	0.0	0.0	0.0	0.0	0.0	0.0	
215.0	35.0	0.0	0.0	0.0	0.0	0.0	0.0	0.0	0.0	0.0	
220.0	30.0	0.0	0.0	0.0	0.0	0.0	0.0	0.0	0.0	0.0	
225.0	25.0	0.0	0.0	0.0	0.0	0.0	0.0	0.0	0.0	0.0	
230.0	20.0	0.0	0.0	0.0	0.0	0.0	0.0	0.0	0.0	0.0	
235.0	15.0	0.0	0.0	0.0	0.0	0.0	0.0	0.0	0.0	0.0	
240.0	10.0	0.0	0.0	0.0	0.0	0.0	0.0	0.0	0.0	0.0	
245.0	5.0	0.0	0.0	0.0	0.0	0.0	0.0	0.0	0.0	0.0	
250.0	0.0	0.0	0.0	0.0	0.0	0.0	0.0	0.0	0.0	0.0	
255.0	355.0	0.0	0.0	0.0	0.0	0.0	0.0	0.0	0.0	0.0	
260.0	350.0	0.0	0.0	0.0	0.0	0.0	0.0	0.0	0.0	0.0	
265.0	345.0	0.0	0.0	0.0	0.0	0.0	0.0	0.0	0.0	0.0	
270.0	340.0	0.0	0.0	0.0	0.0	0.0	0.0	0.0	0.0	0.0	ON SHORE
275.0	335.0	0.0	0.0	0.0	0.0	0.0	0.0	0.0	0.0	0.0	
280.0	330.0	0.0	0.0	0.0	0.0	0.0	0.0	0.0	0.0	0.0	
285.0	325.0	0.0	0.0	0.0	0.0	0.0	0.0	0.0	0.0	0.0	
290.0	320.0	0.0	0.0	0.0	0.0	0.0	0.0	0.0	0.0	0.0	
295.0	315.0	0.0	0.0	0.0	0.0	0.0	0.0	0.0	0.0	0.0	
300.0	310.0	0.0	0.0	0.0	0.0	0.0	0.0	0.0	0.0	0.0	
305.0	305.0	0.0	0.0	0.0	0.0	0.0	0.0	0.0	0.0	0.0	
310.0	300.0	0.0	0.0	0.0	0.0	0.0	0.0	0.0	0.0	0.0	
315.0	295.0	0.0	0.0	0.0	0.0	0.0	0.0	0.0	0.0	0.0	
320.0	290.0	0.0	0.0	0.0	0.0	0.0	0.0	0.0	0.0	0.0	
325.0	285.0	.4	0.0	.4	0.0	10.1	1.0	.4	10.1	0.0	
330.0	280.0	0.0	0.0	0.0	0.0	0.0	0.0	0.0	0.0	0.0	
335.0	275.0	0.0	0.0	0.0	0.0	0.0	0.0	0.0	0.0	0.0	
340.0	270.0	0.0	0.0	0.0	0.0	0.0	0.0	0.0	0.0	0.0	
345.0	265.0	.7	0.0	.7	0.0	10.1	2.0	.7	10.1	0.0	
350.0	260.0	0.0	0.0	0.0	0.0	0.0	0.0	0.0	0.0	0.0	
355.0	255.0	0.0	0.0	0.0	0.0	0.0	0.0	0.0	0.0	0.0	

MEAN SCALAR SPEED = 11.8 CM/S MEAN SQUARE SPEED = 164.0 CM2/S2 VARIANCE = 36.7 CM2/S2

MEAN VELOCITY = 11.3 CM/S, 109 DEG TRUE MEAN TEMPERATURE = 0.0 C TOTAL HOURS = 276

SPEED RANGES
LIGHT= 0.0 - 5.0 MEDIUM= 5.0 - 15.0 HIGH=> 15.0 CM/S

TABLE 3

CURRENT SPEED-DIRECTION HISTOGRAM (TO THE NEAREST TENTH OF A PERCENT)

CONSERVED (WINTER). LAKE ONTARIO DATA. PICKERING. SHORE ANTIPARALLEL CURRENT.

CURRENT VECTORS = 276 TOTAL
SECTOR INCREMENT = 5.0 DEGREES
SPEED INCREMENT = 1.0 CM/SEC.

SPEED BIN 1 HOLDS 0-1 CM/SEC EVENTS, ETC.
SPEED BIN 51 HOLDS >50 CM/SEC EVENTS.

SECTOR DIRECTIONS ARE LABELLED ANTICLOCKWISE STARTING FROM THE 250 DEGREE SHORELINE

CURRENT EVENTS ARE WEIGHTED AVERAGED OVER THE NEAREST NEIGHBOUR SPEED AND DIRECTION BINS.
HENCE THERE MAY BE SOME ROUND OFF ERRORS IN THE INTEGRAL DISPLAY OF THE HISTOGRAM BELOW.

SPEED BIN > / SECTOR !	SUM	1	2	3	4	5	6	7	8	9	10	11	12	13	14	15	16	17	18	19	20	21	22	23	24	25	26	
0.0																												
5.0																												PARALLEL
10.0																												
15.0																												
20.0																												
25.0																												
30.0																												
35.0																												
40.0																												
45.0																												
50.0	3										1	2																
55.0																												
60.0																												
65.0																												
70.0																												
75.0																												
80.0	3		3	1																								
85.0																												
90.0	4		2	2																								
95.0																												OFFSHORE
100.0	1																											
105.0	10			3	2	2					2	1																
110.0	10				2	4											2	1										
115.0	12			3	5		3	1																				
120.0	2					1	1																					
125.0	26					4	2										2	7	2		3	2	2					
130.0	120								2	1	3	1		9	16	6	19	20	5	6	13	10	4	2	3			
135.0	193				2	3	4		2		4	8	9	32	18	27	17	2	5	13	17	18	4	3		6	1	
140.0	172		3	1	2	8	8	4	3	8	6	11	22	16	18	28	7	1	2	4	9	8	2	2				
145.0	109					1	7	8	7	7	24	14	17	5	13	5												
150.0	90			2		4	18	15	7	4	14	9	5	2	3	5	1											
155.0	78			1		3	9	6	3	2	7	5	6	5	5	8	12	6										
160.0	61					3	6	7	11	10	9	3	3	3	1		3	4										
165.0	48					4	8	13	10	4	5	1		1			1											
170.0	32					1	3	12	4		5	6																
175.0	13						2	2		1	6	2																
180.0																												
185.0																												ANTIPARA
190.0																												
195.0																												
200.0	3																3											
205.0																												
210.0																												
215.0																												
220.0																												
225.0																												
230.0																												
235.0																												
240.0																												
245.0																												
250.0																												
255.0																												
260.0																												
265.0																												
270.0																												ON SHORE
275.0																												
280.0																												
285.0																												
290.0																												
295.0																												
300.0																												
305.0																												
310.0																												
315.0																												
320.0																												
325.0	4										1	2																
330.0																												
335.0																												
340.0																												
345.0	6										2	3																
350.0	1											1																
355.0																												
TOTAL	1000	8	13	14	38	70	68	49	37	91	71	62	72	74	79	67	42	13	24	41	39	12	7	3	6	1		

TABLE 4

COMPUTED MEAN CONCENTRATION FIELD
(BASED ON CURRENT SPEED-DIRECTION HISTOGRAM)

TITLE CARD- CONSERVED (WINTER). LAKE ONTARIO DATA. PICKERING. SHORE ANTIPARALLEL CURRENT.

FIRST DAY 80/ 1/18
FINAL DAY 80/ 1/29

I/O DATA		
DIFFUSION CONSTANT	1000.00	CM**2/SEC
SOURCE DISCHARGE RATE	2000.00	L/SEC.
DISCHARGE VELOCITY	50.00	CM/SEC.
DENSITY DIFFERENCE	1.50	PPT.
SOURCE DILUTION RATIO	10.0	(TO 1.0)
MEAN CURRENT SPEED	11.8	CM/SEC.
DIFFUSION LAYER	1.1	M THICK.
DIFFUSER DEPTH	10.0	M.
DIFFUSER LENGTH	200.0	M.
DIFFUSER ANGLE	160.0	DEGREES
SHORELINE ANGLE	250.0	DEGREES
DIFFUSER -SHORE ANGLE	90.0	DEGREES
DISTANCE OFFSHORE	1.3	KM.

MAXIMUM COMPONENTS OF THE CURRENT VECTOR SUM

PARALLEL	1.23	KM.
OFF SHORE	71.42	KM.
ANTIPARALLEL	88.02	KM.
ON SHORE	.39	KM.

CURRENT HISTOGRAM DATA

CURRENT VECTORS	276	TOTAL
SECTOR INCREMENT	5.0	DEGREES
SPEED INCREMENT	1.0	CM/SEC.

THE DIFFUSIVITY INCREASES AS THE 4/3 POWER OF THE SCALE OF THE DIFFUSION FIELD

CONCENTRATIONS ARE NORMALIZED TO SOURCE CONCENTRATION
VALUES PRESENTED ARE 10**4 TIMES ACTUAL VALUES

DIRECTION WRT SHORE	DISTANCE> DEG TRUE	1000.0	2000.0	3000.0	4000.0	5000.0	6000.0	7000.0	8000.0	9000.0	10000.0	M.	ESTIMATED CURRENT RANGE KM.
0.0	250.0	.1	.0	.0	.0	.0	0.0	0.0	0.0	0.0	0.0	PARALLEL	0.00
5.0	245.0	.0	0.0	0.0	0.0	0.0	0.0	0.0	0.0	0.0	0.0		0.00
10.0	240.0	.0	0.0	0.0	0.0	0.0	0.0	0.0	0.0	0.0	0.0		0.00
15.0	235.0	0.0	0.0	0.0	0.0	0.0	0.0	0.0	0.0	0.0	0.0		0.00
20.0	230.0	0.0	0.0	0.0	0.0	0.0	0.0	0.0	0.0	0.0	0.0		0.00
25.0	225.0	0.0	0.0	0.0	0.0	0.0	0.0	0.0	0.0	0.0	0.0		0.00
30.0	220.0	.0	0.0	0.0	0.0	0.0	0.0	0.0	0.0	0.0	0.0		0.00
35.0	215.0	.0	0.0	0.0	0.0	0.0	0.0	0.0	0.0	0.0	0.0		0.00
40.0	210.0	.2	.0	.0	.0	.0	0.0	0.0	0.0	0.0	0.0		0.00
45.0	205.0	2.0	.5	.2	.1	.0	.0	.0	.0	.0	.0		0.00
50.0	200.0	3.4	2.8	2.3	1.9	1.6	1.4	1.2	1.1	1.0	.9		0.00
55.0	195.0	2.3	.8	.4	.2	.2	.2	.1	.1	.1	.1		0.00
60.0	190.0	.5	.1	.0	.0	.0	.0	.0	.0	.0	.0		0.00
65.0	185.0	.4	.1	.1	.1	.0	.0	.0	.0	.0	.0		0.00
70.0	180.0	1.0	.4	.3	.2	.2	.2	.1	.1	.1	.1		0.00
75.0	175.0	2.0	1.0	.7	.5	.4	.3	.3	.2	.2	.2		0.00
80.0	170.0	3.0	1.6	1.1	.8	.6	.5	.4	.4	.3	.3		0.00
85.0	165.0	3.5	1.9	1.3	.9	.7	.6	.5	.4	.4	.3		0.00
90.0	160.0	3.6	1.8	1.2	.9	.7	.6	.5	.4	.4	.3		0.00
95.0	155.0	4.4	1.7	1.1	.8	.7	.6	.5	.4	.4	.3	OFFSHORE	0.00
100.0	150.0	8.9	3.5	2.0	1.5	1.2	1.0	.8	.7	.7	.6		0.00
105.0	145.0	16.7	8.8	6.2	4.9	4.0	3.4	3.0	2.6	2.3	2.1		0.00
110.0	140.0	20.5	11.9	8.5	6.7	5.6	4.7	4.1	3.7	3.3	3.0		0.00
115.0	135.0	18.3	8.7	5.8	4.3	3.5	2.9	2.4	2.1	1.9	1.7		0.00
120.0	130.0	29.2	7.9	4.3	3.1	2.5	2.1	1.8	1.6	1.4	1.3		0.00
125.0	125.0	112.7	35.2	22.5	18.6	16.3	14.6	13.1	11.9	10.9	10.1		0.00
130.0	120.0	267.6	135.9	106.1	91.9	81.6	73.2	66.2	60.2	55.1	50.7		23.99
135.0	115.0	379.8	207.7	162.8	140.0	123.4	110.2	99.2	90.0	82.1	75.4		85.31
140.0	110.0	362.4	183.0	135.4	112.8	97.4	85.7	76.4	68.7	62.2	56.8		112.15
145.0	105.0	273.4	129.4	89.4	71.0	59.5	51.2	44.9	39.9	35.8	32.3		72.74
150.0	100.0	209.5	96.4	64.4	50.0	41.2	35.0	30.4	26.8	23.9	21.6		16.56
155.0	95.0	175.7	92.3	66.4	53.5	45.2	39.2	34.6	30.9	27.9	25.3		9.06
160.0	90.0	143.5	69.3	47.7	37.5	31.1	26.6	23.2	20.6	18.4	16.7		5.54
165.0	85.0	104.4	51.6	34.6	26.4	21.4	18.0	15.5	13.6	12.1	10.9		2.58
170.0	80.0	70.0	35.8	24.4	18.7	15.3	12.9	11.1	9.8	8.7	7.8		.73
175.0	75.0	36.5	16.9	11.3	8.7	7.1	6.0	5.2	4.6	4.1	3.7		0.00
180.0	70.0	11.6	2.9	1.2	.7	.5	.4	.3	.3	.3	.2	ANTIPARA	0.00
185.0	65.0	1.5	.1	.1	.0	.0	.0	.0	.0	.0	.0		0.00
190.0	60.0	.2	.0	.0	.0	.0	.0	.0	.0	.0	.0		0.00
195.0	55.0	2.1	.3	.0	.0	.0	.0	.0	.0	.0	.0		0.00
200.0	50.0	3.5	3.1	2.7	2.4	2.2	1.9	1.7	1.6	1.4	1.3		0.00
205.0	45.0	2.4	.6	.3	.2	.2	.2	.2	.1	.1	.1		0.00
210.0	40.0	.3	.0	.0	.0	.0	.0	.0	.0	.0	.0		0.00
215.0	35.0	.0	.0	0.0	0.0	0.0	0.0	0.0	0.0	0.0	0.0		0.00
220.0	30.0	.0	0.0	0.0	0.0	0.0	0.0	0.0	0.0	0.0	0.0		0.00
225.0	25.0	0.0	0.0	0.0	0.0	0.0	0.0	0.0	0.0	0.0	0.0		0.00
230.0	20.0	0.0	0.0	0.0	0.0	0.0	0.0	0.0	0.0	0.0	0.0		0.00
235.0	15.0	0.0	0.0	0.0	0.0	0.0	0.0	0.0	0.0	0.0	0.0		0.00
240.0	10.0	0.0	0.0	0.0	0.0	0.0	0.0	0.0	0.0	0.0	0.0		0.00
245.0	5.0	0.0	0.0	0.0	0.0	0.0	0.0	0.0	0.0	0.0	0.0		0.00
250.0	0.0	0.0	0.0	0.0	0.0	0.0	0.0	0.0	0.0	0.0	0.0		0.00
255.0	355.0	0.0	0.0	0.0	0.0	0.0	0.0	0.0	0.0	0.0	0.0		0.00
260.0	350.0	0.0	0.0	0.0	0.0	0.0	0.0	0.0	0.0	0.0	0.0		0.00
265.0	345.0	0.0	0.0	0.0	0.0	0.0	0.0	0.0	0.0	0.0	0.0		0.00
270.0	340.0	0.0	0.0	0.0	0.0	0.0	0.0	0.0	0.0	0.0	0.0		0.00
275.0	335.0	0.0	0.0	0.0	0.0	0.0	0.0	0.0	0.0	0.0	0.0	ON SHORE	0.00
280.0	330.0	0.0	0.0	0.0	0.0	0.0	0.0	0.0	0.0	0.0	0.0		0.00
285.0	325.0	0.0	0.0	0.0	0.0	0.0	0.0	0.0	0.0	0.0	0.0		0.00
290.0	320.0	0.0	0.0	0.0	0.0	0.0	0.0	0.0	0.0	0.0	0.0		0.00
295.0	315.0	0.0	0.0	0.0	0.0	0.0	0.0	0.0	0.0	0.0	0.0		0.00
300.0	310.0	0.0	0.0	0.0	0.0	0.0	0.0	0.0	0.0	0.0	0.0		0.00
305.0	305.0	.0	0.0	0.0	0.0	0.0	0.0	0.0	0.0	0.0	0.0		0.00
310.0	300.0	.0	0.0	0.0	0.0	0.0	0.0	0.0	0.0	0.0	0.0		0.00
315.0	295.0	.2	.0	.0	.0	.0	0.0	0.0	0.0	0.0	0.0		0.00
320.0	290.0	2.2	.6	.2	.1	.0	.0	.0	.0	.0	.0		0.00
325.0	285.0	3.5	2.9	2.5	2.1	1.8	1.5	1.4	1.2	1.1	1.0		0.00
330.0	280.0	2.2	.6	.2	.1	.0	.0	.0	.0	.0	.0		0.00
335.0	275.0	.8	.1	.0	.0	.0	.0	.0	.0	.0	.0		0.00
340.0	270.0	3.9	1.2	.5	.3	.2	.2	.1	.1	.1	.1		0.00
345.0	265.0	6.4	4.9	4.0	3.4	2.9	2.5	2.2	1.9	1.7	1.6		0.00
350.0	260.0	4.6	1.9	1.1	.8	.6	.5	.5	.4	.4	.3		0.00
355.0	255.0	1.1	.2	.1	.0	.0	.0	.0	.0	.0	.0		0.00

RELATIVE CENTRELINE DECAY AND DIFFUSION AT MEAN CURRENT SPEED INTO AN ADJACENT CURRENT OR DIFFUSION FIELD SECTOR (100% SOURCE)

5.0	61.3	13.8	3.6	1.3	.6	.3	.2	.1	.1	.1	CURRENT SECTOR
0.0	97.5	85.7	73.4	63.1	54.8	48.2	42.7	38.2	34.5	31.3	CENTRELINE
5.0	61.3	13.8	3.6	1.3	.6	.3	.2	.1	.1	.1	DIFFUSION SECTOR

TABLE 5

Location 043 Operating Log

Location: 79° 31' 54"W; 43° 34' 08"N

Depth of Water: 31.0 feet (9.5 m.)

Depth of Current Meter 9.8 feet (3.0 m) from bottom

Current Meter Details: Serial # 144 and 272, Plessey M021

Date	Time (Hours) In	Out	Service
May 21	1409		Meter installed
Jun 8	1020	1005	Meter checked and found O.K.
Jun 12			Drogue trackings
June 25			Drogue trackings
Jul 2			Drogue trackings
Jul 21	0945	0955	Meter working O.K.
Jul 30	1210	1200	Meter O.K., drogue trackings
Aug 13	1235	1220	Meter changed, drogue trackings
Sep 30	1240	1155	Changed bearings, "O" ring, battery, dessicator and tape. Drogue trackings.
(1971) Dec 9	1440		Meter installed
Dec 15			Surveyed spar
(1972) Feb 9			Drogue trackings
Mar 27		1155	Meter removed

TABLE 6

Summary of Current Meter Results, in the Vicinity of Lakeview WPCP outfall

	Jun 70	Jul 70	Aug 70	Sep 70	Oct 70	Nov 70	Dec 71	Jan 72	Feb 72	Mar 72
Result and direction (0^{o} North)	100	109	176	60	189	68	62	56	57	223
Resultant speed (cm/s)	1.38	0.34	1.24	1.06	0.83	2.31	1.81	5.43	0.44	1.24
Average speed (cm/s)	3.49	2.30	5.39	4.36	4.26	6.06	6.91	7.51	4.55	3.62
Maximum speed (cm/s)	20	14	20	20	17	27	34	29	24	29
Persistence factor	0.39	0.15	0.23	0.24	0.19	0.38	0.26	0.72	0.10	0.34
Percentage of time going in direction of resultant	4	2	4	12	1	13	23	41	18	19
Percentage of time going towards R. L. Clark Intake	5	10	6	12	13	25	23	41	18	12
Total number of readings	4312	4007	4461	4311	4464	4317	1584	2232	2088	1986
Interval of readings (min)	10	10	10	10	10	10	20	20	20	20
Percentage of negligible* speed (% of recording period)	14	25	8	15	10	8	7	9	32	38

TABLE 7

CURRENT SPEED-DIRECTION HISTOGRAM (TO THE NEAREST TENTH OF A PERCENT)

CONSERVED (SUMMER). ALL MOE SUMMER LAKEVIEW DATA. MAY 1,1970 - OCT 31,1970.

CURRENT VECTORS - 3822 TOTAL
SECTOR INCREMENT - 5.0 DEGREES
SPEED INCREMENT - 1.0 CM/SEC.

SPEED BIN 1 HOLDS 0-1 CM/SEC EVENTS, ETC.
SPEED BIN 51 HOLDS >50 CM/SEC EVENTS.

SECTOR DIRECTIONS ARE LABELLED ANTICLOCKWISE STARTING FROM THE 225 DEGREE SHORELINE

CURRENT EVENTS ARE WEIGHTED AVERAGED OVER THE NEAREST NEIGHBOUR SPEED AND DIRECTION BINS.
HENCE THERE MAY BE SOME ROUND OFF ERRORS IN THE INTEGRAL DISPLAY OF THE HISTOGRAM BELOW.

SPEED / SECTOR	BIN > SUM	1	2	3	4	5	6	7	8	9	10	11	12	13	14	15	16	17	18	19	20	21	
0.0	28	4	2	2	1	2	1	1	4	2	1	1	2	2	1								PARALLEL
5.0	18	5	1	1	1	1	1	1	1	1	1	1											
10.0	17	3	2	2	2	2	1	3	2														
15.0	14	4	2	1	1	1	1	1	1														
20.0	14	4	2	2	2	1	1	1															
25.0	13	5	2	2	1	1	1	1															
30.0	11	4	1	1	1	1	1	1	1														
35.0	7	3	1	1	1	1																	
40.0	9	3	2	1	1	2																	
45.0	10	5	2	1		1	1																
50.0	7	4	1	1		1	1																
55.0	7	4	1	1																			
60.0	7	2	2	1	1		1																
65.0	7	3	1	1	1	1																	
70.0	7	4	1	1																			
75.0	8	5	2	1																			
80.0	7	3	2	1																			
85.0	6	2	2	1				1															
90.0	9	4	1	1	1																		OFFSHORE
95.0	8	4	2	1	1																		
100.0	8	4	2	1																			
105.0	11	6	2	1																			
110.0	7	3	2	1																			
115.0	9	4	2	1																			
120.0	8	4	2	1	1																		
125.0	11	5	2	1	1	1																	
130.0	10	4	2	1	1	1																	
135.0	13	7	2	1	1	1																	
140.0	12	7	2	1	1	1	1																
145.0	12	4	2	1	1	1	1	1	1														
150.0	12	4	1	2	1	1	1																
155.0	12	4	2	2	1	1	1																
160.0	16	4	3	3	2	2	1	1															
165.0	16	4	3	2	1	1	1	1	2														
170.0	17	4	1	2	2	2	1	1	1	1	1	1	1										
175.0	30	9	4	2	2	1	1	1	1	2	2	1	1	1									
180.0	40	9	4	3	2	2	2	2	3	2	2	2	2	1	1								ANTIPARA
185.0	51	9	3	3	4	3	4	4	4	4	4	1	3	2	1	1	1						
190.0	54	9	4	5	4	5	5	5	4	5	2	1	2	1									
195.0	51	9	5	6	7	6	4	4	4	3	1		1	1									
200.0	37	5	4	5	7	5	4	3	1	1	1					1							
205.0	29	7	4	4	5	4	1	1					1										
210.0	19	4	4	3	2	3	1	1	1														
215.0	13	4	2	1	1	1					1	1											
220.0	7	1	1	1	1																		
225.0	2	1																					
230.0	3	2	1	1																			
235.0	2	1																					
240.0	3	1		1																			
245.0	5	2	1	1		1																	
250.0	4	1		1			1																
255.0	4	1	1	1																			
260.0	4	2		1		1																	
265.0	4	1	1			1																	ON SHORE
270.0	6	2	1			1	1																
275.0	5	1	1	1																			
280.0	6	1	1	1	1	1	1	1						1									
285.0	8	3		1	2	1	1																
290.0	7	2		1	1	1	1																
295.0	9	2	1	1	1	1	1	1	1														
300.0	7	2	1	1	1	1	1	1															
305.0	9	3	2	1	1	1	1																
310.0	8	2	1	1	1	1		1	1														
315.0	11	3	2	1	1	1	1	1	1														
320.0	11	2	2	2	2	1	1		1														
325.0	11	2	1	2	2	1	1		1		1												
330.0	14	4	1	1	1	1	1	1	1	1	1												
335.0	19	3	1	2	2	2	2	2	1	1	1												
340.0	23	4	1	2	3	2	3	3	1		1	2				1							
345.0	27	4	2	2	2	2	3	2	3	2	2	2	1										
350.0	35	5	2	3	3	4	3	4	3	2	2	2	1		1								
355.0	33	3	1	3	2	3	3	3	3	2	2	3	1		1								
TOTAL	1000	270	123	110	94	84	68	57	53	37	28	22	20	12	9	6	5	2	1	1	1		

TABLE 8

CURRENT SPEED-DIRECTION HISTOGRAM (TO THE NEAREST TENTH OF A PERCENT)

CONSERVED (WINTER). ALL MOE WINTER LAKEVIEW DATA. NOV. 1,1970 - APRIL 31,1971.

CURRENT VECTORS - 1958 TOTAL
SECTOR INCREMENT - 5.0 DEGREES
SPEED INCREMENT - 1.0 CM/SEC.

SPEED BIN 1 HOLDS 0-1 CM/SEC EVENTS, ETC.
SPEED BIN 51 HOLDS >50 CM/SEC EVENTS.

SECTOR DIRECTIONS ARE LABELLED ANTICLOCKWISE STARTING FROM THE 225 DEGREE SHORELINE

CURRENT EVENTS ARE WEIGHTED AVERAGED OVER THE NEAREST NEIGHBOUR SPEED AND DIRECTION BINS.
HENCE THERE MAY BE SOME ROUND OFF ERRORS IN THE INTEGRAL DISPLAY OF THE HISTOGRAM BELOW.

SPEED SECTOR	BIN SUM	> 1	2	3	4	5	6	7	8	9	10	11	12	13	14	15	16	17	18	19	20	21	22	23	24	25	26	27	28	29	30	
0.0	39	3	3	5	6	3	4	3	4	2	2	1	1	1	1																	PARALLEL
5.0	21	6	3	3	2	1	2		1		1	1																				
10.0	12	6	1	1	1	1	1																									
15.0	7	2		2	1	1																										
20.0	6	3		1	1																											
25.0	6	2	1	1	1	1																										
30.0	3	1																														
35.0	3	1	1	1																												
40.0	6	1	2	3	1																											
45.0	7	3	2	2																												
50.0	5	1	3	1																												
55.0	5	3	1	1																												
60.0	2	1	1																													
65.0	3	1	1	1																												
70.0	3	2	1																													
75.0	3	2	1																													
80.0	2	1																														
85.0	2	2																														
90.0	2	1																														
95.0	3	1	1	1																												OFFSHORE
100.0	2	2																														
105.0	3	2																														
110.0	2	1																														
115.0	4	3																														
120.0	7	6	1																													
125.0	5	4	1	1																												
130.0	6	4	2	1																												
135.0	5	3	1	1	1																											
140.0	7	3	1	2	1																											
145.0	5	1	2	2																												
150.0	7	1	1	2	1	1																										
155.0	12	6	1	2	2																											
160.0	15	5	4	2	2	1	1																									
165.0	22	6	3	4	2	2	3	1	1																							
170.0	31	3	2	3	6	6	3	2	1	1	1															1						
175.0	40	6	2	5	5	6	4	3	2	3	2																					
180.0	57	6	5	5	5	8	5	6	5	4	5	1																				ANTIPARA
185.0	69	4	4	3	5	5	8	10	8	6	4	6	2	1																		
190.0	53	2	5	7	8	5	4	2	5	4	2	2	2	1				1	1	1												
195.0	47	2	4	7	6	4	2	2	2	2	1	1	2	2	1	1	1	1	1		1	1		1	1	1		1	1			
200.0	28	3	3	5	3	2	2	2	1	1	1							1		1	1		1	1								
205.0	16	2	2	2	2	2		1		2	1						1							1								
210.0	6	1	2			1																										
215.0	5	1	1	1																												
220.0	2	1	1																													
225.0																																
230.0																																
235.0	1	1																														
240.0	2	1																														
245.0	2	1																														
250.0	2	1																														
255.0	2	1																														
260.0	1																															
265.0	2	1																														
270.0	2	1																														ON SHORE
275.0	2	1																														
280.0	2																															
285.0	2	1																														
290.0	1																															
295.0	4	2																														
300.0	4	1	1	1			1																									
305.0	4	2		1																												
310.0	3	2																														
315.0	7	5	1			1																										
320.0	5	1			1			1						1																		
325.0	6	2	1			1																										
330.0	7	1	1	1	1	1	1																									
335.0	11	1	2	1	1	2	2		1																							
340.0	22	4	4	2	2	2	3	2	1	1																						
345.0	60	4	2	3	4	3	5	5	4	3	3	2	3	4	2	2	2	2	1	2	2	1		1								
350.0	145	6	3	5	6	9	10	11	9	7	9	6	7	7	6	5	7	6	2	4	6	3	2	3	1	1	1	2				
355.0	109	2	2	6	9	9	8	10	9	8	7	5	4	7	8	3	3	2	2	1							1	1	1			
TOTAL	1000	167	89	98	94	79	73	63	56	47	41	28	23	25	19	13	13	13	8	9	10	5	3	6	3	3	4	4	3	1		

TABLE 9

Summer Current Episodes (Shore Parallel)
(Lakeview W.P.C.P.)

Speed 0-5 cm/s (frequency 8.5%)

Episode Time and Date	Duration (hours)	Average Velocity (cm/s & deg. true)
18:00 8/06/70 - 23:00 11/06/70	78	1.9 at 245°
12:00 4/09/70 - 23:00 7/09/70	84	4.5 at 226°
6:00 1/10/70 - 17:00 5/10/70	108	2.5 at 223°
12:00 11/10/70 - 17:00 13/10/70	54	4.2 at 221°
Average episode	40.5	3.1 at 227°

Speed 5-15 cm/s (frequency 11.0%)

Episode Time and Date	Duration (hours)	Average Velocity (cm/s & deg. true)
0:00 22/07/70 - 23:00 25/08/70	96	5.1 at 240°
0:00 27/08/70 - 11:00 29/08/70	60	7.1 at 230°
12:00 1/09/70 - 17:00 3/09/70	54	5.8 at 235°
0:00 11/09/70 - 17:00 12/09/70	42	8.6 at 231°
0:00 17/09/70 - 5:00 18/09/70	30	8.1 at 236°
6:00 28/09/70 - 5:00 30/09/70	48	4.3 at 230°
0:00 17/10/70 - 11:00 19/10/70	60	6.2 at 232°
12:00 23/10/70 - 17:00 24/10/70	30	6.4 at 230°
Average episode	52.5	6.2 at 233°

Speed 15 cm/s (frequency 0%)

No episodes observed

TABLE 10

Summer Current Episodes (Shore Antiparallel)
(Lakeview W.P.C.P.)

Speed 0-5 cm/s (frequency 8.9%)

Episode Time and Date	Duration (hours)	Average Velocity (cm/s & deg. true)
0:00 28/05/70 - 23:00 4/06/70	186	1.9 at 46°
0:00 18/08/70 - 17:00 19/08/70	42	4.0 at 38°
0:00 9/10/70 - 11:00 11/10/70	60	3.1 at 44°
12:00 29/10/70 - 17:00 31/10/70	54	3.7 at 24°
Average episode	85.5	2.6 at 39°

Speed 5-15 cm/s (frequency 13.8%)

Episode Time and Date	Duration (hours)	Average Velocity (cm/s & deg. true)
12:00 24/05/70 - 17:00 25/05/70	30	7.5 at 40°
12:00 14/06/70 - 11:00 17/06/70	72	7.4 at 49°
0:00 8/08/70 - 23:00 10/08/70	72	8.0 at 43°
0:00 22/08/70 - 23:00 23/08/70	48	4.7 at 43°
6:00 8/09/70 - 17:00 10/09/70	60	4.5 at 42°
6:00 14/09/70 - 5:00 16/09/70	48	8.7 at 41°
18:00 19/10/70 - 11:00 23/10/70	90	4.9 at 43°
0:00 25/10/70 - 11:00 29/10/70	108	6.0 at 31°
Average episode	66.0	6.3 at 41°

Speed 15 cm/s (frequency 0%)

No episodes observed

TABLE 11
Winter Current Episodes (Shore Parallel)
(Lakeview W.P.C.P.)

Speed 0-5 cm/s (frequency 10.0%)

Episode Time and Date	Duration (hours)	Average Velocity (cm/s & deg. true)
12:00 29/11/70 - 5:00 1/12/70	41	3.2 at 224°
18:00 18/02/71 - 23:00 20/02/71	54	3.3 at 238°
18:00 8/03/71 - 23:00 9/03/71	30	5.2 at 240°
6:00 31/03/71 - 5:00 3/04/71	72	4.3 at 233°
Average episode	49.3	3.9 at 234°

Speed 5-15 cm/s (frequency 25.7%)

Episode Time and Date	Duration (hours)	Average Velocity (cm/s & deg. true)
06:00 6/11/70 - 11:00 7/11/70	30	10.3 at 235°
12:00 16/11/70 - 23:00 21/11/70	138	7.4 at 234°
00:00 25/11/70 - 11:00 27/11/70	60	10.4 at 234°
00:00 2/12/70 - 17:00 3/12/70	42	5.7 at 234°
06:00 5/12/70 - 11:00 6/12/70	30	10.5 at 241°
12:00 8/12/70 - 11:00 10/12/70	48	5.3 at 232°
18:00 25/02/71 - 17:00 28/02/71	71	6.4 at 233°
18:00 4/04/71 - 05:00 8/04/71	84	7.9 at 230°
Average episode	63.0	7.7 at 234°

Speed 15 cm/s (frequency 7.0%)

Episode Time and Date	Duration (hours)	Average Velocity (cm/s & deg. true)
06:00 22/11/70 - 03:00 24/11/70	46	15.4 at 235°
06:00 2/03/71 - 23:00 4/03/71	66	14.8 at 235°
14:00 11/03/71 - 14:00 12/03/71	25	16.7 at 235°
Average episode	45.7	15.3 at 235°

TABLE 12
Winter Current Episodes (Shore Antiparallel)
(Lakeview W.P.C.P.)

Speed 0-5 cm/s (frequency 12.3%)

Episode Time and Date	Duration (hours)	Average Velocity (cm/s & deg. true)
6:00 11/11/70 - 23:00 15/11/70	114	3.2 at 43°
12:00 6/12/70 - 5:00 8/12/70	42	3.1 at 51°
12:00 29/03/71 - 5:00 31/03/71	42	2.8 at 35°
18:00 9/04/71 - 11:00 11/04/71	42	1.5 at 61°
Average episode	60.0	2.8 at 45°

Speed 5-15 cm/s (frequency 17.2%)

Episode Time and Date	Duration (hours)	Average Velocity (cm/s & deg. true)
12:00 2/11/70 - 17:00 3/11/70	30	8.5 at 3°
18:00 8/11/70 - 5:00 10/11/70	36	6.5 at 38°
0:00 28/11/70 - 11:00 29/11/70	36	6.7 at 41°
18:00 3/12/70 - 5:00 5/12/70	36	7.1 at 32°
0:00 1/03/71 - 5:00 2/03/71	30	7.2 at 41°
0:00 6/03/71 - 11:00 8/03/71	60	5.3 at 55°
12:00 26/03/71 - 11:00 29/03/71	72	5.4 at 42°
6:00 3/04/71 - 17:00 4/04/71	36	6.3 at 39°
Average episode	42.0	6.3 at 41°

Speed 15 cm/s (frequency 4.9%)

Episode Time and Date	Duration (hours)	Average Velocity (cm/s & deg. true)
0:00 21/02/71 - 17:00 22/02/71	42	10.4 at 30°
10:00 24/02/71 - 17:00 25/02/71	31	16.6 at 35°
15:00 10/03/71 - 12:00 11/03/71	22	15.5 at 29°
Average episode	31.7	13.6 at 32°

TABLE 13
Plume Dimensions at the Lakeview W.P.C.P

The plume dimensions are the length and width of a specified dilution contour averaged over several episodes. The maximum and minimum ranges of the contour are also given. The diffuser, effluent, and current episode descriptors are listed in Table 15, the most useful ones being repeated below. They are the specified dilution (s), the frequency of occurrence, and the diffusion time (t) required to achieve the specified dilution.

S = 100 : 1

SUMMER

			Shore Parallel Flow								Shore Antiparallel Flow					
			Length (km)			Width (km)					Length (km)			Width (km)		
Speed (cm/s)	Frequency (%)	Diffusion Time (min)	min	mean	max	min	mean	max	Frequency (%)	Diffusion Time (min)	min	mean	max	min	mean	max
0-5	8.5	805	1.2	1.5	2.4	0.4	0.6	0.9	8.9	1155	1.3	1.8	4.0	0.3	0.6	0.9
5-15	11.0	670	1.0	2.5	6.0	0.3	0.5	1.0	13.8	900	1.3	3.4	7.4	0.3	0.5	1.3
15	-								-							

WINTER

			Shore Parallel Flow								Shore Antiparallel Flow					
			Length (km)			Width (km)					Length (km)			Width (km)		
Speed (cm/s)	Frequency (%)	Diffusion Time (min)	min	mean	max	min	mean	max	Frequency (%)	Diffusion Time (min)	min	mean	max	min	mean	max
0-5	10.0	1370	2.7	3.2	4.2	0.3	0.5	1.0	12.3	1665	1.3	2.8	3.7	0.3	0.8	1.5
5-15	25.7	1340	3.7	6.2	11.0	0.3	0.6	1.1	17.2	1215	1.3	4.6	7.1	0.3	0.5	1.5
15	7.0	1765	16.1	16.2	16.3	1.0	1.0	1.0	4.9	1190	4.0	9.7	14.6	0.5	0.5	0.9

TABLE 14

Input Parameters for Effluent Plume Simulations

Initial Dilution - 13:1 (as per section 9.3)

Diffuser length - 200 m

Diffuser orientation - 135 deg. true (axis direction)

Shore parallel direction - 225 deg. true

Eddy diffusivity - 1200 cm^2/s.

The computer simulations are based on the inertial sub-range diffusion model, i.e. the eddy diffusivity increases as the 4/3 power of the plume width. The diffusion constant K = 1200 cm^2/sec corresponds to an initial plume width of 200 m.

TABLE B5

Source Description

Discharge rate	2100 l/sec	(typical)
Discharge velocity	48 cm/s	"
Density anomaly	1.5 ppt.	"
Initial dilution	13:1	"
Diffuser Depth	9.5 m	
Diffuser Length	210 m	
Diffuser Orientation	135 deg. true (axis direction)	
Shoreline Orientation	225 deg. true	
Distance Offshore	1.3 km	
Diffuser Location	As per Figure A1	

TABLE 15

Alongshore Current Frequency Table
Lakeview W.P.C.P.

Summer (May 1 - Oct 31)
(based on 3822 hourly averaged events)

Speed (cm/s)	Parallel (%)	Antiparallel (%)
0-5	8.5	8.9
5-15	11.0	13.8
15	-	-
Sum	19.5	22.7

Percentage of alongshore current episodes = 42.2

Percentage of miscellaneous current events = 57.8

Winter (Nov 1 - April 30)
(based on 1958 hourly averaged events)

Speed (cm/s)	Parallel (%)	Antiparallel (%)
0-15	10.0	12.3
5-15	25.7	17.2
15	7.0	4.9
Sum	42.7	34.4

Percentage of alongshore current episodes = 77.1

Percentage of miscellaneous current events = 22.9

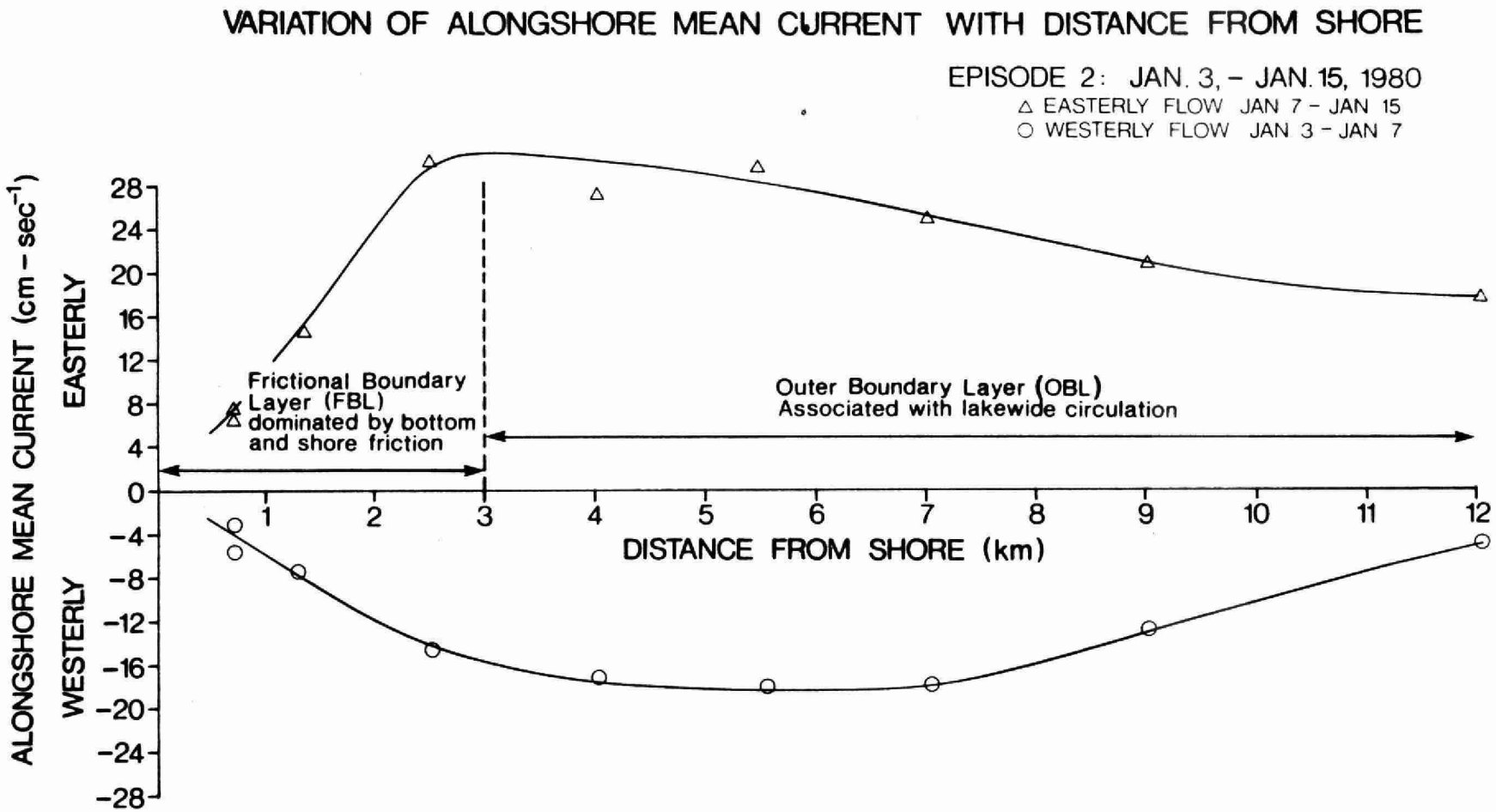

Figure 1. (After Bull & Murthy 1980)

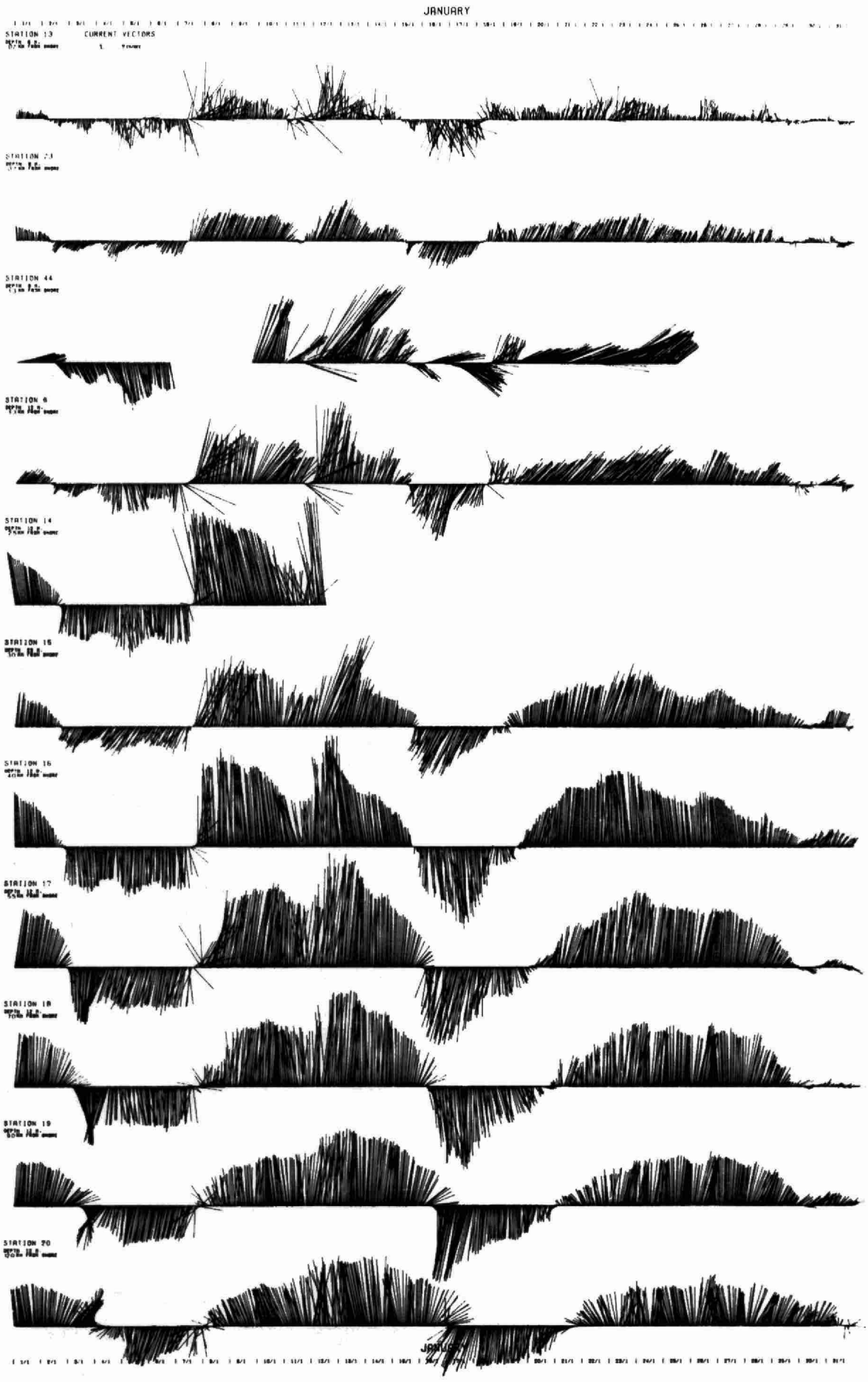

Figure 2. MONTHLY VECTOR TIME–SERIES PLOT PICKERING, (After Bull & Murthy, 1980) LAKE ONTARIO, JANUARY 1980

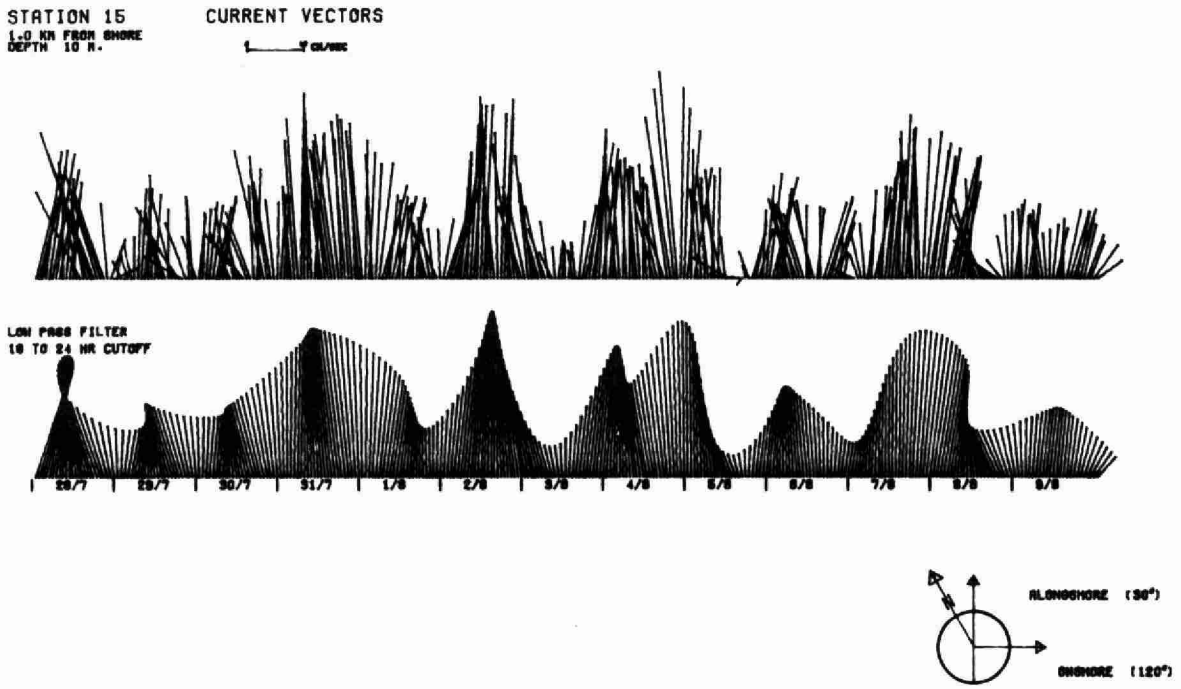

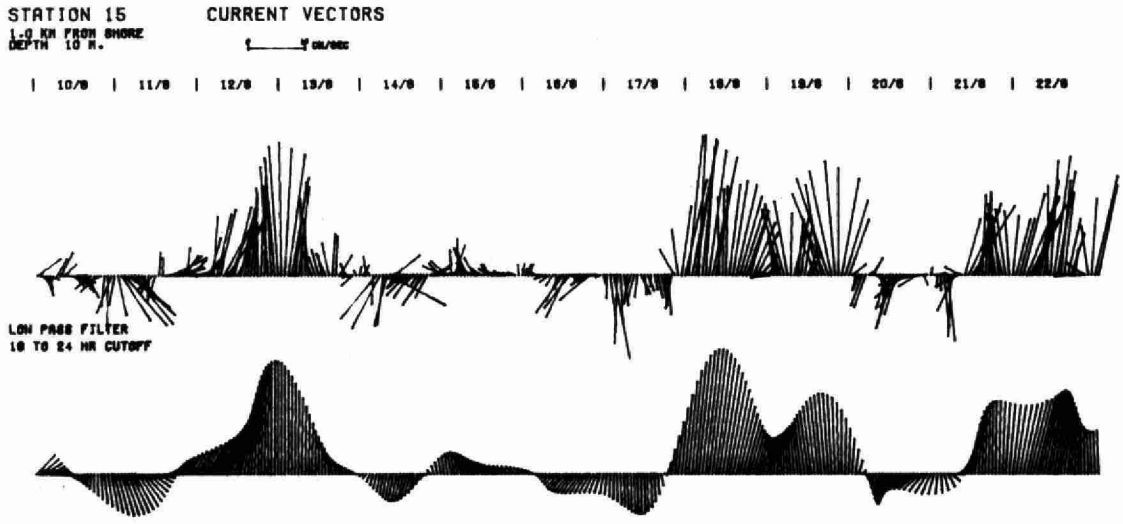

VECTOR TIME-SERIES PLOT, DOUGLAS POINT, LAKE HURON, JULY 28-AUG 22, 1974

Figure 3.

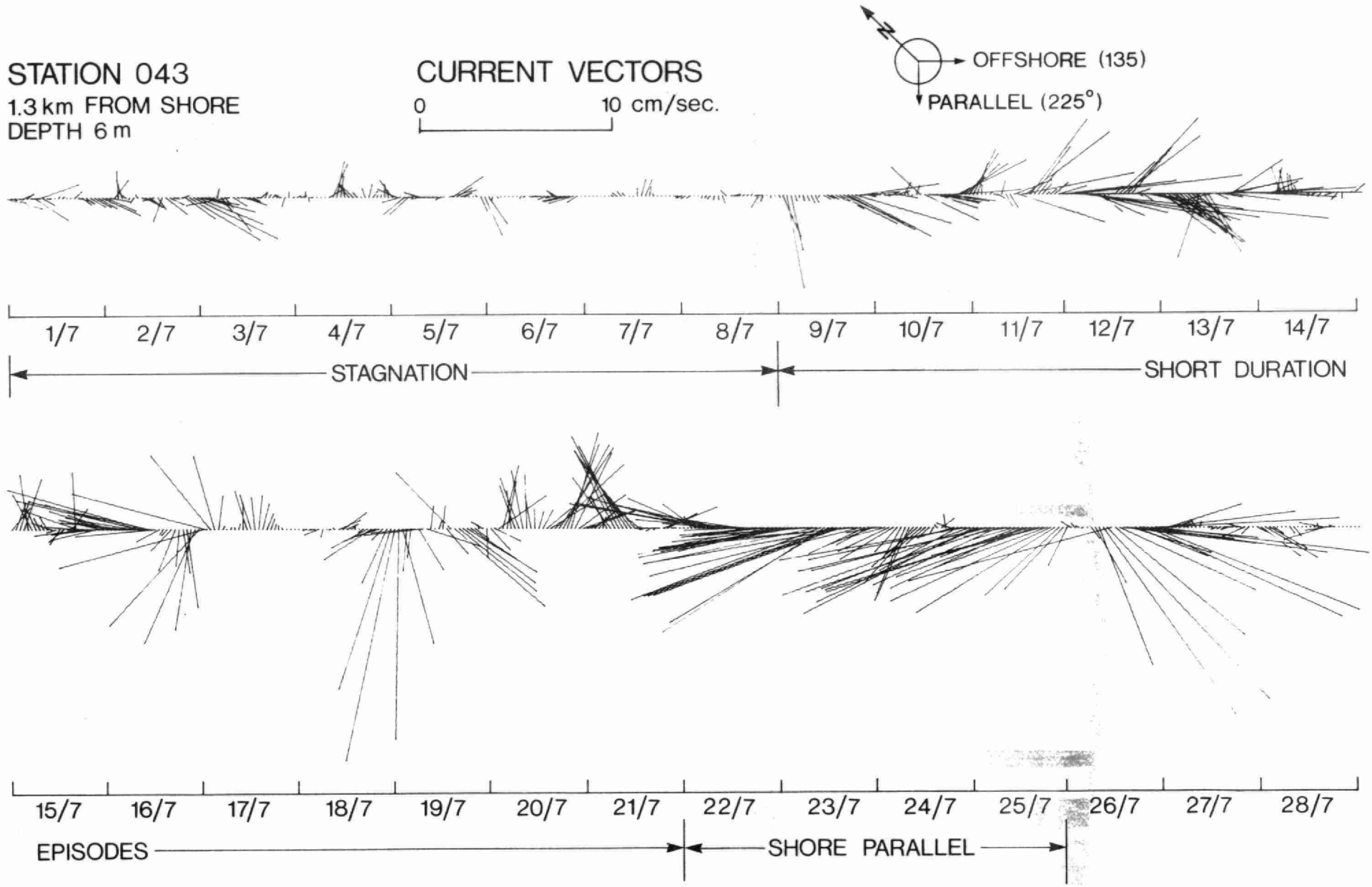

VECTOR TIME—SERIES PLOT, LAKEVIEW, LAKE ONTARIO, JULY 1—JULY 28, 1972

Figure 4.

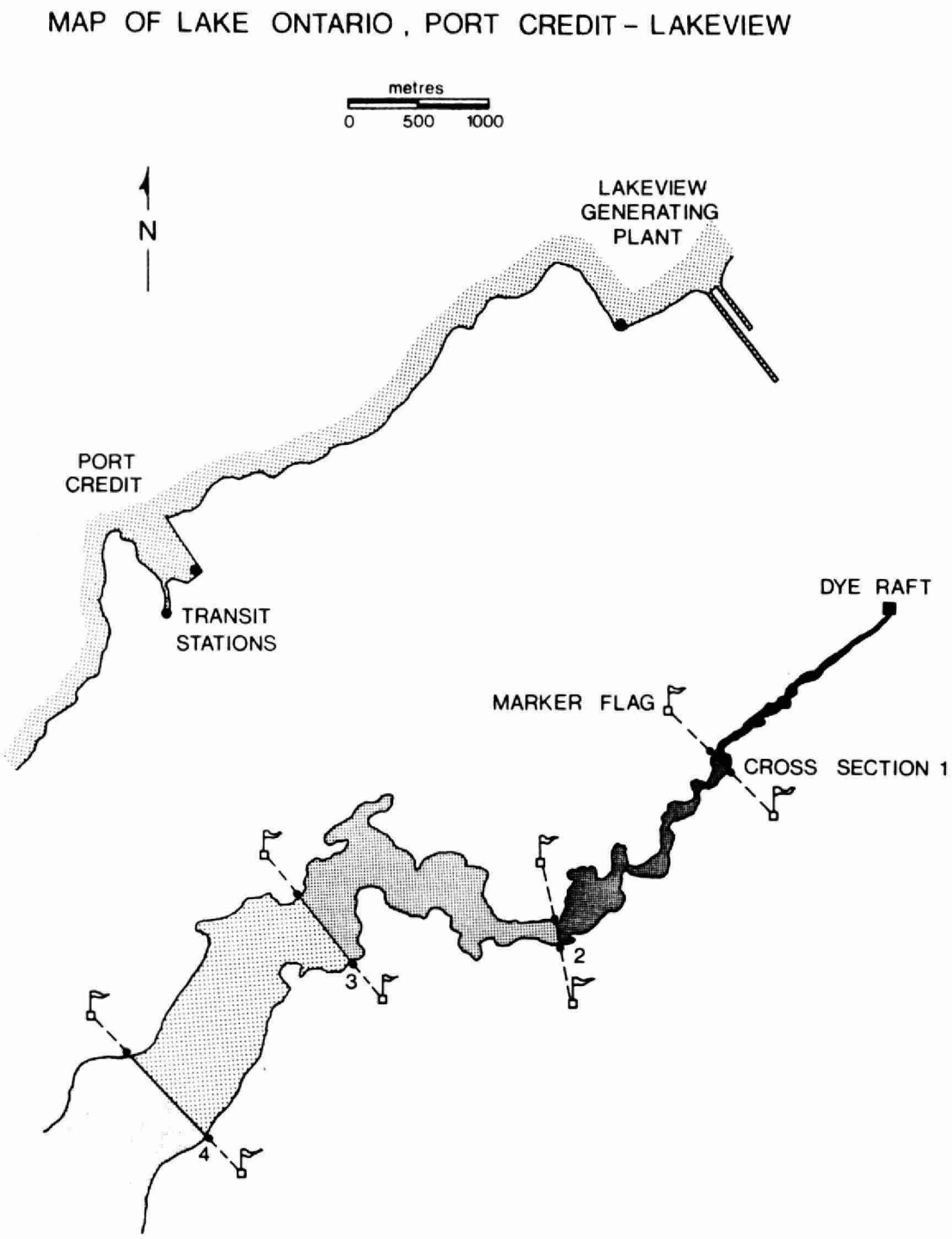

Figure 5. Schematic of a Continuous Plume Experiment

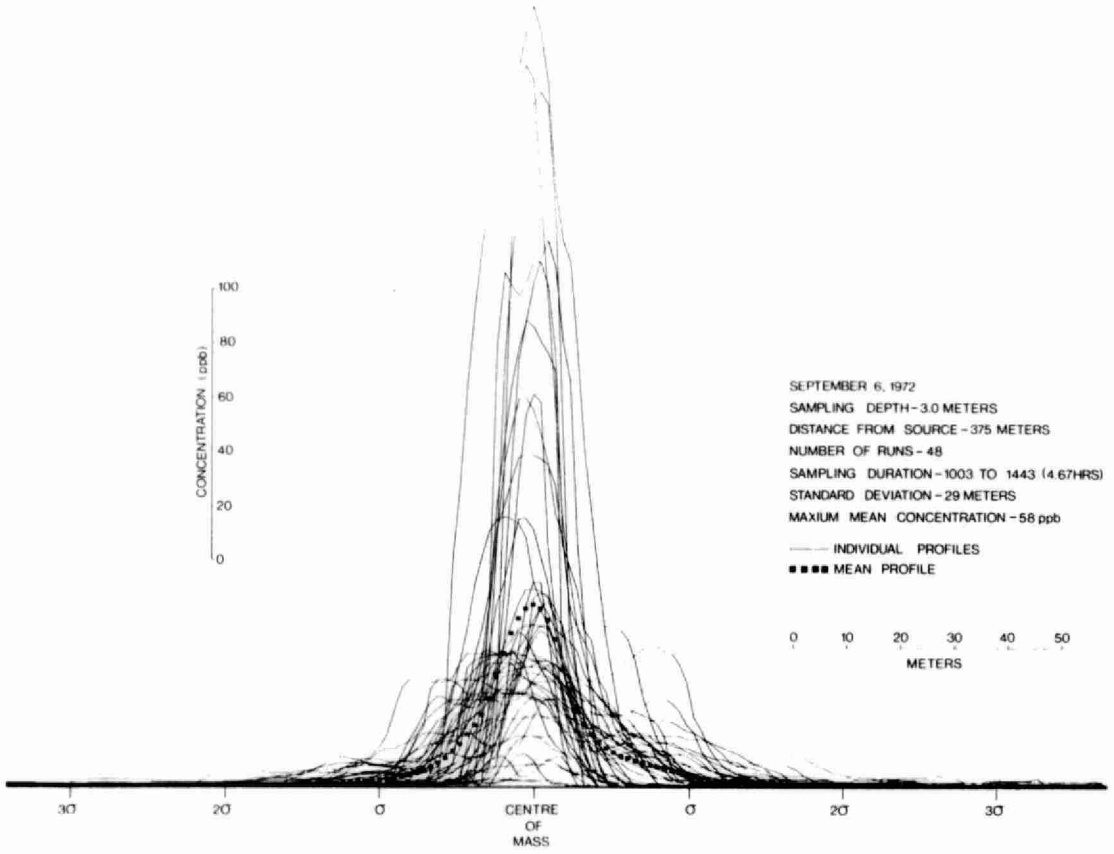

Figure 6. CROSSPLUME CONCENTRATION DISTRIBUTION - RELATIVE
(After Murthy & Miners, 1978)

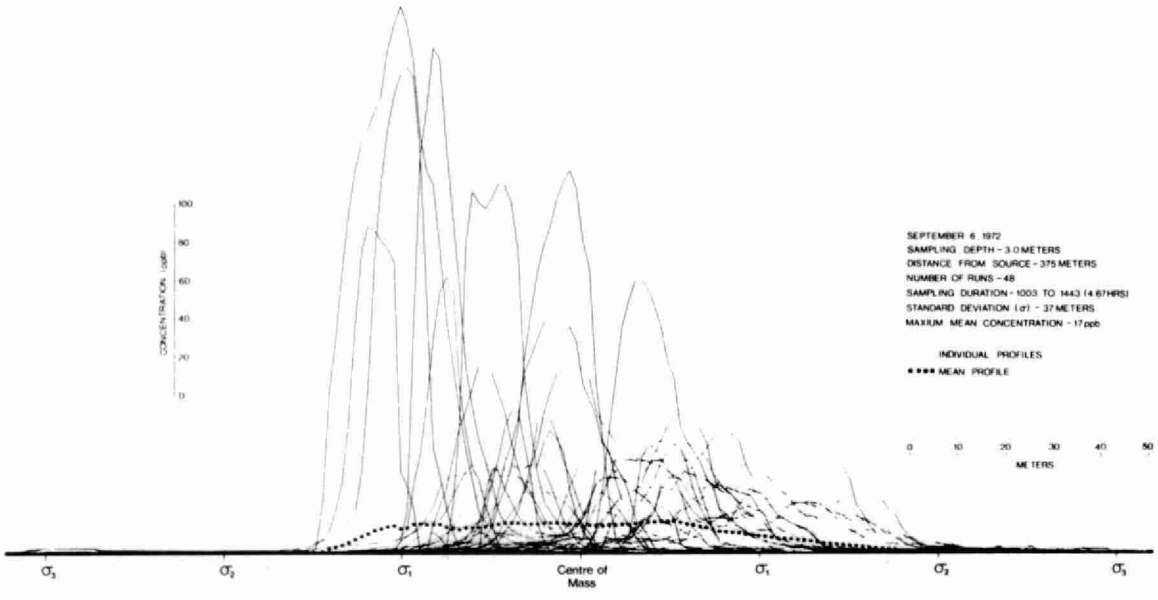

Figure 7. CROSSPLUME CONCENTRATION DISTRIBUTION - ABSOLUTE
(After Murthy & Miners, 1978)

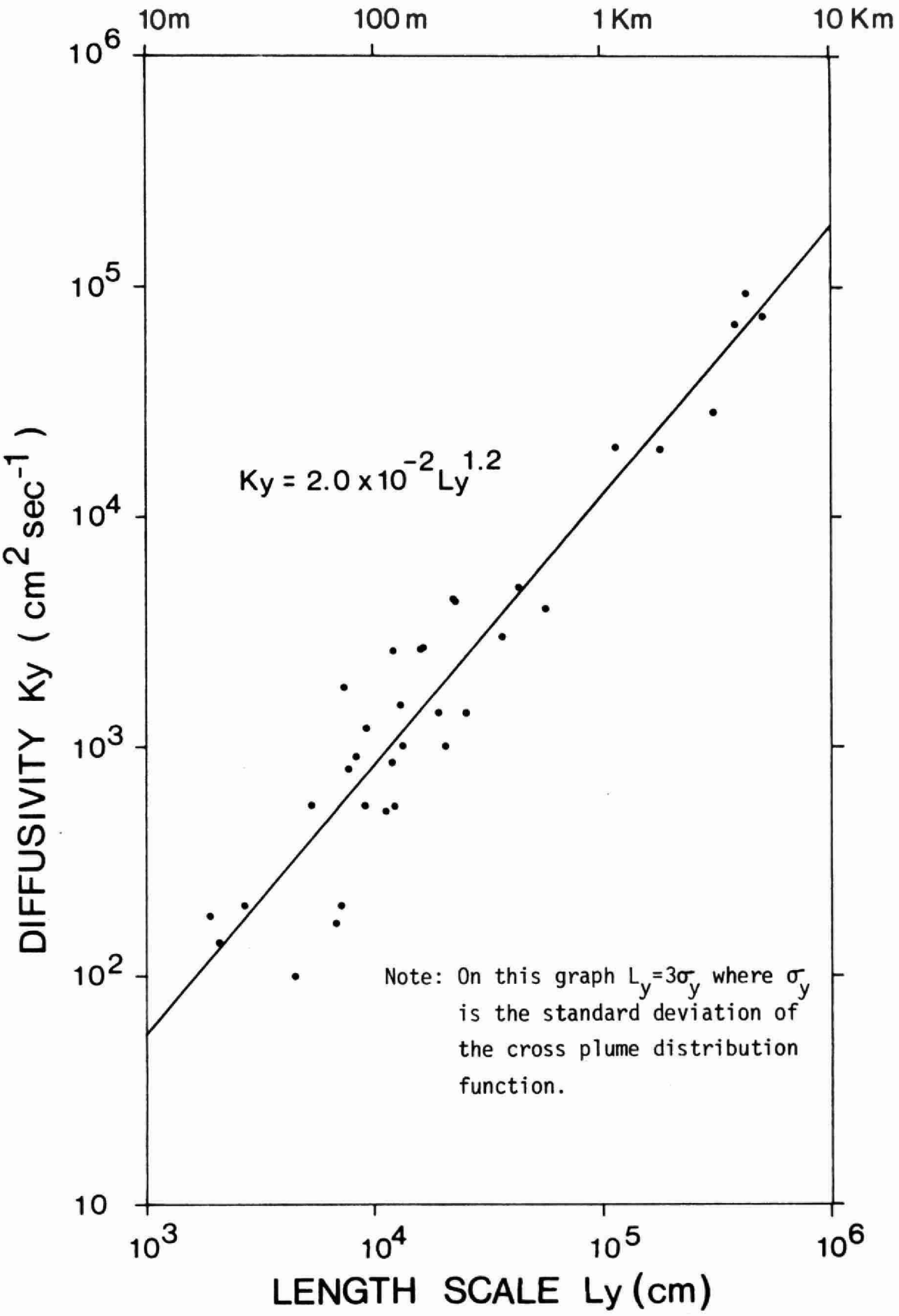

Figure 8. **HORIZONTAL EDDY DIFFUSIVITY vs LENGTH SCALE OF DIFFUSION**
(After Murthy and Kenney 1974)

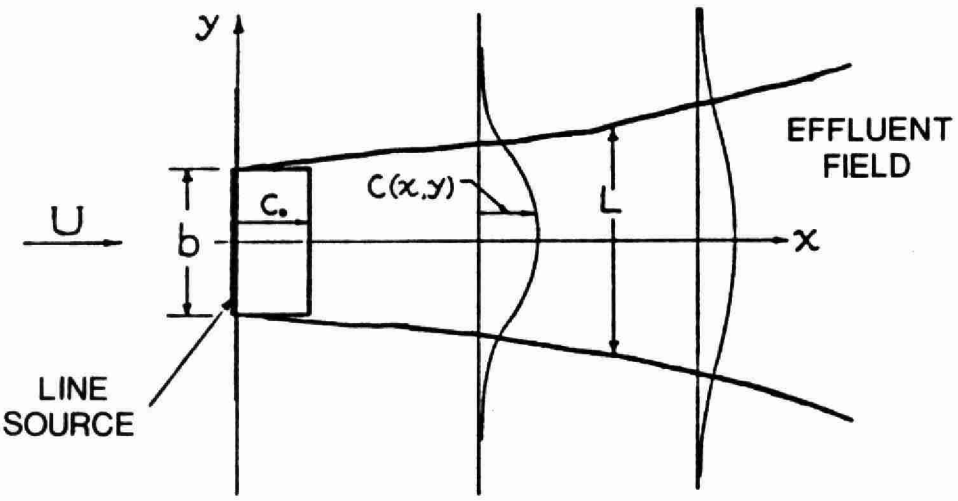

Figure 9. Schematic of a laterally diffusing effluent field in a steady current.

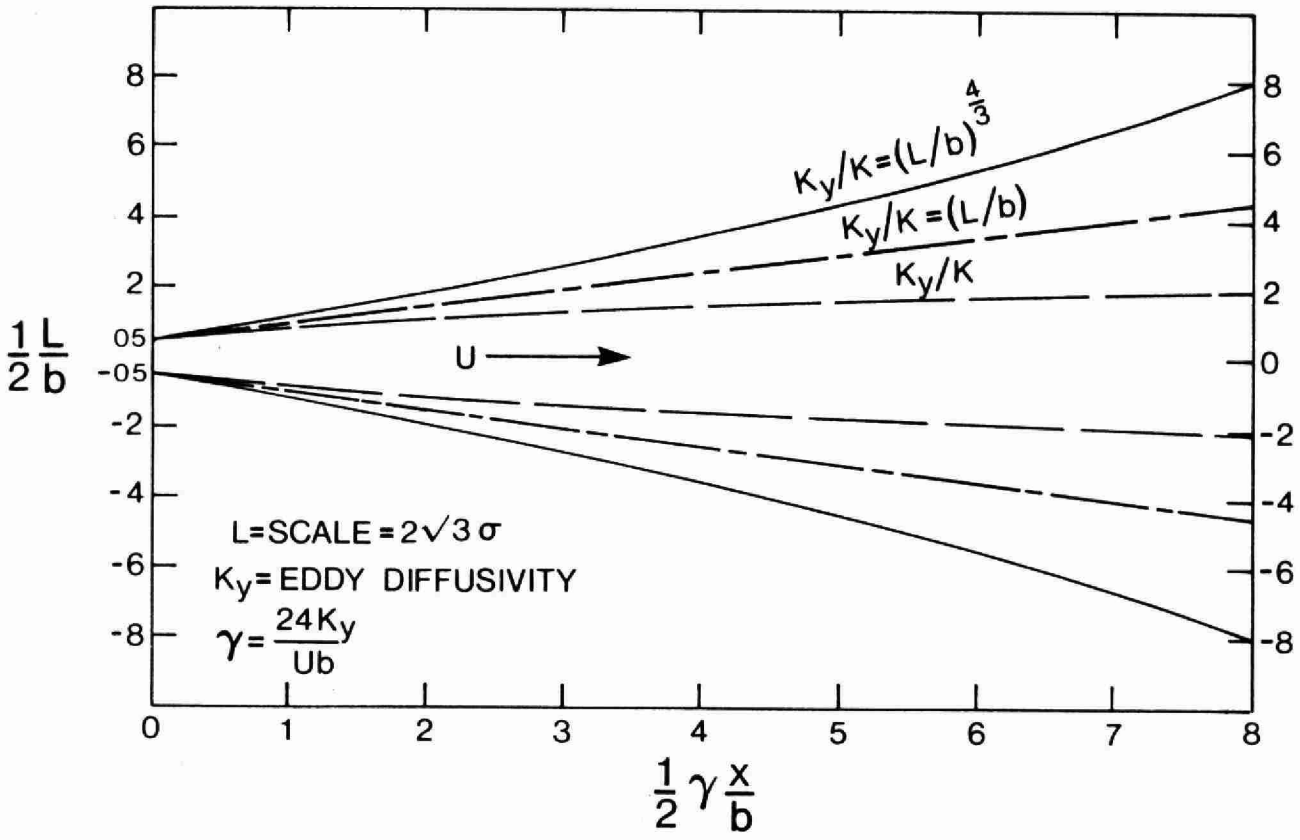

Figure 9A. Schematic of Plume Dispersal with Different Diffusion Mechanisms. (After Brooks, 1960)

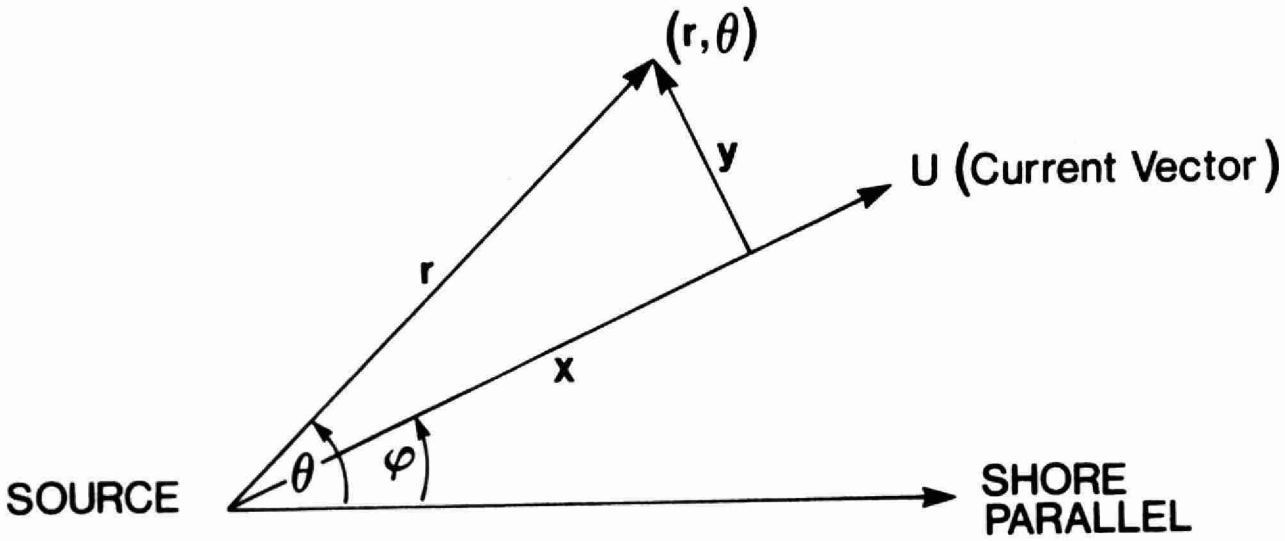

Figure 10. Coordinate System for Gaussian Plume Calculations.

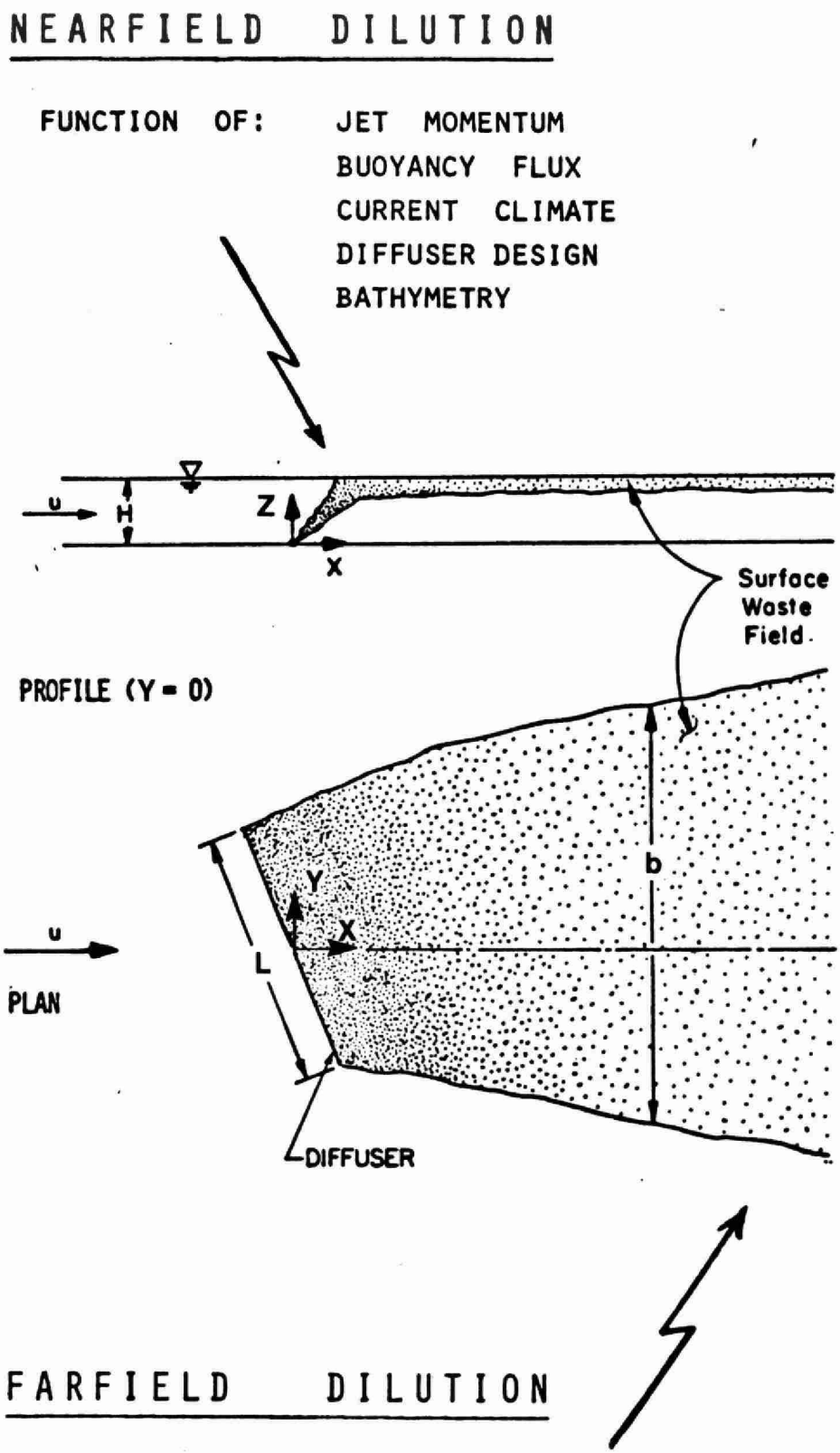

Figure 11. Schematic of the Farfield Dilution.

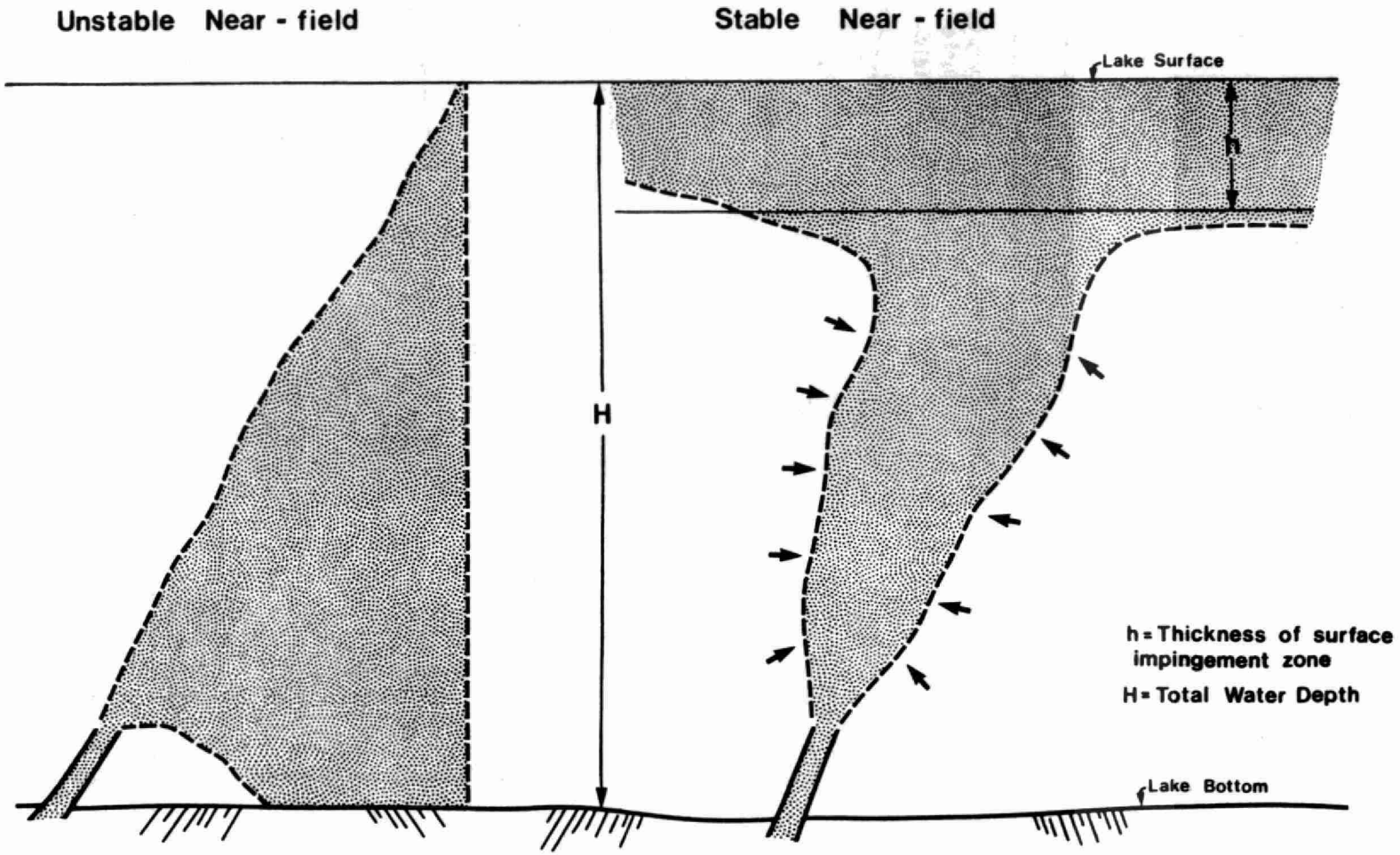

FIGURE 12 NEAR-FIELD FLOW STABILITY

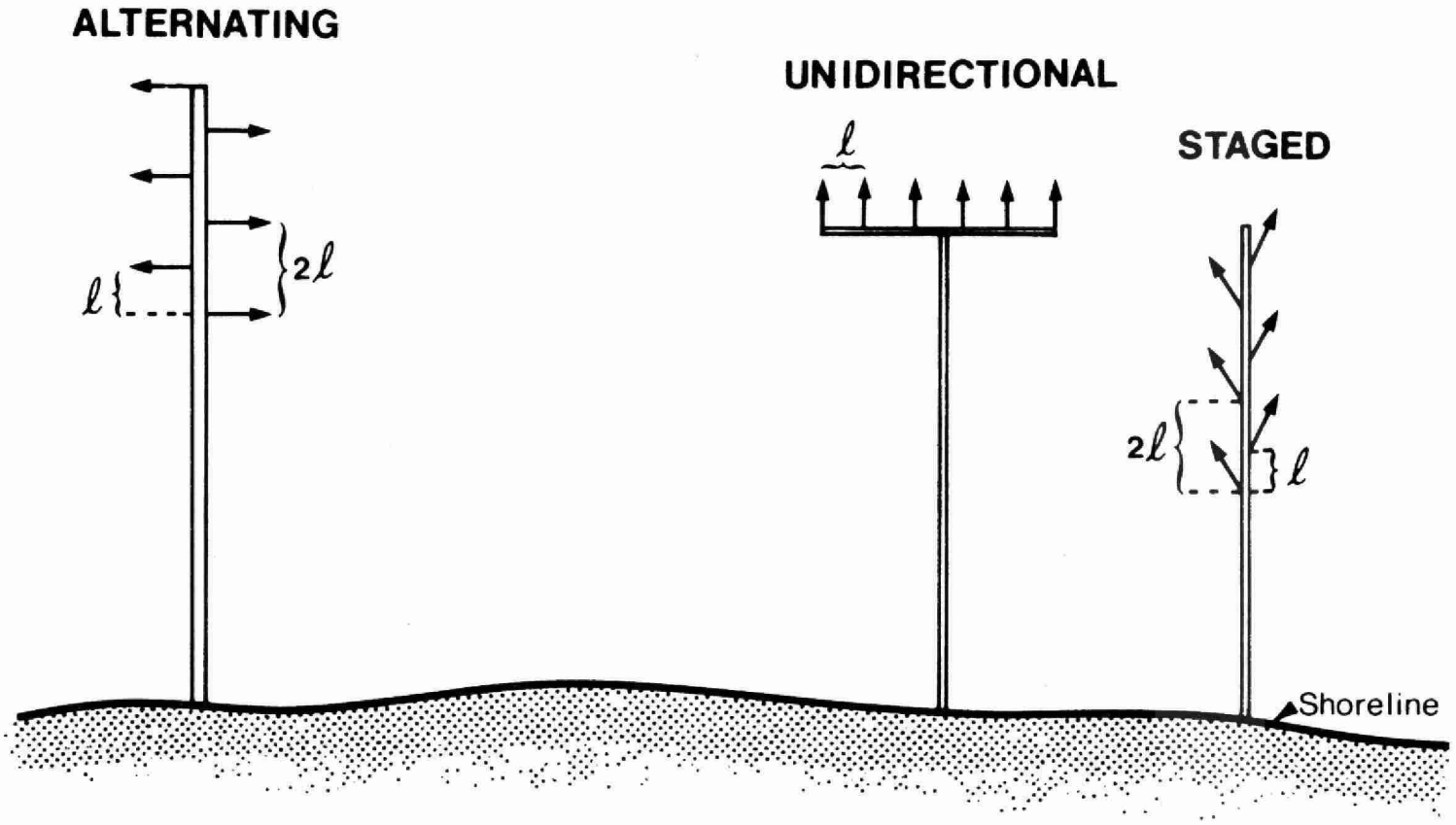

FIGURE 13 DIFFUSER TYPES

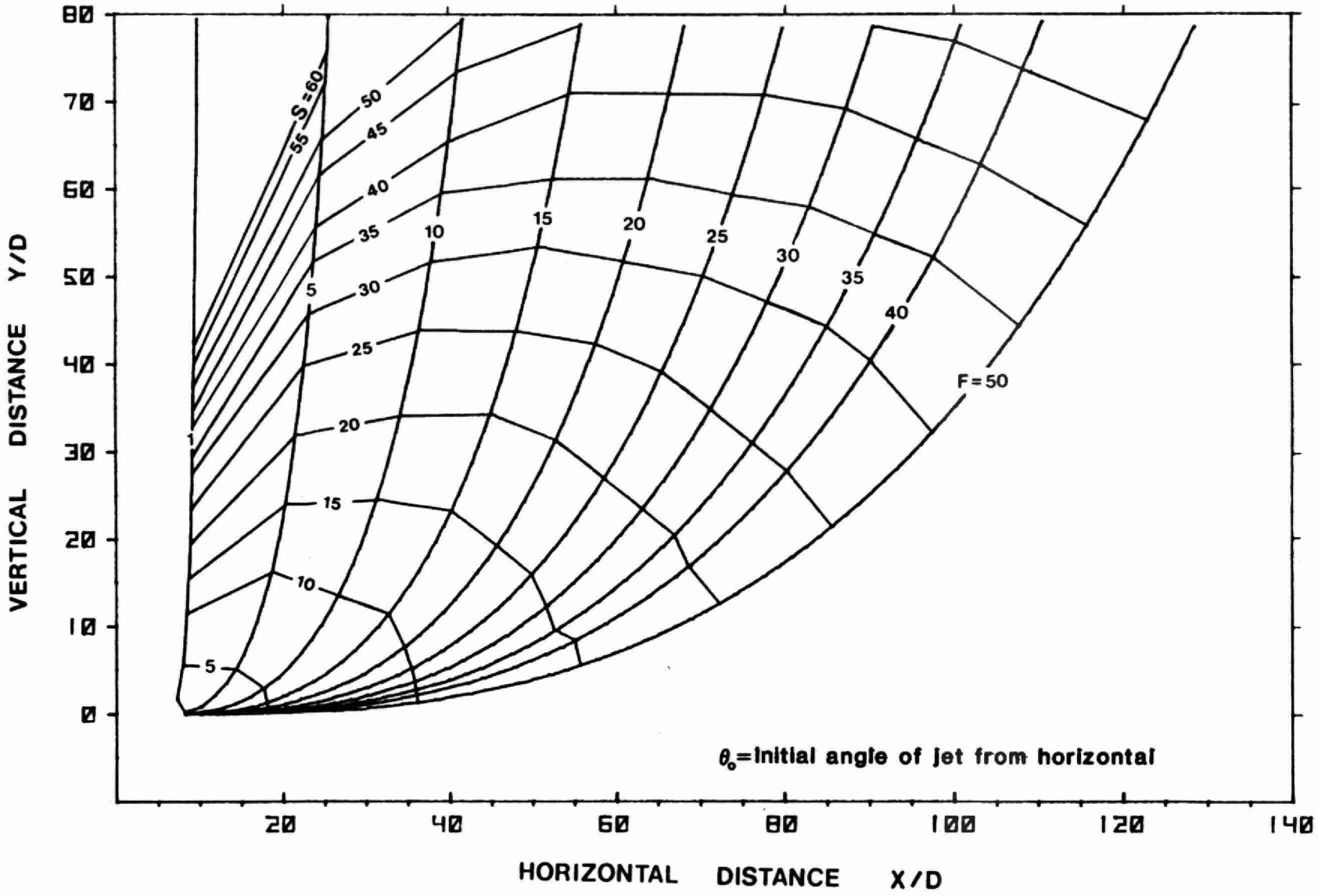

FIGURE 14 DILUTION NO INTERFERENCE $\theta_o = 0°$

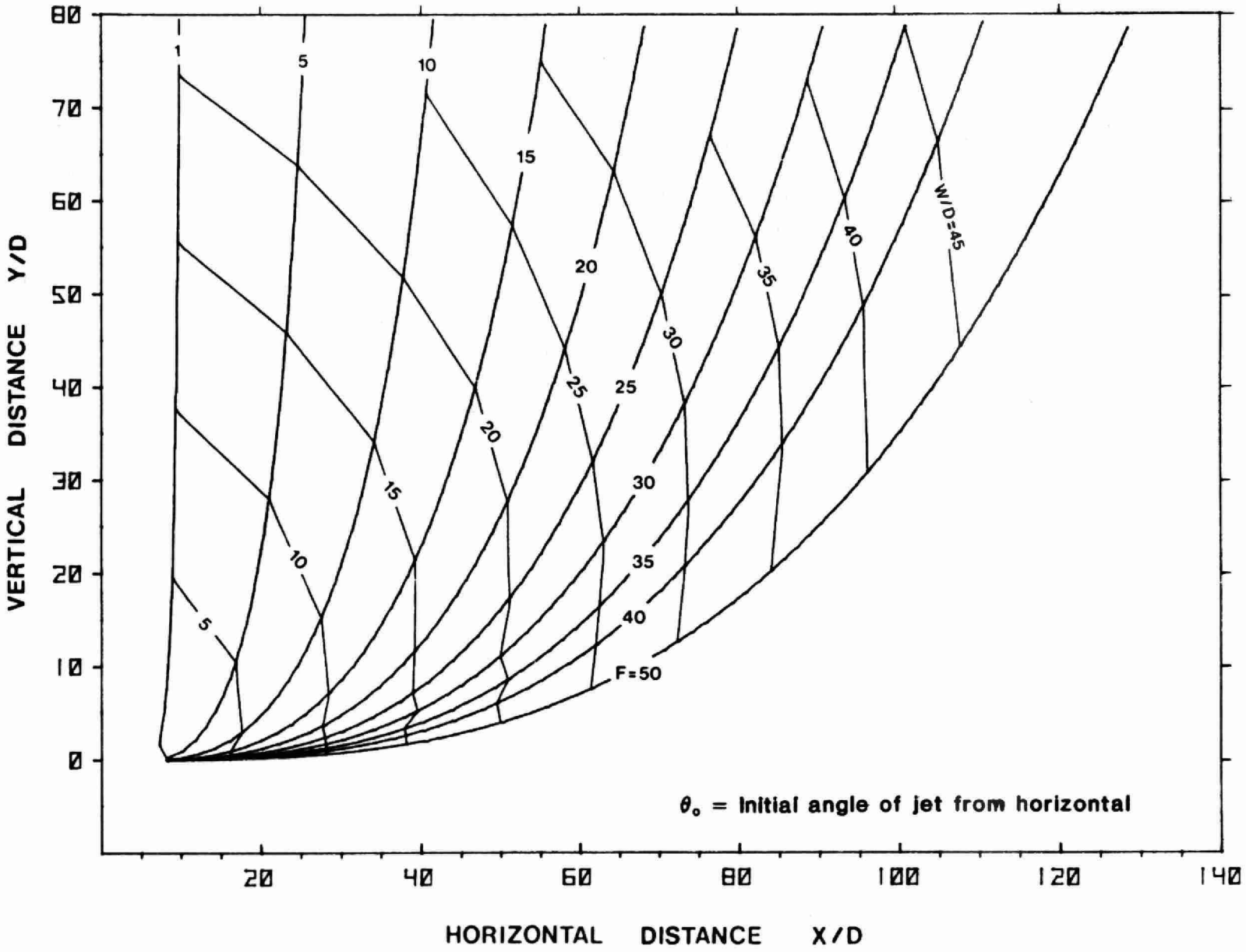

FIGURE 15 JET WIDTH NO INTERFERENCE $\theta_o = 0°$

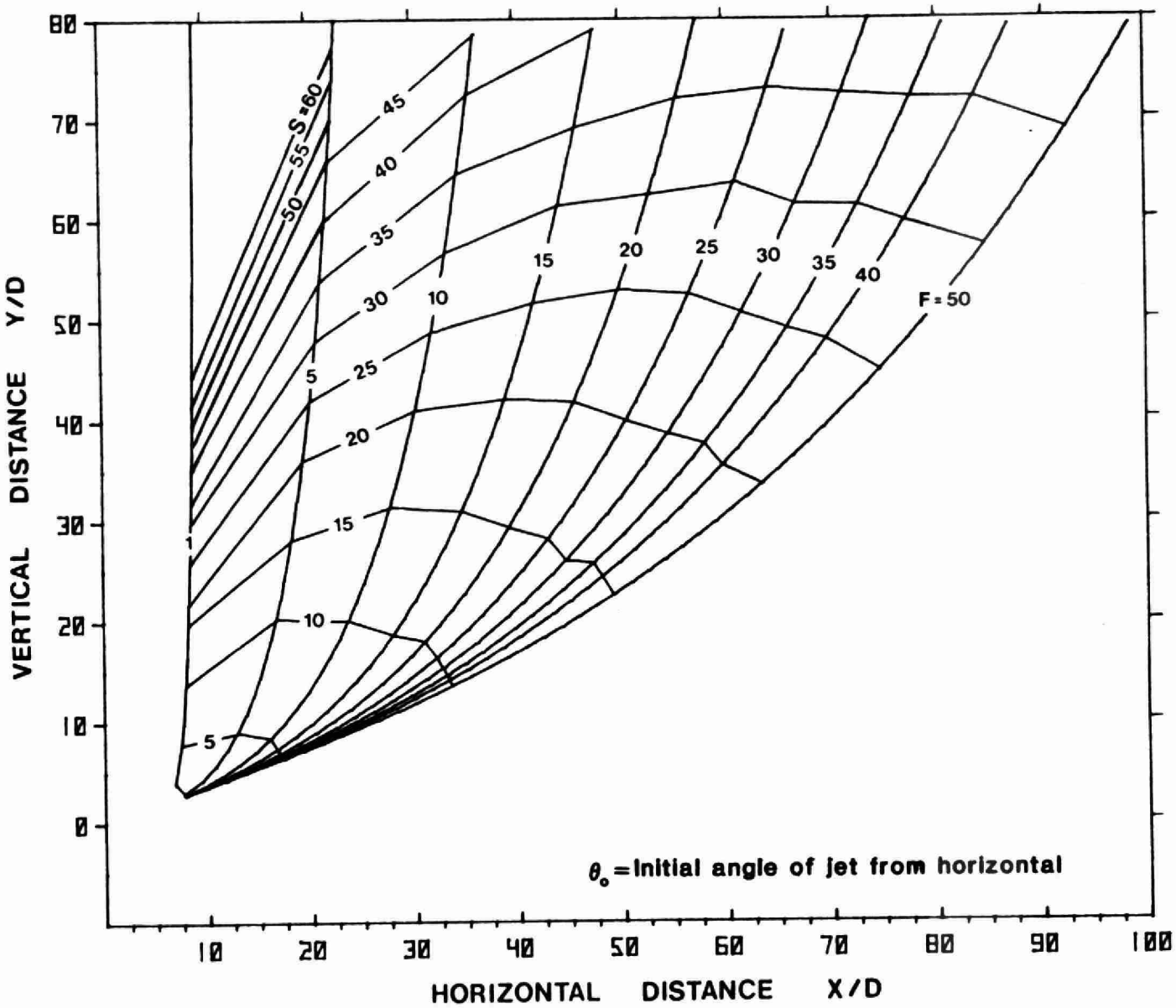

FIGURE 16 DILUTION NO INTERFERENCE $\theta_o = 20°$

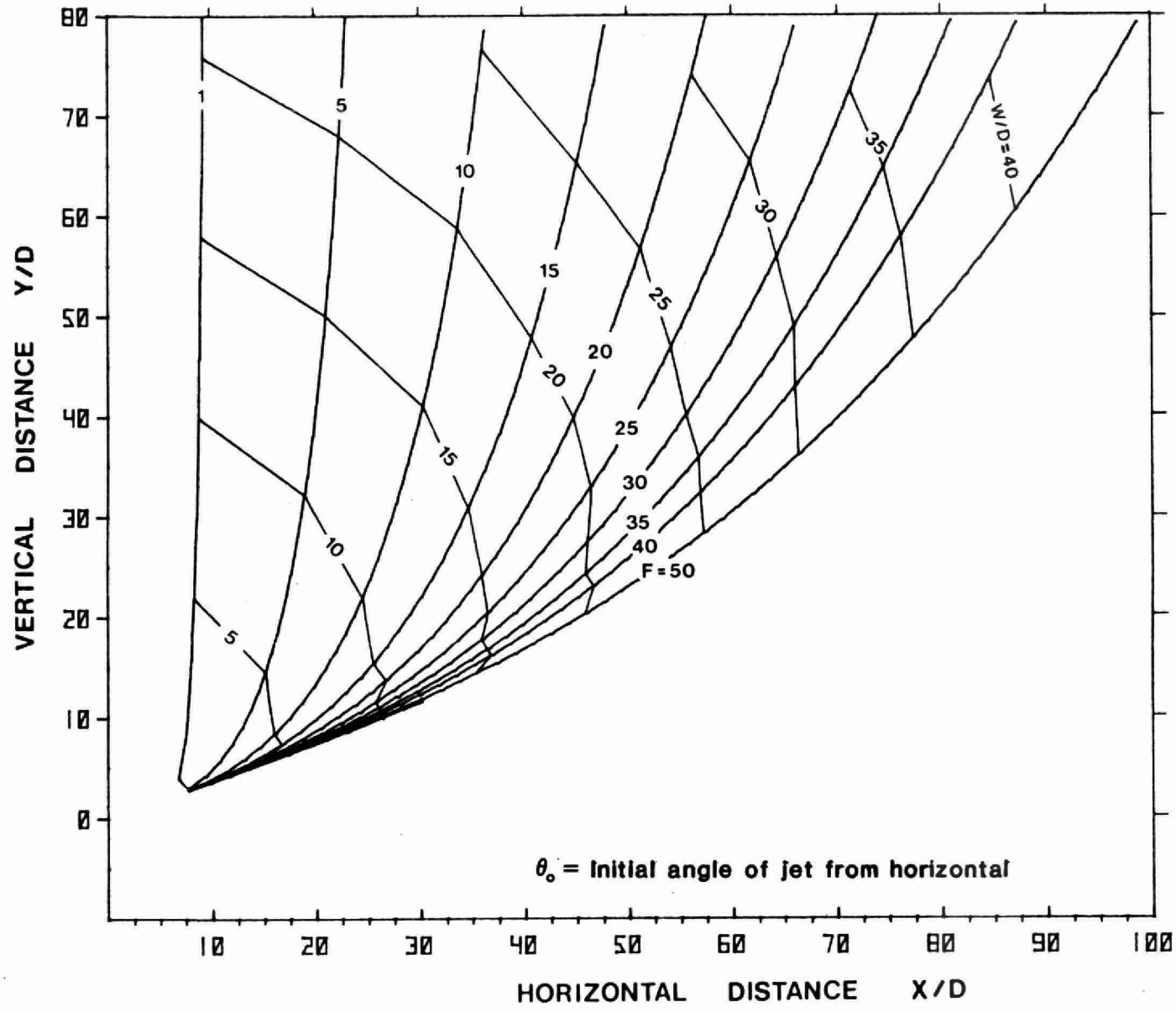

FIGURE 17 JET WIDTH NO INTERFERENCE $\theta_o = 20°$

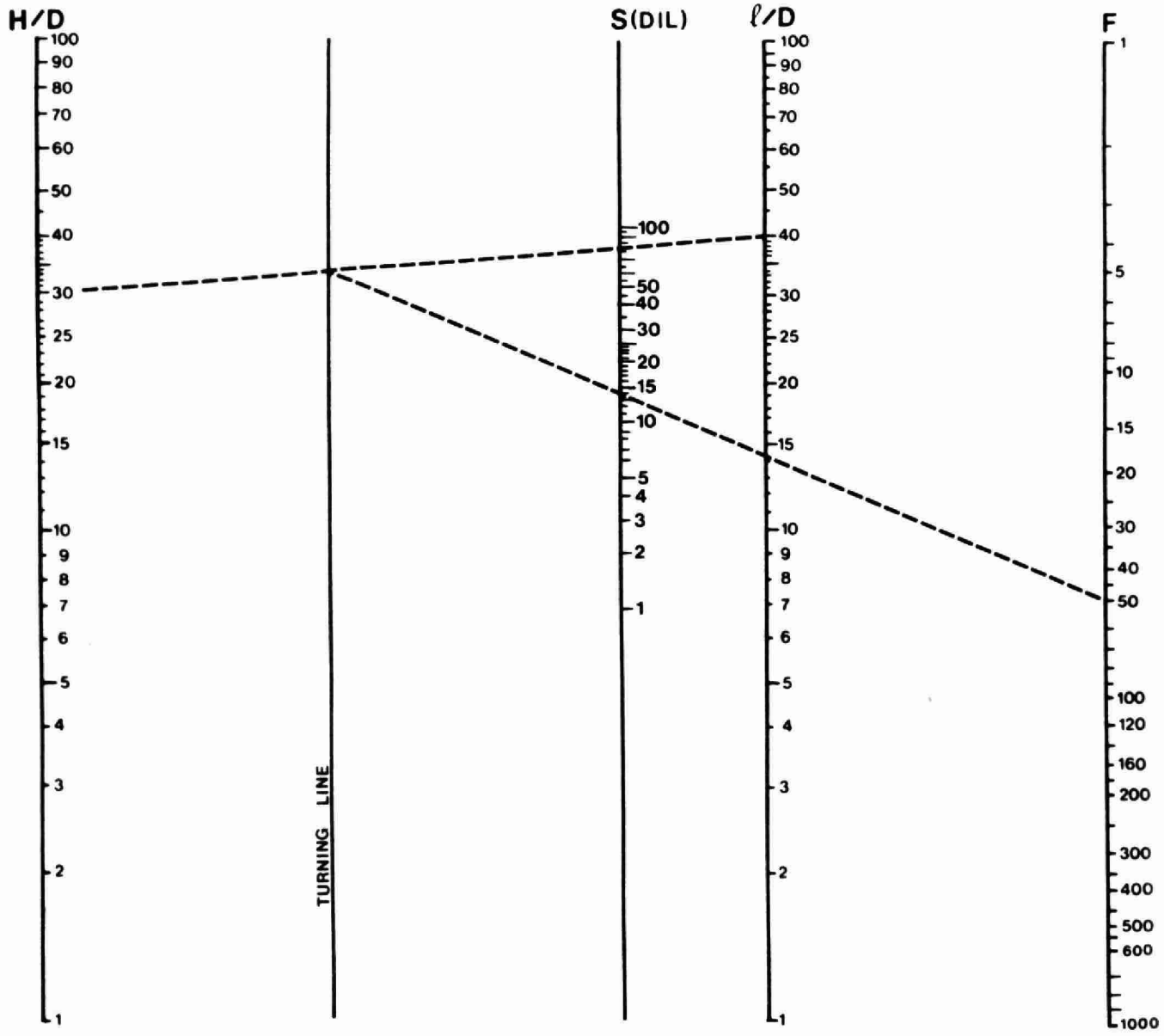

FIGURE 18 DILUTION FACTORS FOR AN ALTERNATING DIFFUSER (STRONG FAR-FIELD FRICTION EFFECTS)

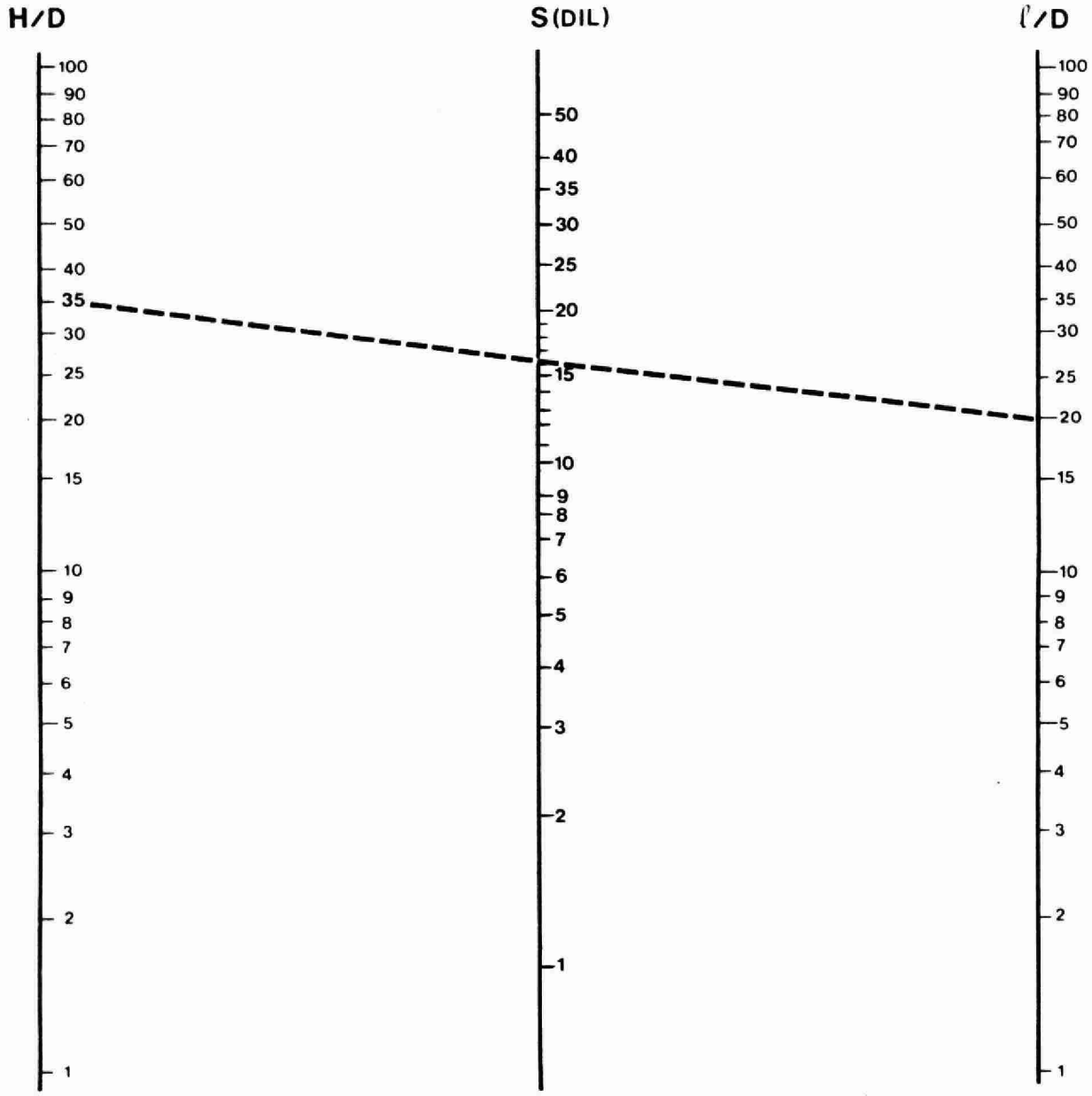

FIGURE 19 DILUTION FACTORS FOR A STAGED DIFFUSER

CURRENT DILUTION

EXPERIMENTAL MEASUREMENTS OF MINIMUM SURFACE DILUTION OF A FINITE LINE SOURCE OF BUOYANCY FLUX IN A CURRENT.

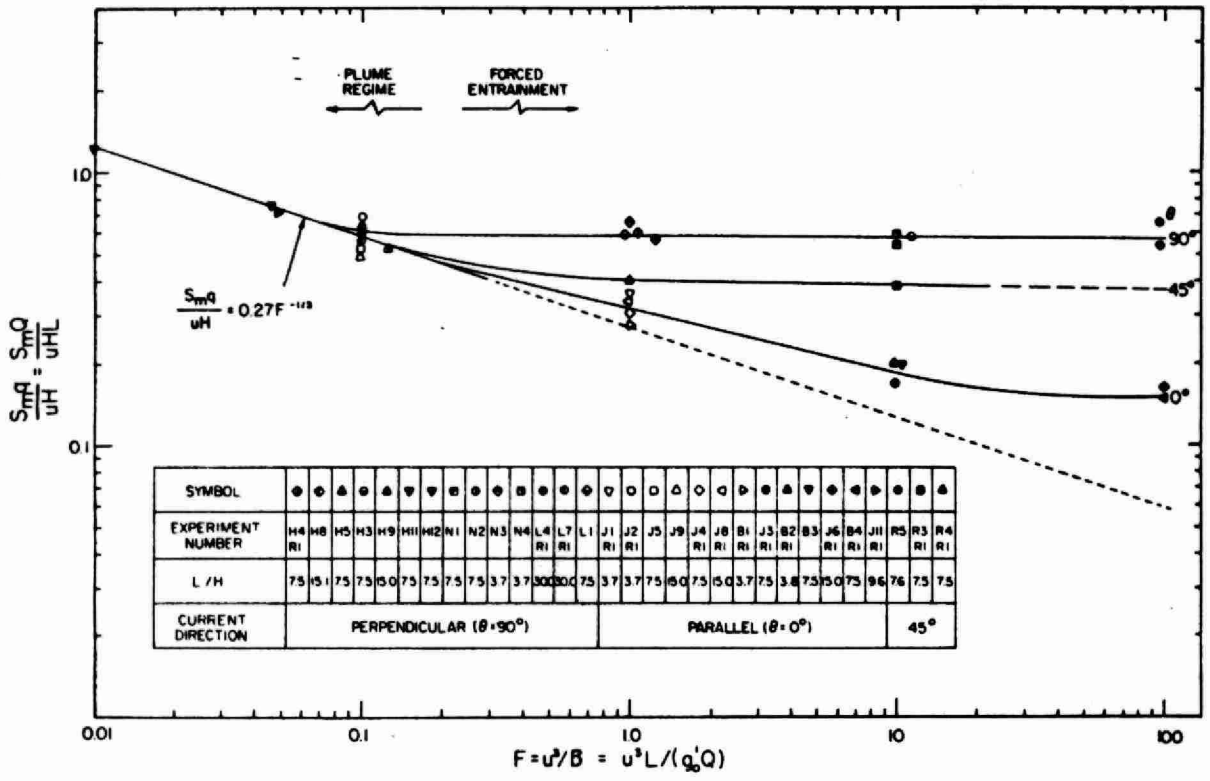

S_m = MINIMUM SURFACE DILUTION
Q = LINE SOURCE DISCHARGE RATE
L = LINE SOURCE LENGTH
H = WATER DEPTH
U = CURRENT SPEED
B = BUOYANCY FLUX PER UNIT LENGTH
$g'_o = g(\rho_r - \rho_o)/\rho_o$
g = ACCELERATION DUE TO GRAVITY
ρ_r = MASS DENSITY OF RECEIVING WATER
ρ_o = MASS DENSITY OF EFFLUENT

Figure 20. Current Dilution (After Roberts 1977)

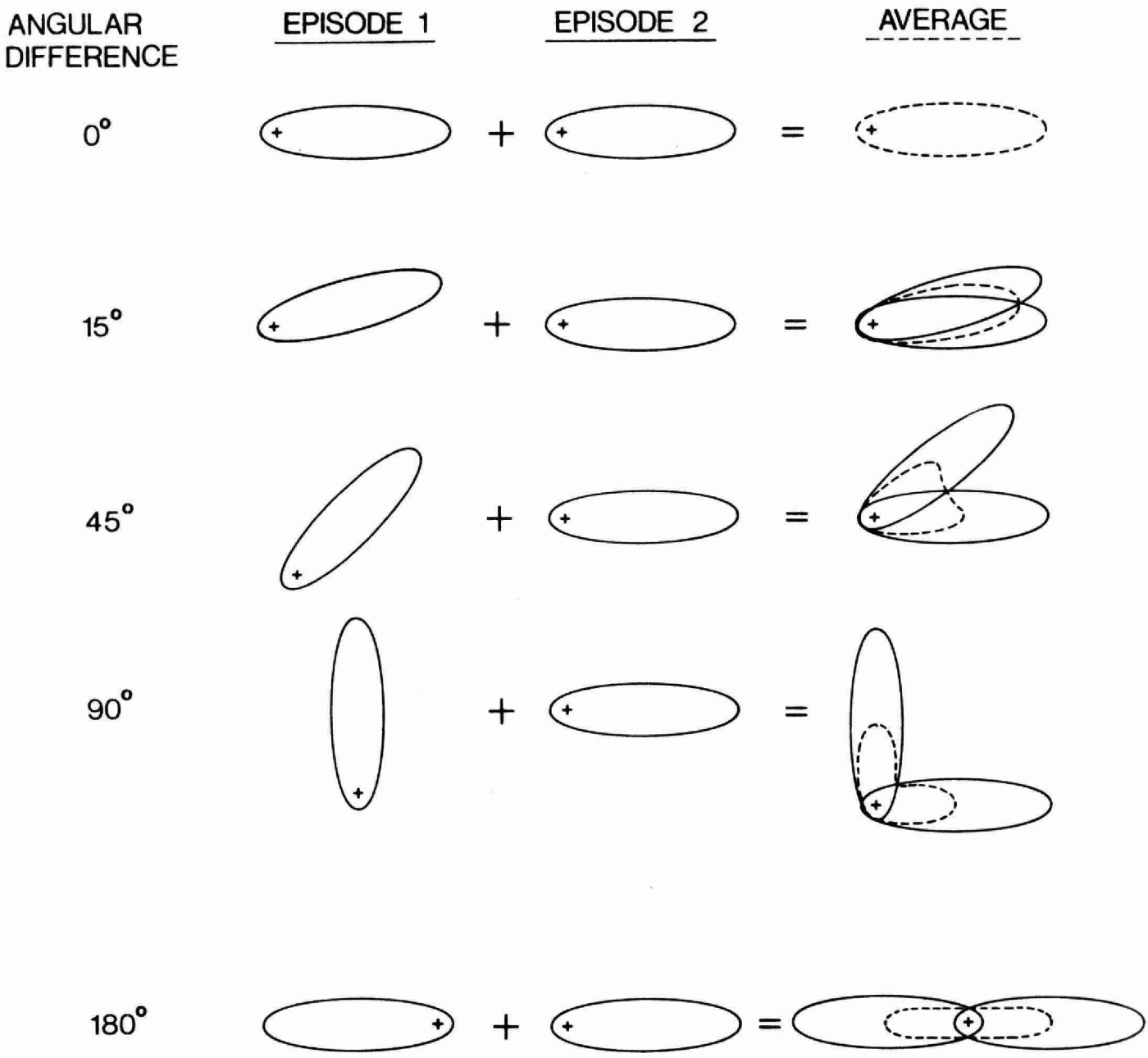

Figure 21. Schematic of the Average Concentration Field obtained when Combining Plumes with Different Orientations.

*** CURRENT ADVECTION DIAGRAM ***

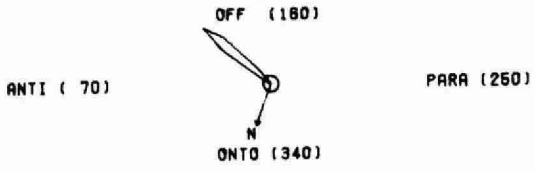

THE IRREGULAR CONTOUR CIRCUMSCRIBES THE ESTIMATED MAXIMUM ADVECTION OF THE SECTOR CURRENT SUMS.

THE ABOVE CIRCLE REPRESENTS THE OUTER 10.00 KM RADIUS CIRCLE OF THE MAIN PLOT.

*** CURRENT HISTOGRAM ***
(276 EVENTS. 5.0° SECTORS)

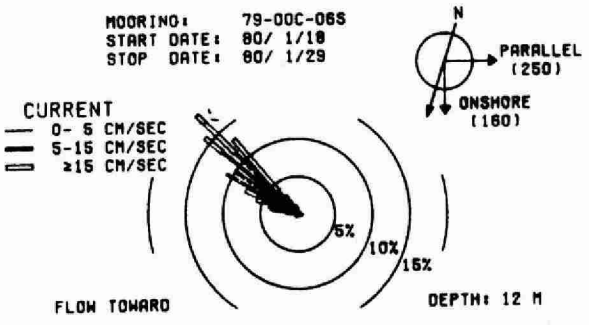

*** AVERAGE CONCENTRATION FIELD ***
(BASED ON CURRENT SPEED-DIRECTION HISTOGRAM)

CONSERVED (WINTER). LAKE ONTARIO DATA.
PICKERING. SHORE ANTIPARALLEL CURRENT.

CM MOORING:	79-00C-06S	START DATE:	80/ 1/18
CM DEPTH:	12.0 M.	STOP DATE:	80/ 1/29

DIFFUSIVITY:	1000.0	CM**2/SEC.
DISCHARGE RATE:	2000.0	L/SEC.
DISCHARGE SPEED:	50.0	CM/SEC.
DENSITY ANOMALY:	1.5	PPT.
SOURCE DILUTION:	10.0	(TO 1.0)
CURRENT SPEED:	11.8	CM/SEC.
DIFFUSION LAYER:	1.1	M THICK.
DIFFUSER DEPTH:	10.0	M.
DIFFUSER WIDTH:	200.0	M.
DIFFUSER ANGLE:	160.0	DEGREES.
SHORELINE ANGLE:	250.0	DEGREES.
DIFFUSER-SHORE:	90.0	DEGREES.
DISTANCE-SHORE:	1.3	KM.

* THE CONCENTRATIONS ARE SCALED BY 10**4
* THE DIFFUSIVITY INCREASES AS THE 4/3 POWER OF THE SCALE OF THE DIFFUSION FIELD.

OUTER RADIUS:	10.00	KM.
ANGULAR INCREMENT:	5.0	DEGREES.
RADIAL INCREMENT:	1000.0	METRES.
CURRENT HISTOGRAM:	276.0	EVENTS
SECTOR INCREMENT:	5.0	DEGREES.
SPEED INCREMENT:	1.0	CM/SEC.

Figure 22. The average concentration field of a single alongshore current episode.

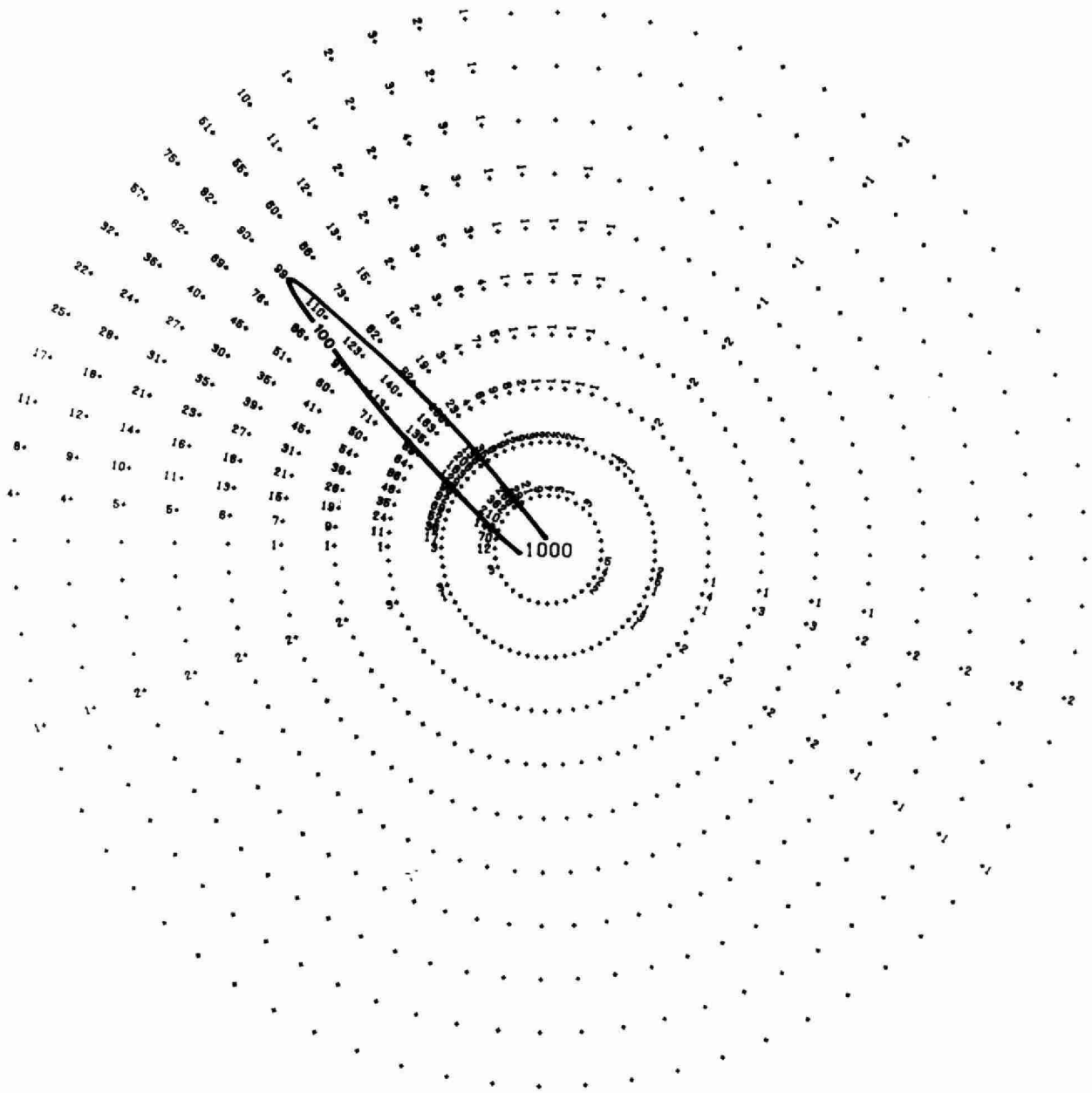

Figure 22 (cont'd)

*** CURRENT ADVECTION DIAGRAM ***

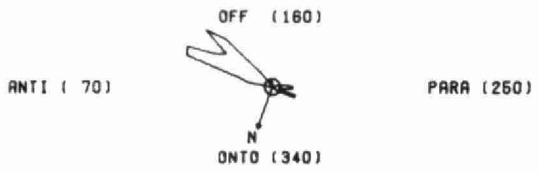

THE IRREGULAR CONTOUR CIRCUMSCRIBES THE ESTIMATED MAXIMUM ADVECTION OF THE SECTOR CURRENT SUMS.

THE ABOVE CIRCLE REPRESENTS THE OUTER 10.00 KM RADIUS CIRCLE OF THE MAIN PLOT.

*** CURRENT HISTOGRAM ***
(1320 EVENTS, 5.0° SECTORS)

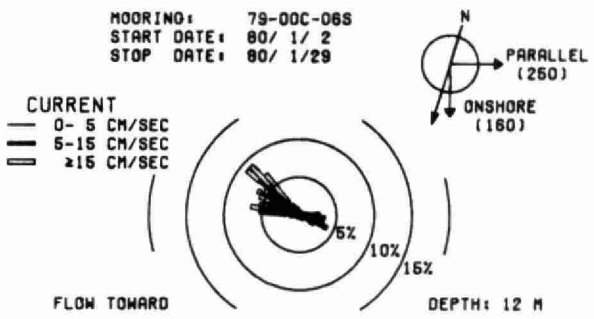

*** AVERAGE CONCENTRATION FIELD ***
(BASED ON CURRENT SPEED-DIRECTION HISTOGRAM)

CONSERVED (WINTER). 0.01 CONTOUR RANGE.
LAKE ONTARIO. PICKERING. JANUARY 1980.

CM MOORING:	79-00C-06S	START DATE:	80/ 1/ 2
CM DEPTH:	12.0 M.	STOP DATE:	80/ 1/29

DIFFUSIVITY:	1000.0	CM**2/SEC.
DISCHARGE RATE:	2000.0	L/SEC.
DISCHARGE SPEED:	50.0	CM/SEC.
DENSITY ANOMALY:	1.5	PPT.
SOURCE DILUTION:	10.0	(TO 1.0)
CURRENT SPEED:	12.6	CM/SEC.
DIFFUSION LAYER:	1.2	M THICK.
DIFFUSER DEPTH:	10.0	M.
DIFFUSER WIDTH:	200.0	M.
DIFFUSER ANGLE:	160.0	DEGREES.
SHORELINE ANGLE:	250.0	DEGREES.
DIFFUSER-SHORE:	90.0	DEGREES.
DISTANCE-SHORE:	1.3	KM.

* THE CONCENTRATIONS ARE SCALED BY 10**4
* THE DIFFUSIVITY INCREASES AS THE 4/3 POWER OF THE SCALE OF THE DIFFUSION FIELD.

OUTER RADIUS:	10.00	KM.
ANGULAR INCREMENT:	5.0	DEGREES.
RADIAL INCREMENT:	1000.0	METRES.
CURRENT HISTOGRAM:	660.0	EVENTS
SECTOR INCREMENT:	5.0	DEGREES.
SPEED INCREMENT:	1.0	CM/SEC.

Figure 23. The average concentration field of shore parallel and antiparallel current episodes.

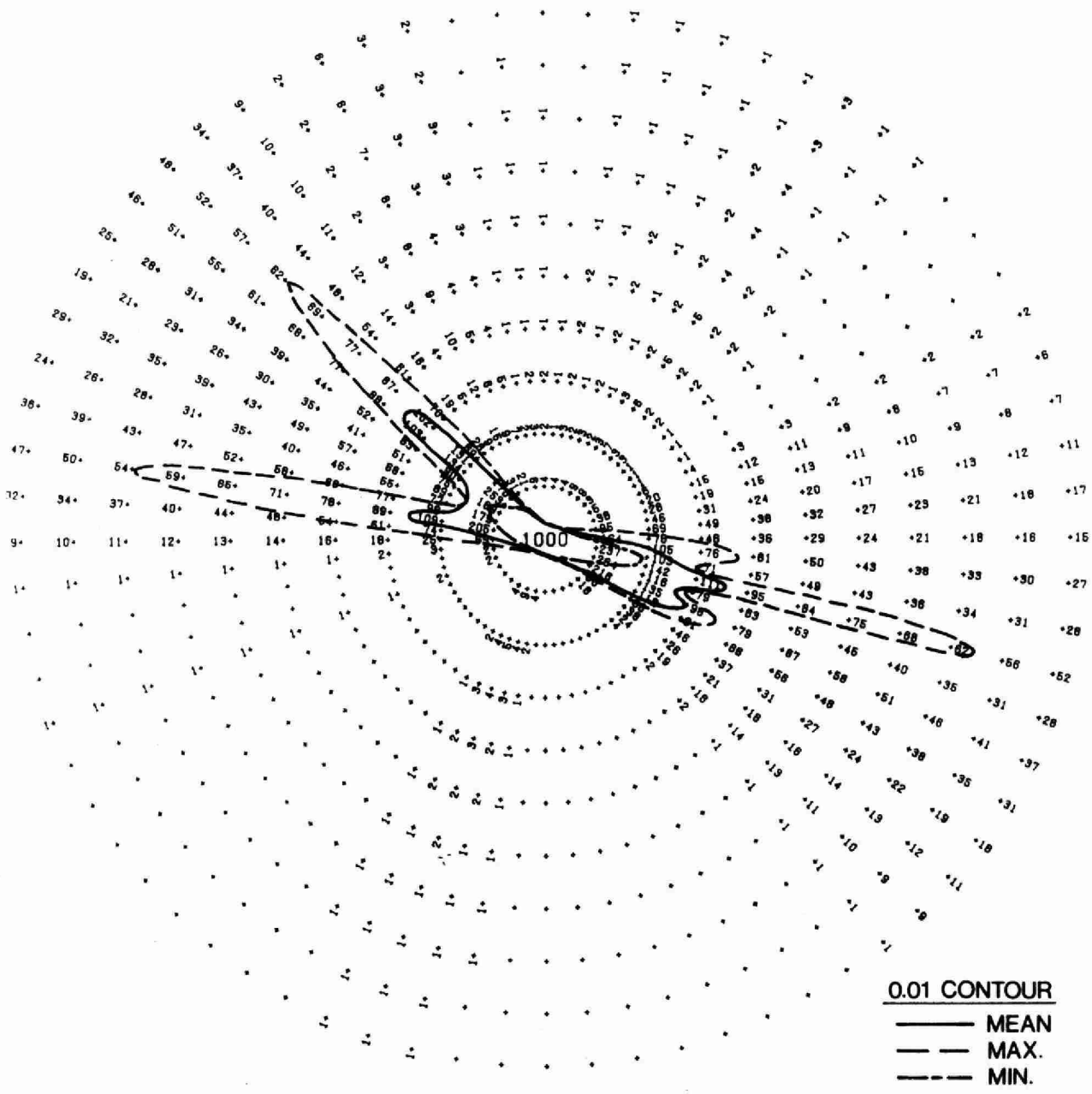

Figure 23(cont'd.)

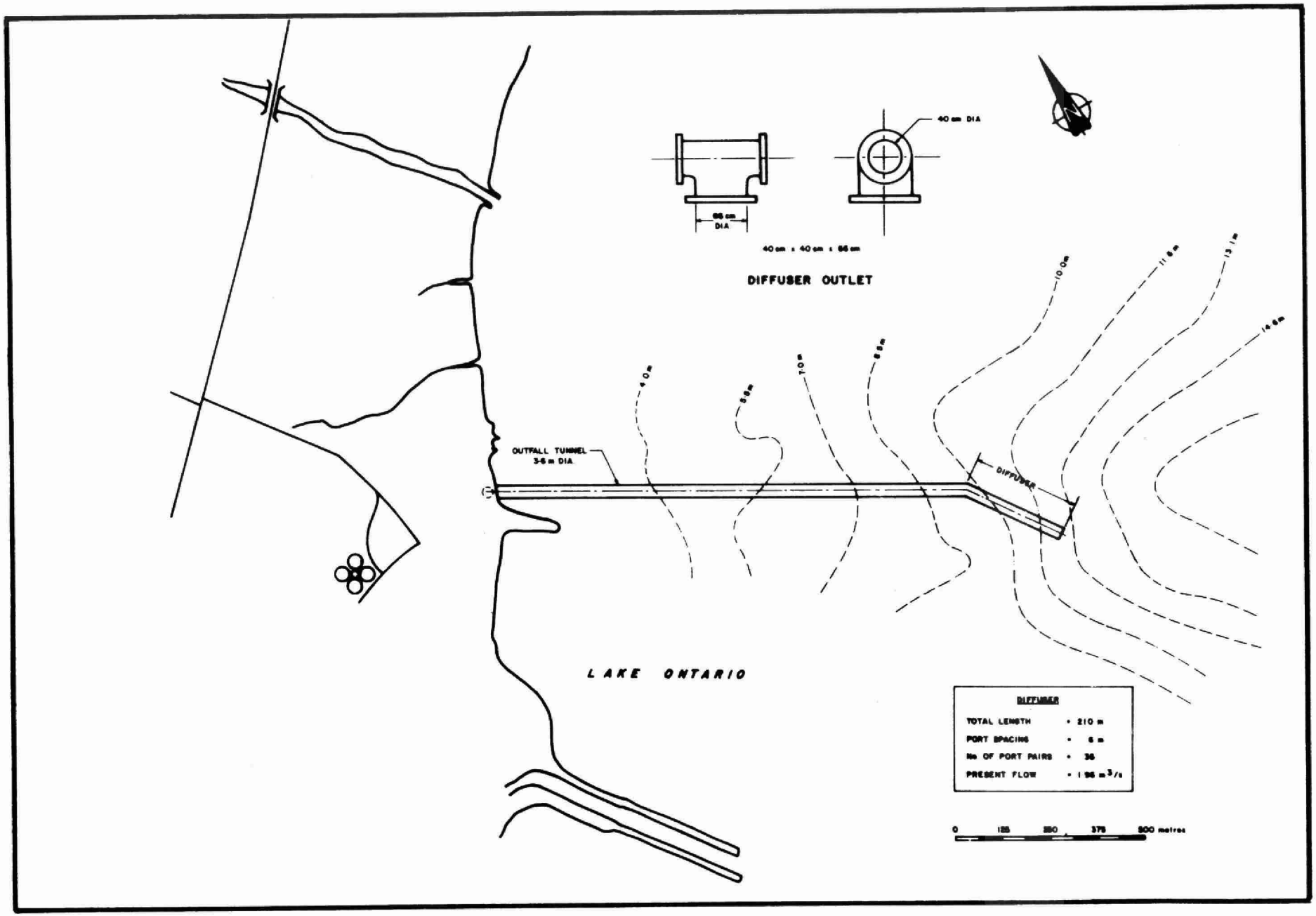

Figure 24 : Lakeview WPCP Outfall Diffuser

A COASTAL DISPERSION MODEL

FOR EFFLUENT PLUMES

APPENDIX

Contours of the mean concentration field and the extent (minimum, mean, and maximum) of the 100 concentration contour (when the effluent concentration of a conservative substance was 10000) for different current flow regimes are presented in Figures 1.01 to 1.20. Monthly summaries and stick vector plots of the current meter data (including water temperature) are presented in Figures 1.21 to 1.31.

*** CURRENT ADVECTION DIAGRAM ***

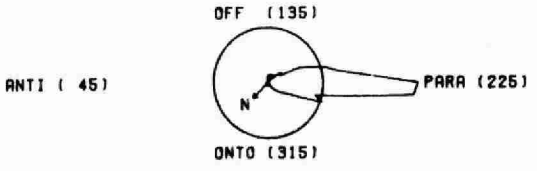

THE IRREGULAR CONTOUR CIRCUMSCRIBES THE ESTIMATED MAXIMUM ADVECTION OF THE SECTOR CURRENT SUMS.

THE ABOVE CIRCLE REPRESENTS THE OUTER 5.0 KM RADIUS CIRCLE OF THE MAIN PLOT.

*** CURRENT HISTOGRAM ***
(324 EVENTS, 5.0° SECTORS)

MOORING: 70-00C-006
START DATE: 70/ 6/ 8
STOP DATE: 70/10/13

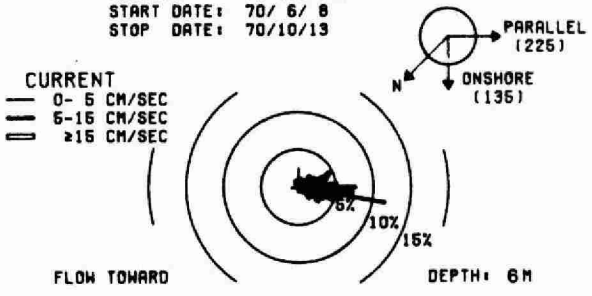

*** AVERAGE CONCENTRATION FIELD ***
(BASED ON CURRENT SPEED-DIRECTION HISTOGRAM)

CONSERVED (SUMMER). MEAN LAKEVIEW FIELD.
SPEED 0-5 CM/SEC. SHORE PARALLEL.

CM MOORING: 70-00C-006 START DATE: 70/ 6/ 8
CM DEPTH: 6.0 M. STOP DATE: 70/10/13

DIFFUSIVITY:	1200.0	CM**2/SEC.
DISCHARGE RATE:	2100.0	L/SEC.
DISCHARGE SPEED:	48.0	CM/SEC.
DENSITY ANOMALY:	1.5	PPT.
SOURCE DILUTION:	13.0	(TO 1.0)
CURRENT SPEED:	4.2	CM/SEC.
DIFFUSION LAYER:	3.9	M THICK.
DIFFUSER DEPTH:	9.5	M.
DIFFUSER WIDTH:	200.0	M.
DIFFUSER ANGLE:	135.0	DEGREES.
SHORELINE ANGLE:	225.0	DEGREES.
DIFFUSER-SHORE:	90.0	DEGREES.
DISTANCE-SHORE:	1.3	KM.

- THE CONCENTRATIONS ARE SCALED BY 10**4
- THE DIFFUSIVITY INCREASES AS THE 4/3 POWER OF THE SCALE OF THE DIFFUSION FIELD.

OUTER RADIUS:	5.0	KM.
ANGULAR INCREMENT:	5.0	DEGREES.
RADIAL INCREMENT:	500.0	METRES.
CURRENT HISTOGRAM:	324.0	EVENTS
SECTOR INCREMENT:	5.0	DEGREES.
SPEED INCREMENT:	1.0	CM/SEC.

Figure 1.01 Contours of the Mean Concentration Field

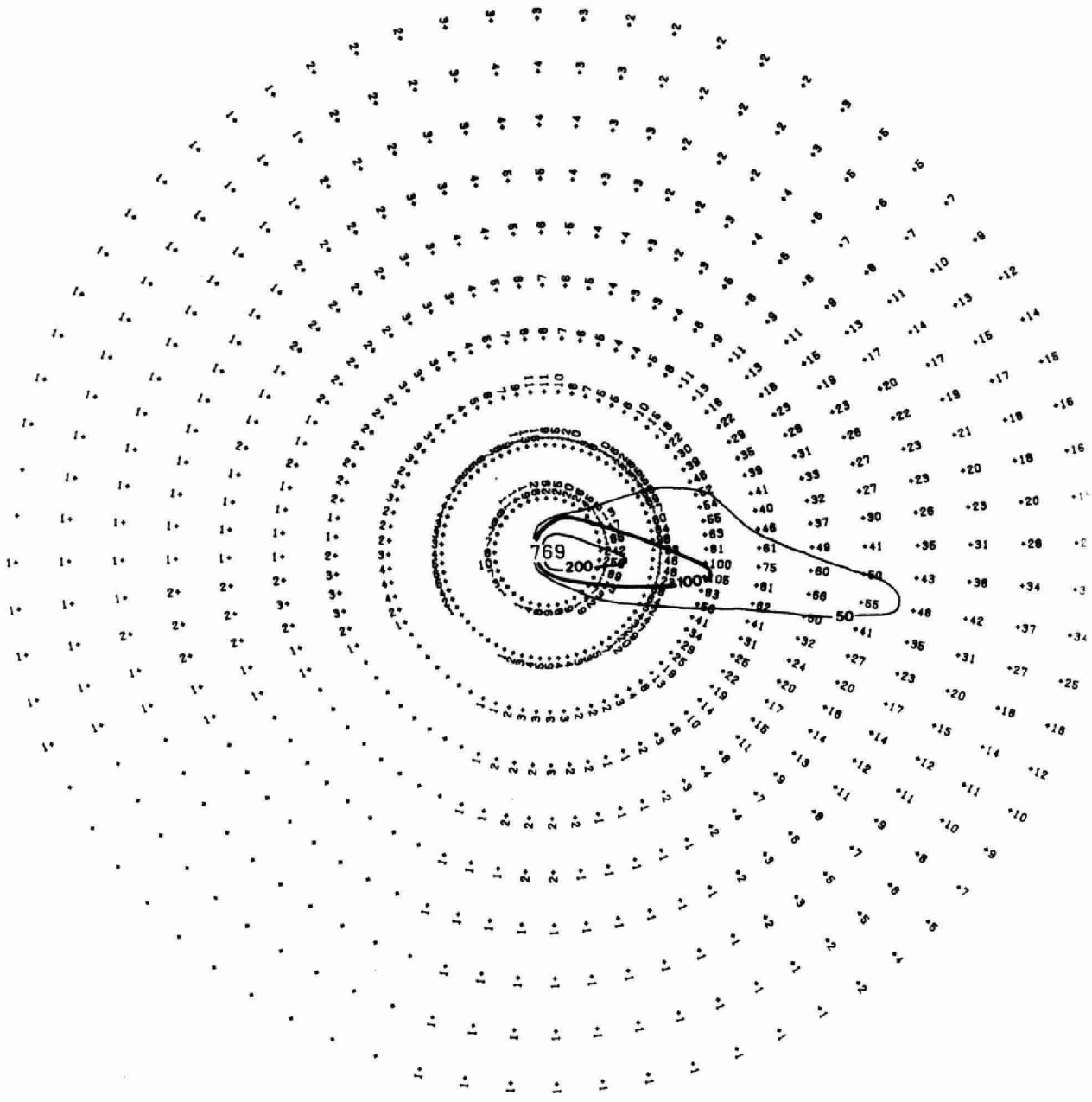

Figure 1.01 Contours of the Mean Concentration Field

*** CURRENT ADVECTION DIAGRAM ***

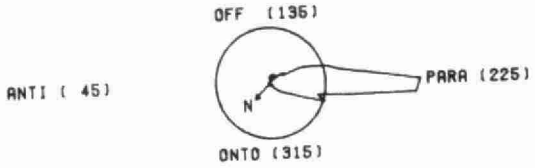

THE IRREGULAR CONTOUR CIRCUMSCRIBES THE ESTIMATED MAXIMUM ADVECTION OF THE SECTOR CURRENT SUMS.

THE ABOVE CIRCLE REPRESENTS THE OUTER 5.0 KM RADIUS CIRCLE OF THE MAIN PLOT.

*** CURRENT HISTOGRAM ***
(324 EVENTS. 5.0° SECTORS)

MOORING: 70-00C-006
START DATE: 70/ 6/ 8
STOP DATE: 70/10/13

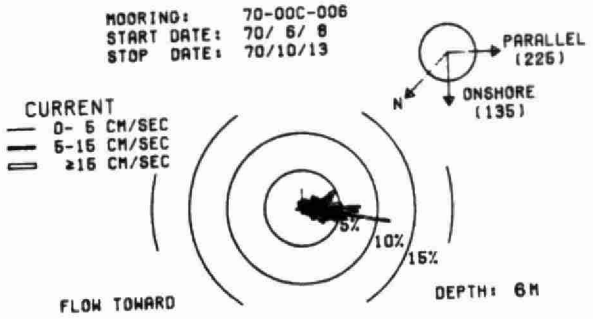

*** AVERAGE CONCENTRATION FIELD ***
(BASED ON CURRENT SPEED-DIRECTION HISTOGRAM)

CONSERVED (SUMMER). 0.01 CONTOUR RANGE.
LAKEVIEW MIN. MEAN. MAX. (0-5 CM/S. P)

CM MOORING: 70-00C-006 START DATE: 70/ 6/ 8
CM DEPTH: 6.0 M. STOP DATE: 70/10/13

DIFFUSIVITY: o	1200.0	CM**2/SEC.
DISCHARGE RATE:	2100.0	L/SEC.
DISCHARGE SPEED:	48.0	CM/SEC.
DENSITY ANOMALY:	1.5	PPT.
SOURCE DILUTION:	13.0	(TO 1.0)
CURRENT SPEED:	4.2	CM/SEC.
DIFFUSION LAYER:	3.9	M THICK.
DIFFUSER DEPTH:	9.5	M.
DIFFUSER WIDTH:	200.0	M.
DIFFUSER ANGLE:	135.0	DEGREES.
SHORELINE ANGLE:	225.0	DEGREES.
DIFFUSER-SHORE:	90.0	DEGREES.
DISTANCE-SHORE:	1.3	KM.

* THE CONCENTRATIONS ARE SCALED BY 10**4
* THE DIFFUSIVITY INCREASES AS THE 4/3 POWER OF THE SCALE OF THE DIFFUSION FIELD.

OUTER RADIUS:	5.0	KM.
ANGULAR INCREMENT:	5.0	DEGREES.
RADIAL INCREMENT:	500.0	METRES.
CURRENT HISTOGRAM:	324.0	EVENTS
SECTOR INCREMENT:	5.0	DEGREES.
SPEED INCREMENT:	1.0	CM/SEC.

Figure 1.02 Extent of the 100 Concentration Contour

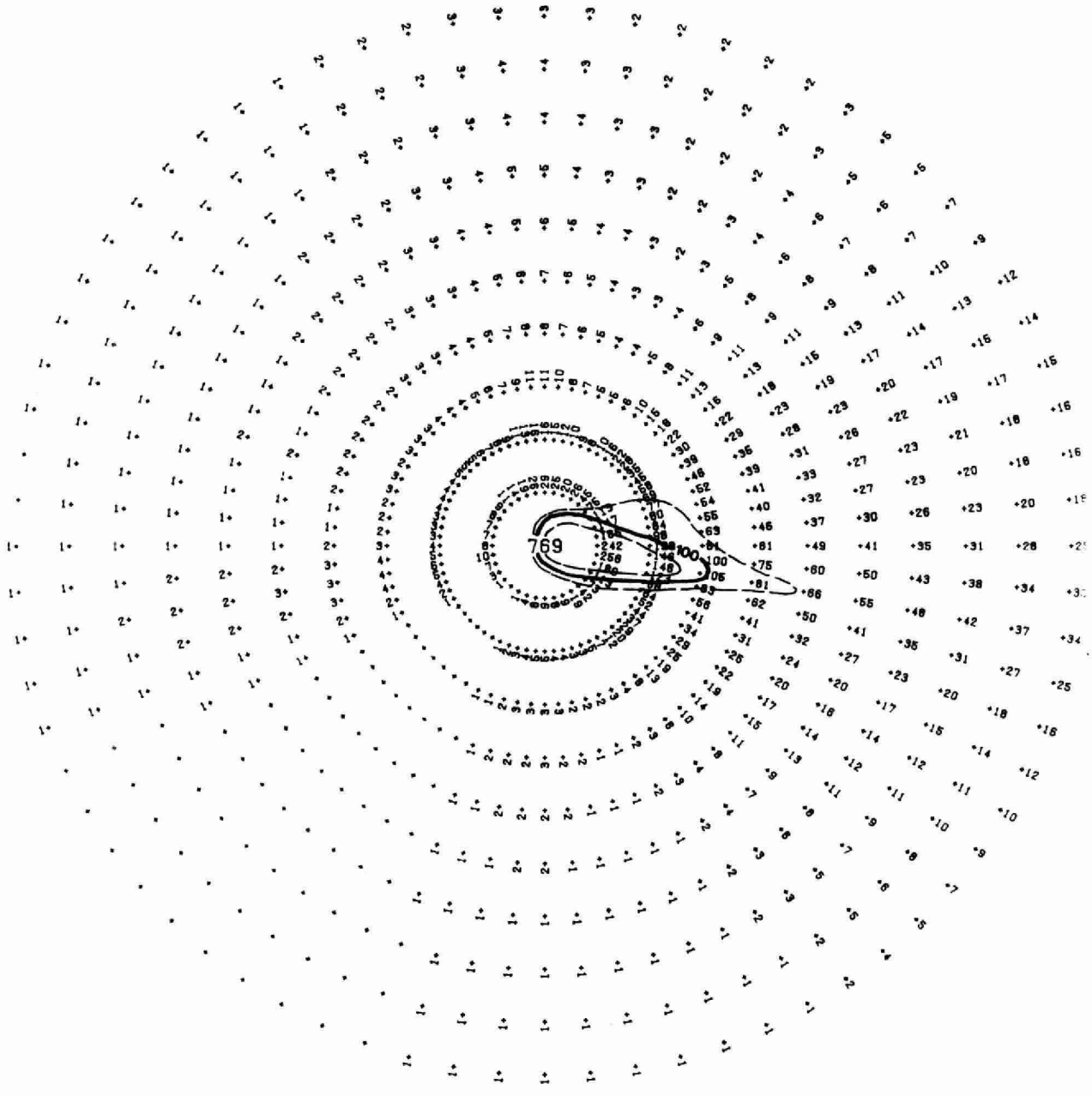

Figure 1.02 Extent of the 100 Concentration Contour

*** CURRENT ADVECTION DIAGRAM ***

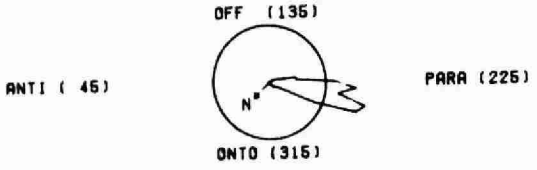

THE IRREGULAR CONTOUR CIRCUMSCRIBES THE ESTIMATED MAXIMUM ADVECTION OF THE SECTOR CURRENT SUMS.

THE ABOVE CIRCLE REPRESENTS THE OUTER 10.0 KM RADIUS CIRCLE OF THE MAIN PLOT.

*** CURRENT HISTOGRAM ***
(420 EVENTS. 5.0° SECTORS)

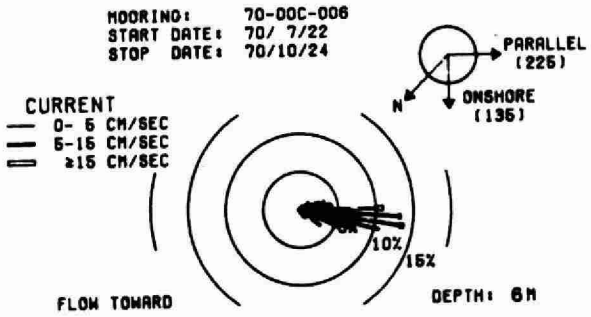

*** AVERAGE CONCENTRATION FIELD ***
(BASED ON CURRENT SPEED-DIRECTION HISTOGRAM)

CONSERVED (SUMMER). MEAN LAKEVIEW FIELD.
SPEED 5-15 CM/SEC. SHORE PARALLEL.

CM MOORING: 70-00C-006 START DATE: 70/ 7/22
CM DEPTH: 6.0 M. STOP DATE: 70/10/24

DIFFUSIVITY:	1200.0	CM**2/SEC.
DISCHARGE RATE:	2100.0	L/SEC.
DISCHARGE SPEED:	48.0	CM/SEC.
DENSITY ANOMALY:	1.5	PPT.
SOURCE DILUTION:	13.0	(TO 1.0)
CURRENT SPEED:	6.9	CM/SEC.
DIFFUSION LAYER:	2.7	M THICK.
DIFFUSER DEPTH:	9.5	M.
DIFFUSER WIDTH:	200.0	M.
DIFFUSER ANGLE:	135.0	DEGREES.
SHORELINE ANGLE:	226.0	DEGREES.
DIFFUSER-SHORE:	90.0	DEGREES.
DISTANCE-SHORE:	1.3	KM.

* THE CONCENTRATIONS ARE SCALED BY 10**4
* THE DIFFUSIVITY INCREASES AS THE 4/3 POWER OF THE SCALE OF THE DIFFUSION FIELD.

OUTER RADIUS:	10.0	KM.
ANGULAR INCREMENT:	5.0	DEGREES.
RADIAL INCREMENT:	1000.0	METRES.
CURRENT HISTOGRAM:	420.0	EVENTS
SECTOR INCREMENT:	5.0	DEGREES.
SPEED INCREMENT:	1.0	CM/SEC.

Figure 1.03 Contours of the Mean Concentration Field

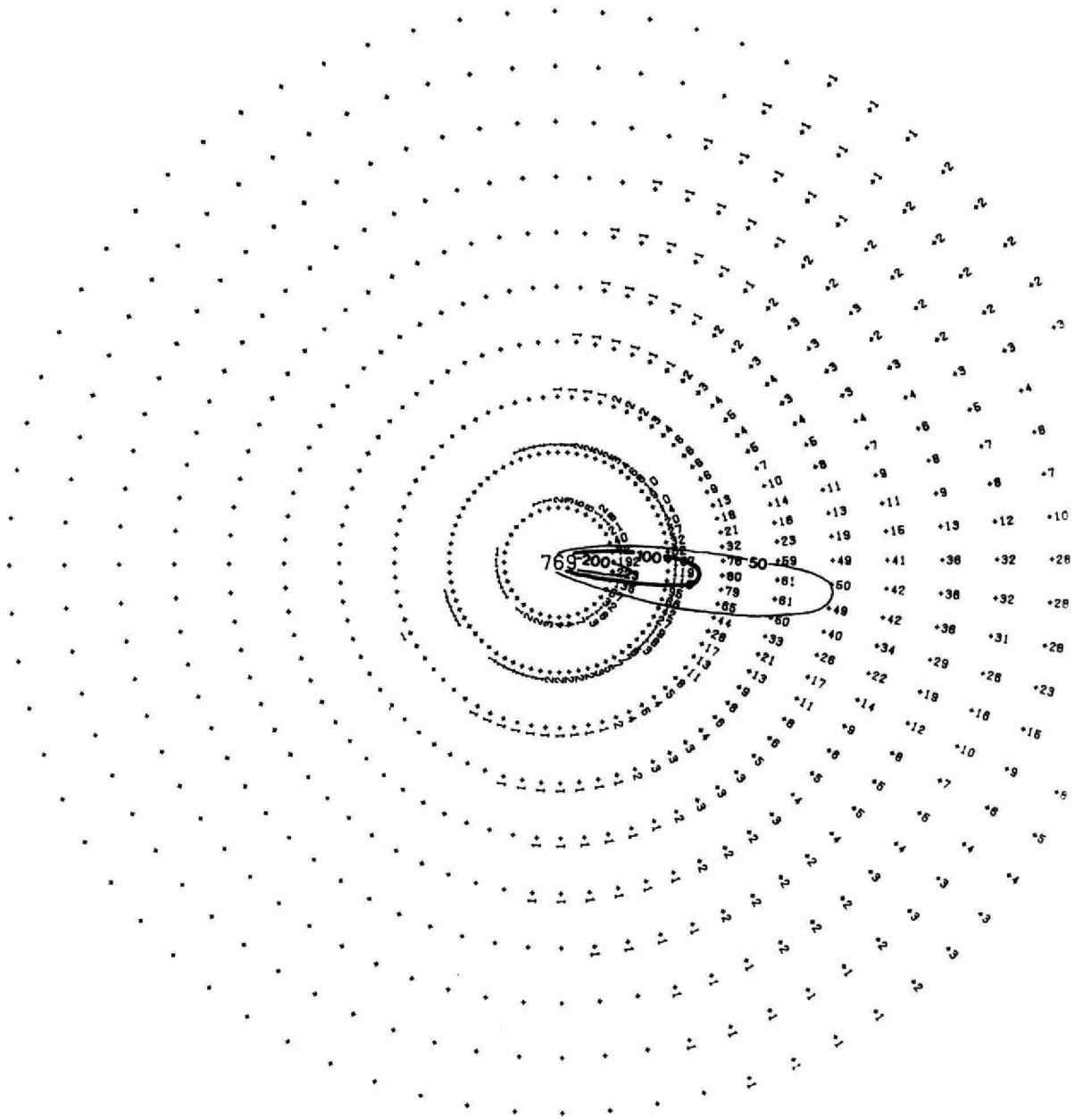

Figure 1.03 Contours of the Mean Concentration Field

*** CURRENT ADVECTION DIAGRAM ***

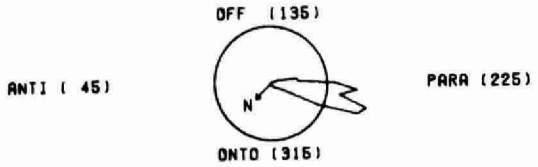

THE IRREGULAR CONTOUR CIRCUMSCRIBES THE ESTIMATED MAXIMUM ADVECTION OF THE SECTOR CURRENT SUMS.

THE ABOVE CIRCLE REPRESENTS THE OUTER 10.00 KM RADIUS CIRCLE OF THE MAIN PLOT.

*** CURRENT HISTOGRAM ***
(420 EVENTS. 5.0° SECTORS)

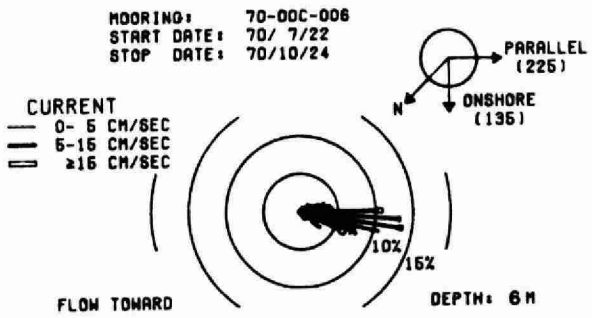

*** AVERAGE CONCENTRATION FIELD ***
(BASED ON CURRENT SPEED-DIRECTION HISTOGRAM)

CONSERVED (SUMMER). 0.01 CONTOUR RANGE.
LAKEVIEW MIN. MEAN. MAX. (5-15 CM/S. P)

CM MOORING: 70-00C-006 START DATE: 70/ 7/22
CM DEPTH: 6.0 M. STOP DATE: 70/10/24

DIFFUSIVITY:	1200.0	CM**2/SEC.
DISCHARGE RATE:	2100.0	L/SEC.
DISCHARGE SPEED:	48.0	CM/SEC.
DENSITY ANOMALY:	1.5	PPT.
SOURCE DILUTION:	13.0	(TO 1.0)
CURRENT SPEED:	6.9	CM/SEC.
DIFFUSION LAYER:	2.7	M THICK.
DIFFUSER DEPTH:	9.5	M.
DIFFUSER WIDTH:	200.0	M.
DIFFUSER ANGLE:	135.0	DEGREES.
SHORELINE ANGLE:	225.0	DEGREES.
DIFFUSER-SHORE:	90.0	DEGREES.
DISTANCE-SHORE:	1.9	KM.

- THE CONCENTRATIONS ARE SCALED BY 10**4
- THE DIFFUSIVITY INCREASES AS THE 4/3 POWER OF THE SCALE OF THE DIFFUSION FIELD.

OUTER RADIUS:	10.00	KM.
ANGULAR INCREMENT:	5.0	DEGREES.
RADIAL INCREMENT:	1000.0	METRES.
CURRENT HISTOGRAM:	420.0	EVENTS
SECTOR INCREMENT:	5.0	DEGREES.
SPEED INCREMENT:	1.0	CM/SEC.

Figure 1.04 Extent of the 100 Concentration Contour

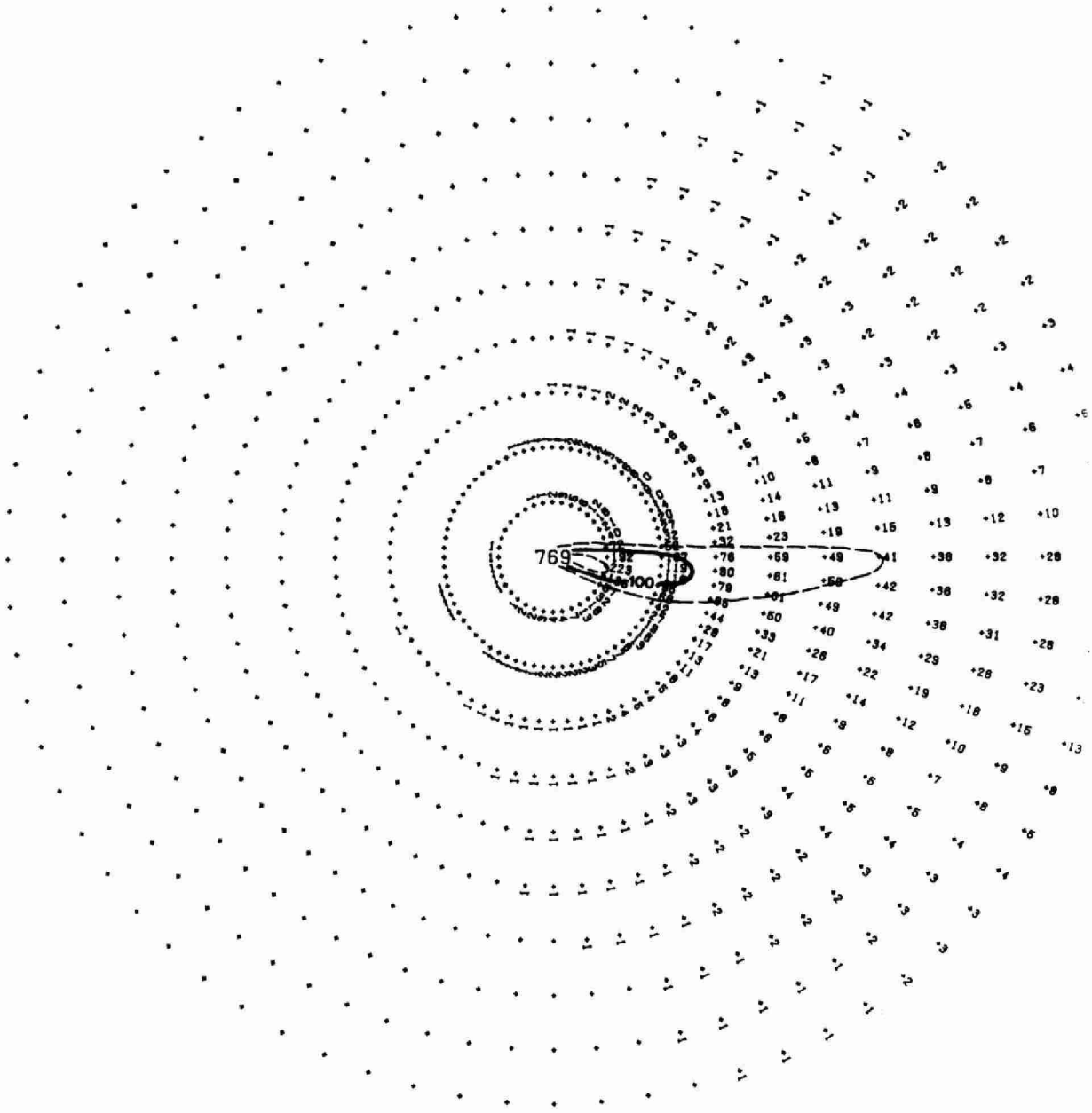

Figure 1.04 Extent of the 100 Concentration Contour

*** CURRENT ADVECTION DIAGRAM ***

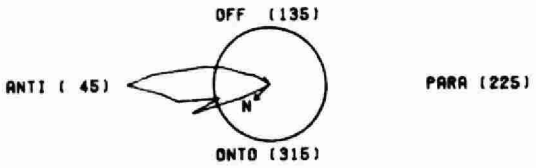

THE IRREGULAR CONTOUR CIRCUMSCRIBES THE ESTIMATED MAXIMUM ADVECTION OF THE SECTOR CURRENT SUMS.

THE ABOVE CIRCLE REPRESENTS THE OUTER 5.0 KM RADIUS CIRCLE OF THE MAIN PLOT.

*** CURRENT HISTOGRAM ***
(342 EVENTS, 5.0° SECTORS)

MOORING: 70-00C-006
START DATE: 70/ 5/28
STOP DATE: 70/10/31

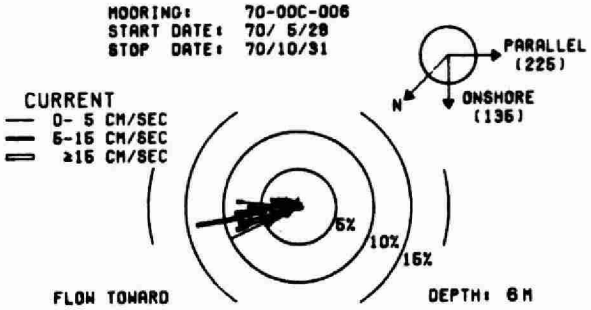

*** AVERAGE CONCENTRATION FIELD ***
(BASED ON CURRENT SPEED-DIRECTION HISTOGRAM)

CONSERVED (SUMMER). MEAN LAKEVIEW FIELD.
SPEED 0-5 CM/SEC. SHORE ANTIPARALLEL.

CM MOORING: 70-00C-006 START DATE: 70/ 5/28
CM DEPTH: 6.0 M. STOP DATE: 70/10/31

DIFFUSIVITY:	1200.0	CM**2/SEC.
DISCHARGE RATE:	2100.0	L/SEC.
DISCHARGE SPEED:	48.0	CM/SEC.
DENSITY ANOMALY:	1.5	PPT.
SOURCE DILUTION:	13.0	(TO 1.0)
CURRENT SPEED:	4.1	CM/SEC.
DIFFUSION LAYER:	4.1	M THICK.
DIFFUSER DEPTH:	9.5	M.
DIFFUSER WIDTH:	200.0	M.
DIFFUSER ANGLE:	135.0	DEGREES.
SHORELINE ANGLE:	225.0	DEGREES.
DIFFUSER-SHORE:	90.0	DEGREES.
DISTANCE-SHORE:	1.3	KM.

* THE CONCENTRATIONS ARE SCALED BY 10**4
* THE DIFFUSIVITY INCREASES AS THE 4/3 POWER OF THE SCALE OF THE DIFFUSION FIELD.

OUTER RADIUS:	5.0	KM.
ANGULAR INCREMENT:	5.0	DEGREES.
RADIAL INCREMENT:	500.0	METRES.
CURRENT HISTOGRAM:	342.0	EVENTS
SECTOR INCREMENT:	5.0	DEGREES.
SPEED INCREMENT:	1.0	CM/SEC.

Figure 1.05 Contours of the Mean Concentration Field

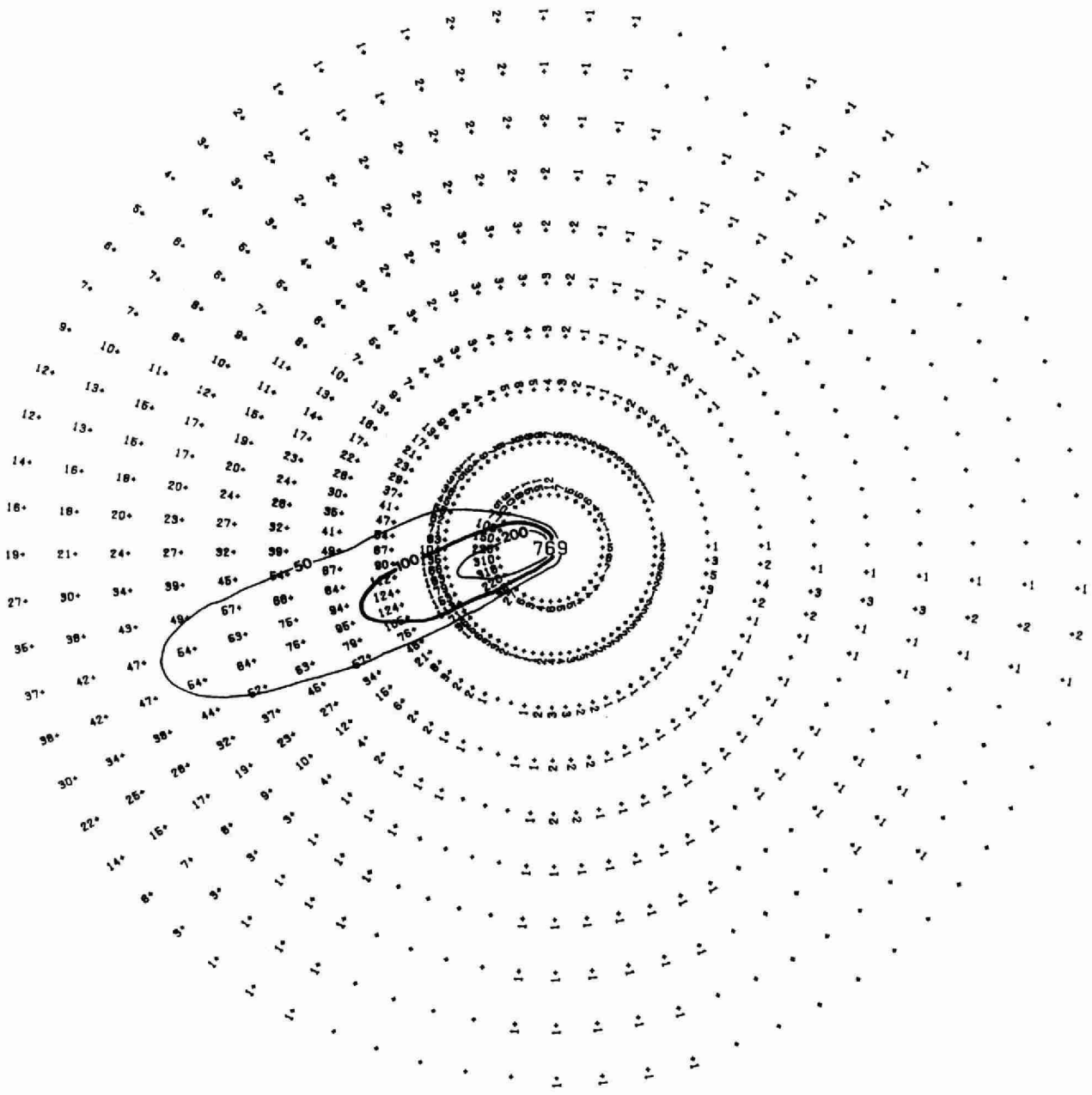

Figure 1.05 Contours of the Mean Concentration Field

*** CURRENT ADVECTION DIAGRAM ***

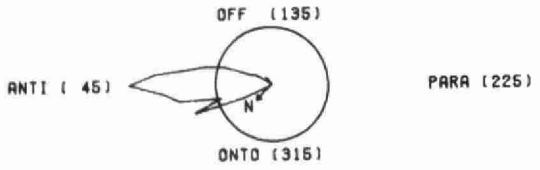

THE IRREGULAR CONTOUR CIRCUMSCRIBES THE ESTIMATED MAXIMUM ADVECTION OF THE SECTOR CURRENT SUMS.

THE ABOVE CIRCLE REPRESENTS THE OUTER 5.0 KM RADIUS CIRCLE OF THE MAIN PLOT.

*** CURRENT HISTOGRAM ***
(342 EVENTS. 5.0° SECTORS)

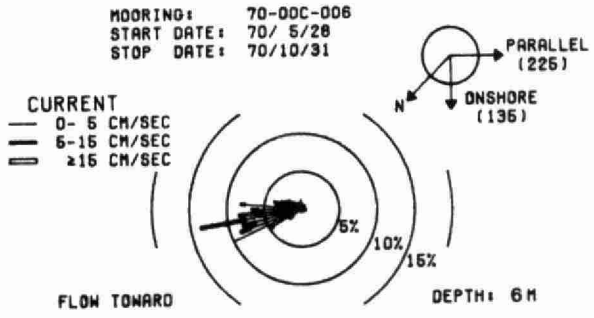

*** AVERAGE CONCENTRATION FIELD ***
(BASED ON CURRENT SPEED-DIRECTION HISTOGRAM)

CONSERVED (SUMMER). 0.01 CONTOUR RANGE.
LAKEVIEW MIN. MEAN. MAX. (0-5 CM/S. AP)

CM MOORING: 70-00C-006 START DATE: 70/ 5/28
CM DEPTH: 6.0 M. STOP DATE: 70/10/31

DIFFUSIVITY:	1200.0	CM**2/SEC.
DISCHARGE RATE:	2100.0	L/SEC.
DISCHARGE SPEED:	48.0	CM/SEC.
DENSITY ANOMALY:	1.5	PPT.
SOURCE DILUTION:	13.0	(TO 1.0)
CURRENT SPEED:	4.1	CM/SEC.
DIFFUSION LAYER:	4.1	M THICK.
DIFFUSER DEPTH:	9.5	M.
DIFFUSER WIDTH:	200.0	M.
DIFFUSER ANGLE:	135.0	DEGREES.
SHORELINE ANGLE:	225.0	DEGREES.
DIFFUSER-SHORE:	90.0	DEGREES.
DISTANCE-SHORE:	1.3	KM.

* THE CONCENTRATIONS ARE SCALED BY 10**4
* THE DIFFUSIVITY INCREASES AS THE 4/3 POWER OF THE SCALE OF THE DIFFUSION FIELD.

OUTER RADIUS:	5.0	KM.
ANGULAR INCREMENT:	5.0	DEGREES.
RADIAL INCREMENT:	500.0	METRES.
CURRENT HISTOGRAM:	342.0	EVENTS
SECTOR INCREMENT:	5.0	DEGREES.
SPEED INCREMENT:	1.0	CM/SEC.

Figure 1.06 Extent of the 100 Concentration Contour

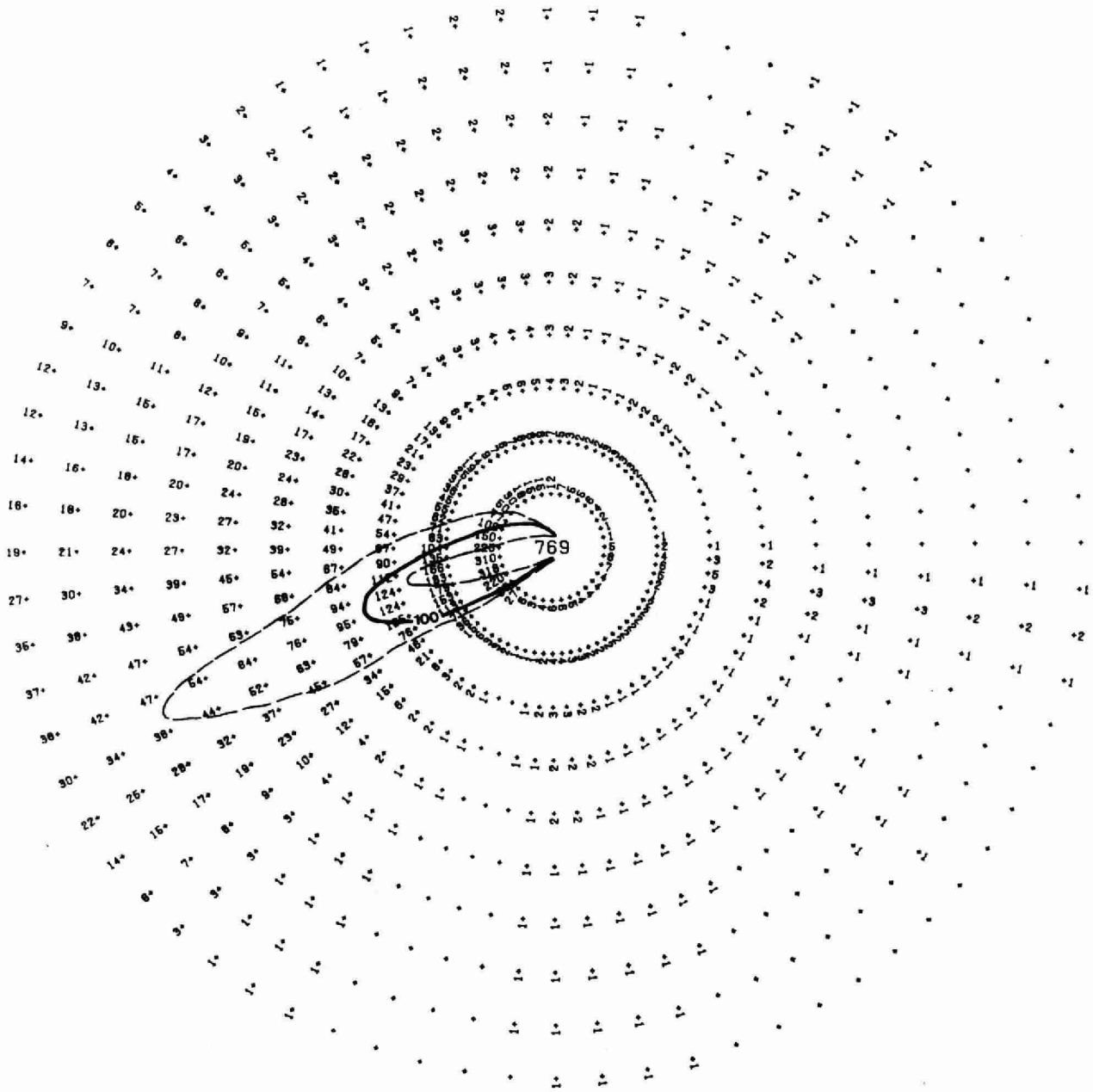

Figure 1.06 Extent of the 100 Concentration Contour

*** CURRENT ADVECTION DIAGRAM ***

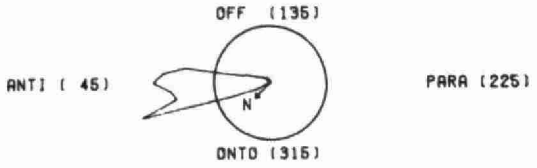

THE IRREGULAR CONTOUR CIRCUMSCRIBES THE ESTIMATED MAXIMUM ADVECTION OF THE SECTOR CURRENT SUMS.

THE ABOVE CIRCLE REPRESENTS THE OUTER 10.0 KM RADIUS CIRCLE OF THE MAIN PLOT.

*** CURRENT HISTOGRAM ***
(528 EVENTS. 5.0° SECTORS)

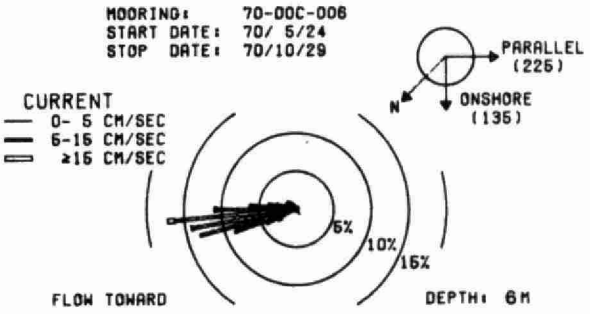

*** AVERAGE CONCENTRATION FIELD ***
(BASED ON CURRENT SPEED-DIRECTION HISTOGRAM)

CONSERVED (SUMMER). MEAN LAKEVIEW FIELD.
SPEED 5-15 CM/SEC. SHORE ANTIPARALLEL.

CM MOORING:	70-00C-006	START DATE:	70/ 5/24
CM DEPTH:	6.0 M.	STOP DATE:	70/10/29

DIFFUSIVITY:	1200.0	CM**2/SEC.
DISCHARGE RATE:	2100.0	L/SEC.
DISCHARGE SPEED:	48.0	CM/SEC.
DENSITY ANOMALY:	1.6	PPT.
SOURCE DILUTION:	13.0	(TO 1.0)
CURRENT SPEED:	6.9	CM/SEC.
DIFFUSION LAYER:	2.6	M THICK.
DIFFUSER DEPTH:	9.5	M.
DIFFUSER WIDTH:	200.0	M.
DIFFUSER ANGLE:	135.0	DEGREES.
SHORELINE ANGLE:	225.0	DEGREES.
DIFFUSER-SHORE:	90.0	DEGREES.
DISTANCE-SHORE:	1.3	KM.

- THE CONCENTRATIONS ARE SCALED BY 10**4
- THE DIFFUSIVITY INCREASES AS THE 4/3 POWER OF THE SCALE OF THE DIFFUSION FIELD.

OUTER RADIUS:	10.0	KM.
ANGULAR INCREMENT:	5.0	DEGREES.
RADIAL INCREMENT:	1000.0	METRES.
CURRENT HISTOGRAM:	528.0	EVENTS
SECTOR INCREMENT:	5.0	DEGREES.
SPEED INCREMENT:	1.0	CM/SEC.

Figure 1.07 Contours of the Mean Concentration Field

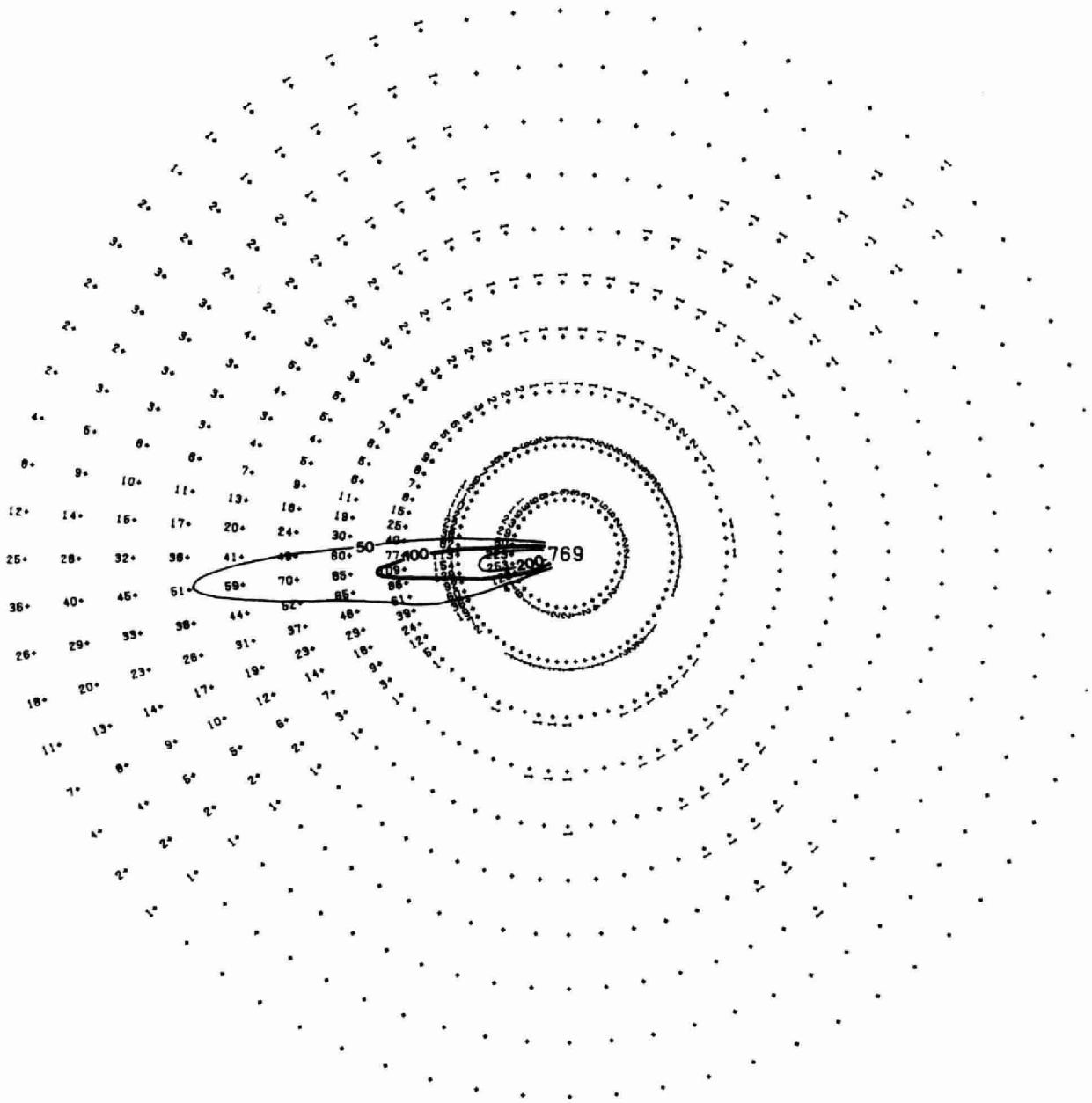

Figure 1.07 Contours of the Mean Concentration Field

*** CURRENT ADVECTION DIAGRAM ***

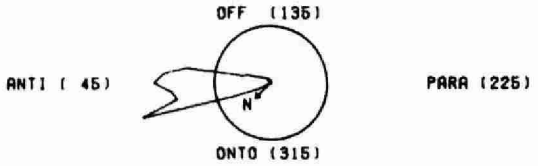

THE IRREGULAR CONTOUR CIRCUMSCRIBES THE ESTIMATED MAXIMUM ADVECTION OF THE SECTOR CURRENT SUMS.

THE ABOVE CIRCLE REPRESENTS THE OUTER 10.00 KM RADIUS CIRCLE OF THE MAIN PLOT.

*** CURRENT HISTOGRAM ***
(528 EVENTS, 5.0° SECTORS)

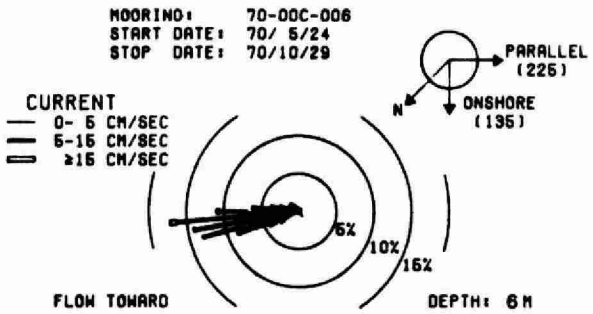

*** AVERAGE CONCENTRATION FIELD ***
(BASED ON CURRENT SPEED-DIRECTION HISTOGRAM)

CONSERVED (SUMMER). 0.01 CONTOUR RANGE.
LAKEVIEW MIN, MEAN, MAX. (5-15 CM/S, AP)

CM MOORING:	70-00C-006	START DATE:	70/ 5/24
CM DEPTH:	6.0 M.	STOP DATE:	70/10/29

DIFFUSIVITY:	1200.0	CM**2/SEC.
DISCHARGE RATE:	2100.0	L/SEC.
DISCHARGE SPEED:	48.0	CM/SEC.
DENSITY ANOMALY:	1.5	PPT.
SOURCE DILUTION:	13.0	(TO 1.0)
CURRENT SPEED:	6.9	CM/SEC.
DIFFUSION LAYER:	2.6	M THICK.
DIFFUSER DEPTH:	9.5	M.
DIFFUSER WIDTH:	200.0	M.
DIFFUSER ANGLE:	135.0	DEGREES.
SHORELINE ANGLE:	225.0	DEGREES.
DIFFUSER-SHORE:	90.0	DEGREES.
DISTANCE-SHORE:	1.3	KM.

* THE CONCENTRATIONS ARE SCALED BY 10**4
* THE DIFFUSIVITY INCREASES AS THE 4/3 POWER OF THE SCALE OF THE DIFFUSION FIELD.

OUTER RADIUS:	10.00	KM.
ANGULAR INCREMENT:	5.0	DEGREES.
RADIAL INCREMENT:	1000.0	METRES.
CURRENT HISTOGRAM:	528.0	EVENTS
SECTOR INCREMENT:	5.0	DEGREES.
SPEED INCREMENT:	1.0	CM/SEC.

Figure 1.08 Extent of the 100 Concentration Contour

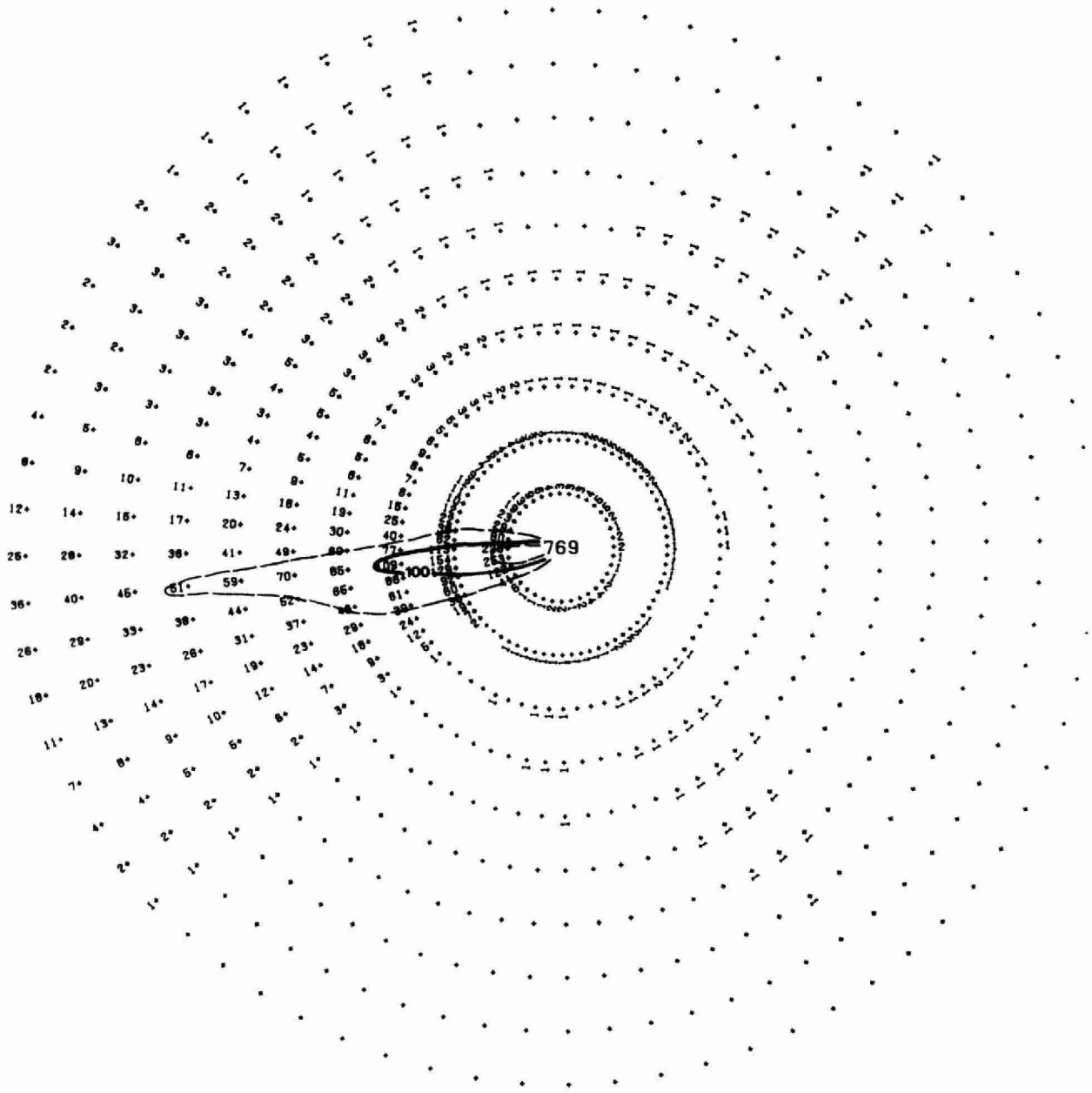

Figure 1.08 Extent of the 100 Concentration Contour

*** CURRENT ADVECTION DIAGRAM ***

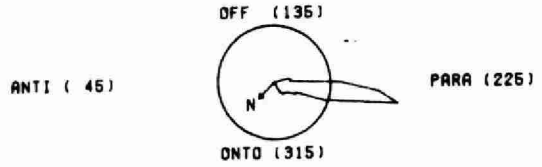

THE IRREGULAR CONTOUR CIRCUMSCRIBES THE ESTIMATED MAXIMUM ADVECTION OF THE SECTOR CURRENT SUMS.

THE ABOVE CIRCLE REPRESENTS THE OUTER 5.0 KM RADIUS CIRCLE OF THE MAIN PLOT.

*** CURRENT HISTOGRAM ***
(197 EVENTS. 5.0° SECTORS)

MOORING: SEVERAL
START DATE: 70/11/29
STOP DATE: 71/ 4/ 3

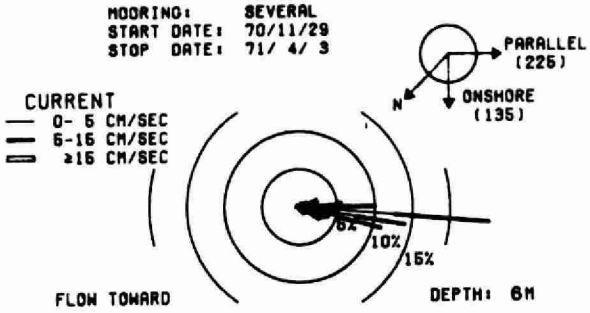

*** AVERAGE CONCENTRATION FIELD ***
(BASED ON CURRENT SPEED-DIRECTION HISTOGRAM)

CONSERVED (WINTER). MEAN LAKEVIEW FIELD.
SPEED 0-5 CM/SEC. SHORE PARALLEL.

CM MOORING: SEVERAL — START DATE: 70/11/29
CM DEPTH: 6.0 M. — STOP DATE: 71/ 4/ 3

DIFFUSIVITY:	1200.0	CM**2/SEC.
DISCHARGE RATE:	2100.0	L/SEC.
DISCHARGE SPEED:	48.0	CM/SEC.
DENSITY ANOMALY:	1.5	PPT.
SOURCE DILUTION:	13.0	(TO 1.0)
CURRENT SPEED:	4.6	CM/SEC.
DIFFUSION LAYER:	3.7	M THICK.
DIFFUSER DEPTH:	9.5	M.
DIFFUSER WIDTH:	200.0	M.
DIFFUSER ANGLE:	135.0	DEGREES.
SHORELINE ANGLE:	225.0	DEGREES.
DIFFUSER-SHORE:	90.0	DEGREES.
DISTANCE-SHORE:	1.3	KM.

- THE CONCENTRATIONS ARE SCALED BY 10**4
- THE DIFFUSIVITY INCREASES AS THE 4/3 POWER OF THE SCALE OF THE DIFFUSION FIELD.

OUTER RADIUS:	5.0	KM.
ANGULAR INCREMENT:	5.0	DEGREES.
RADIAL INCREMENT:	500.0	METRES.
CURRENT HISTOGRAM:	197.0	EVENTS
SECTOR INCREMENT:	5.0	DEGREES.
SPEED INCREMENT:	1.0	CM/SEC.

Figure 1.09 Contours of the Mean Concentration Field

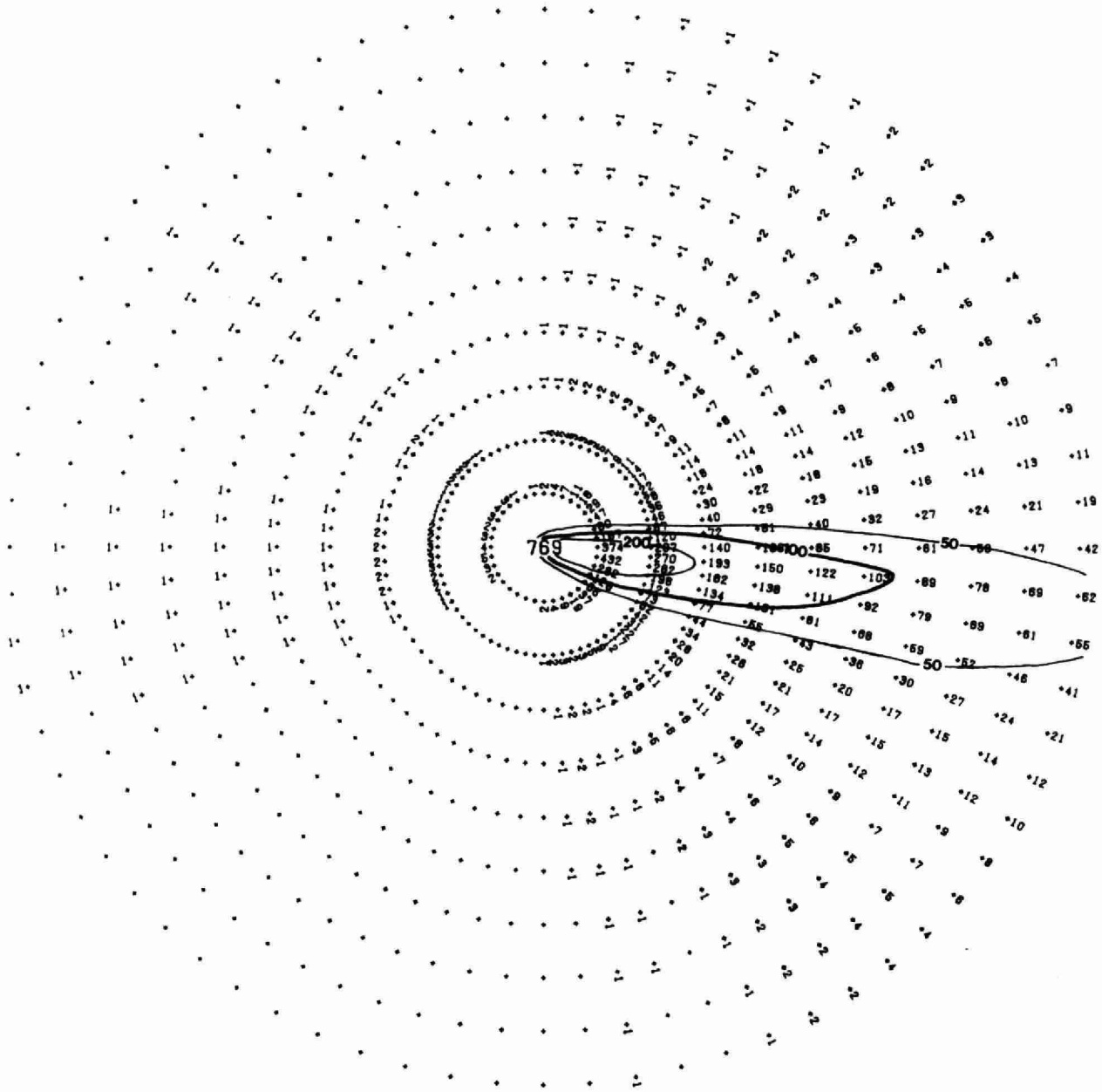

Figure 1.09 Contours of the Mean Concentration Field

*** CURRENT ADVECTION DIAGRAM ***

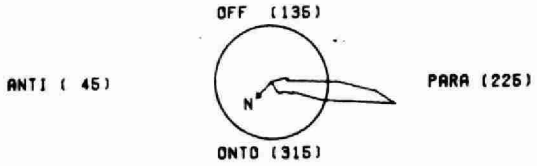

THE IRREGULAR CONTOUR CIRCUMSCRIBES THE ESTIMATED MAXIMUM ADVECTION OF THE SECTOR CURRENT SUMS.

THE ABOVE CIRCLE REPRESENTS THE OUTER 5.0 KM RADIUS CIRCLE OF THE MAIN PLOT.

*** CURRENT HISTOGRAM ***
(197 EVENTS. 5.0° SECTORS)

MOORING: SEVERAL
START DATE: 70/11/29
STOP DATE: 71/ 4/ 3

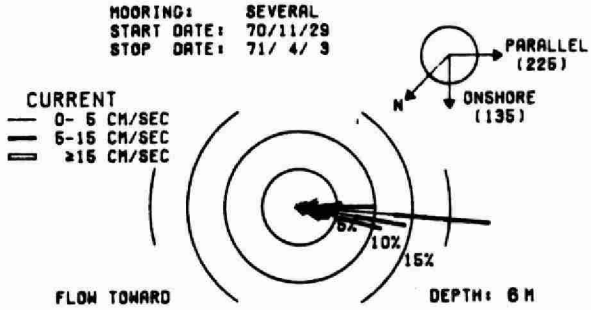

*** AVERAGE CONCENTRATION FIELD ***
(BASED ON CURRENT SPEED-DIRECTION HISTOGRAM)

CONSERVED (WINTER). 0.01 CONTOUR RANGE.
LAKEVIEW MIN. MEAN. MAX. (0-5 CM/S. P)

CM MOORING: SEVERAL START DATE: 70/11/29
CM DEPTH: 6.0 M. STOP DATE: 71/ 4/ 3

DIFFUSIVITY:	1200.0	CM**2/SEC.
DISCHARGE RATE:	2100.0	L/SEC.
DISCHARGE SPEED:	48.0	CM/SEC.
DENSITY ANOMALY:	1.5	PPT.
SOURCE DILUTION:	13.0	(TO 1.0)
CURRENT SPEED:	4.5	CM/SEC.
DIFFUSION LAYER:	3.7	M THICK.
DIFFUSER DEPTH:	9.5	M.
DIFFUSER WIDTH:	200.0	M.
DIFFUSER ANGLE:	135.0	DEGREES.
SHORELINE ANGLE:	225.0	DEGREES.
DIFFUSER-SHORE:	90.0	DEGREES.
DISTANCE-SHORE:	1.3	KM.

* THE CONCENTRATIONS ARE SCALED BY 10**4
* THE DIFFUSIVITY INCREASES AS THE 4/3 POWER OF THE SCALE OF THE DIFFUSION FIELD.

OUTER RADIUS:	5.0	KM.
ANGULAR INCREMENT:	5.0	DEGREES.
RADIAL INCREMENT:	500.0	METRES.
CURRENT HISTOGRAM:	197.0	EVENTS
SECTOR INCREMENT:	5.0	DEGREES.
SPEED INCREMENT:	1.0	CM/SEC.

Figure 1.10 Extent of the 100 Concentration Contour

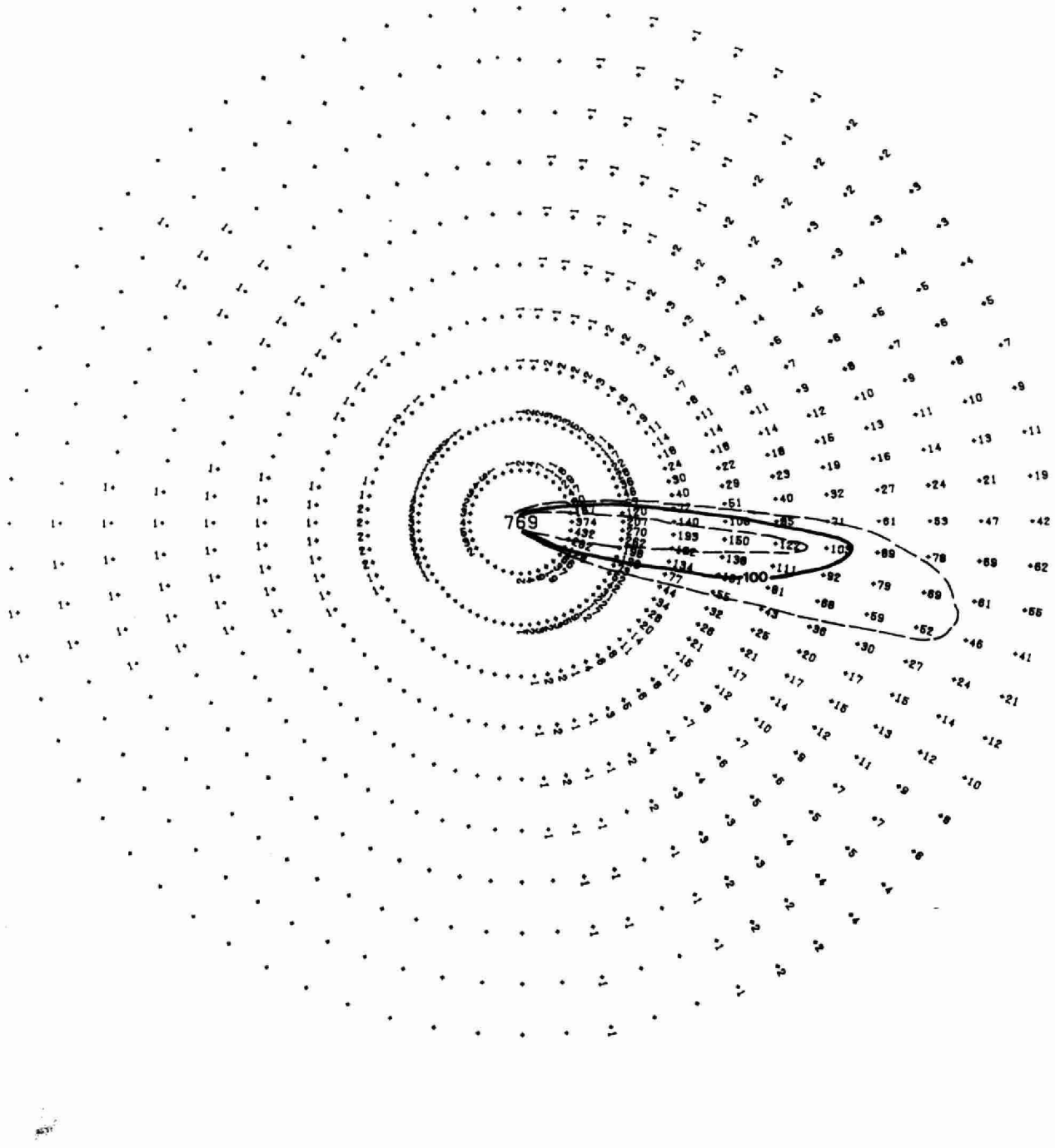

Figure 1.10 Extent of the 100 Concentration Contour

*** CURRENT ADVECTION DIAGRAM ***

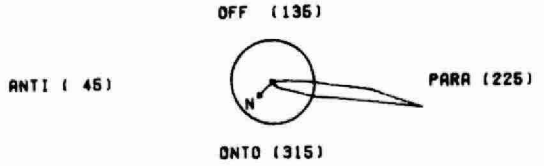

THE IRREGULAR CONTOUR CIRCUMSCRIBES THE ESTIMATED MAXIMUM ADVECTION OF THE SECTOR CURRENT SUMS.

THE ABOVE CIRCLE REPRESENTS THE OUTER 10.0 KM RADIUS CIRCLE OF THE MAIN PLOT.

*** CURRENT HISTOGRAM ***
(504 EVENTS, 5.0° SECTORS)

MOORING: SEVERAL
START DATE: 70/11/ 6
STOP DATE: 71/ 4/ 8

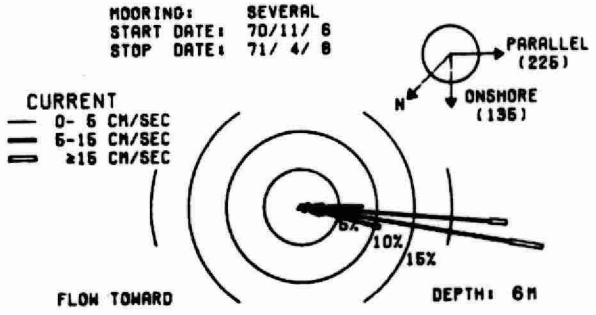

*** AVERAGE CONCENTRATION FIELD ***
(BASED ON CURRENT SPEED-DIRECTION HISTOGRAM)

CONSERVED (WINTER). MEAN LAKEVIEW FIELD.
SPEED 5-15 CM/SEC. SHORE PARALLEL.

CM MOORING: SEVERAL — START DATE: 70/11/ 6
CM DEPTH: 6.0 M. — STOP DATE: 71/ 4/ 8

DIFFUSIVITY:	1200.0	CM**2/SEC.
DISCHARGE RATE:	2100.0	L/SEC.
DISCHARGE SPEED:	48.0	CM/SEC.
DENSITY ANOMALY:	1.5	PPT.
SOURCE DILUTION:	13.0	(TO 1.0)
CURRENT SPEED:	8.3	CM/SEC.
DIFFUSION LAYER:	2.4	M THICK.
DIFFUSER DEPTH:	9.5	M.
DIFFUSER WIDTH:	200.0	M.
DIFFUSER ANGLE:	135.0	DEGREES.
SHORELINE ANGLE:	225.0	DEGREES.
DIFFUSER-SHORE:	90.0	DEGREES.
DISTANCE-SHORE:	1.3	KM.

* THE CONCENTRATIONS ARE SCALED BY 10**4
* THE DIFFUSIVITY INCREASES AS THE 4/3 POWER OF THE SCALE OF THE DIFFUSION FIELD.

OUTER RADIUS:	10.0	KM.
ANGULAR INCREMENT:	5.0	DEGREES.
RADIAL INCREMENT:	1000.0	METRES.
CURRENT HISTOGRAM:	504.0	EVENTS
SECTOR INCREMENT:	5.0	DEGREES.
SPEED INCREMENT:	1.0	CM/SEC.

Figure 1.11 Contours of the Mean Concentration Field

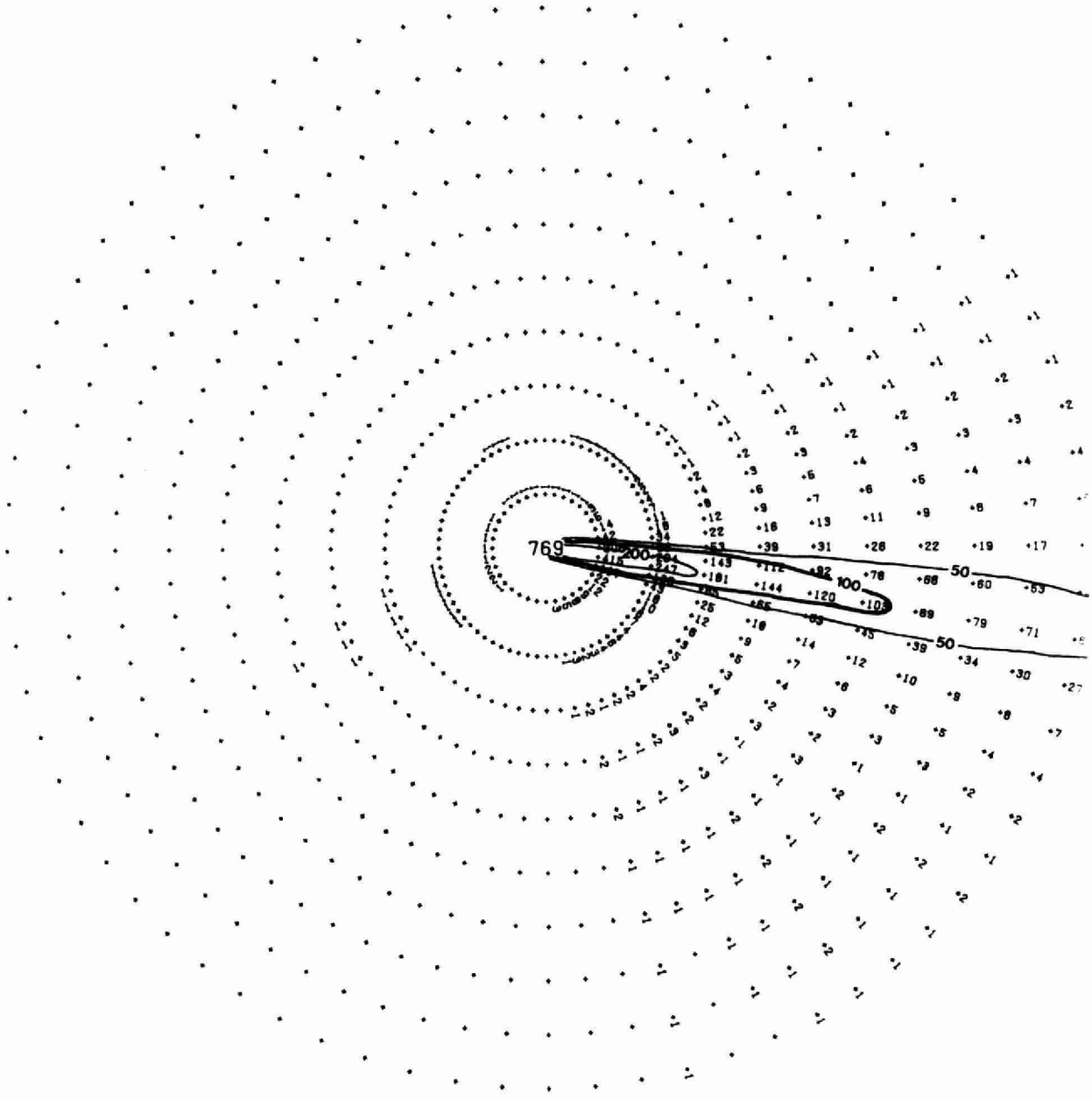

Figure 1.11 Contours of the Mean Concentration Field

*** CURRENT ADVECTION DIAGRAM ***

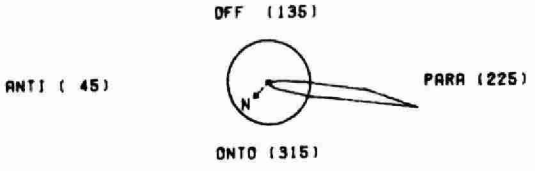

THE IRREGULAR CONTOUR CIRCUMSCRIBES THE ESTIMATED MAXIMUM ADVECTION OF THE SECTOR CURRENT SUMS.

THE ABOVE CIRCLE REPRESENTS THE OUTER 10.00 KM RADIUS CIRCLE OF THE MAIN PLOT.

*** CURRENT HISTOGRAM ***
(504 EVENTS. 5.0° SECTORS)

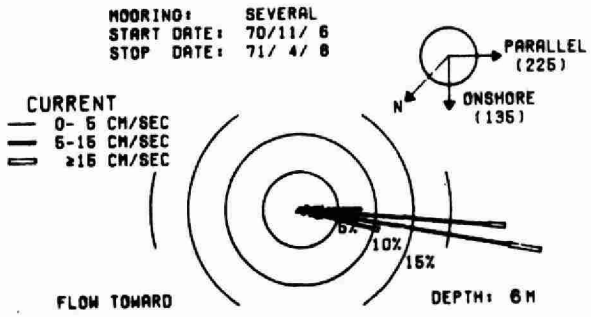

*** AVERAGE CONCENTRATION FIELD ***
(BASED ON CURRENT SPEED-DIRECTION HISTOGRAM)

CONSERVED (WINTER). 0.01 CONTOUR RANGE.
LAKEVIEW MIN. MEAN. MAX. (5-15 CM/S. P)

CM MOORING:	SEVERAL	START DATE:	70/11/ 6
CM DEPTH:	6.0 M.	STOP DATE:	71/ 4/ 8

DIFFUSIVITY:	1200.0	CM**2/SEC.
DISCHARGE RATE:	2100.0	L/SEC.
DISCHARGE SPEED:	48.0	CM/SEC.
DENSITY ANOMALY:	1.6	PPT.
SOURCE DILUTION:	13.0	(TO 1.0)
CURRENT SPEED:	8.3	CM/SEC.
DIFFUSION LAYER:	2.4	M THICK.
DIFFUSER DEPTH:	9.5	M.
DIFFUSER WIDTH:	200.0	M.
DIFFUSER ANGLE:	135.0	DEGREES.
SHORELINE ANGLE:	225.0	DEGREES.
DIFFUSER-SHORE:	90.0	DEGREES.
DISTANCE-SHORE:	1.3	KM.

* THE CONCENTRATIONS ARE SCALED BY 10**4
* THE DIFFUSIVITY INCREASES AS THE 4/3 POWER OF THE SCALE OF THE DIFFUSION FIELD.

OUTER RADIUS:	10.00	KM.
ANGULAR INCREMENT:	5.0	DEGREES.
RADIAL INCREMENT:	1000.0	METRES.
CURRENT HISTOGRAM:	504.0	EVENTS
SECTOR INCREMENT:	5.0	DEGREES.
SPEED INCREMENT:	1.0	CM/SEC.

Figure 1.12 Extent of the 100 Concentration Contour

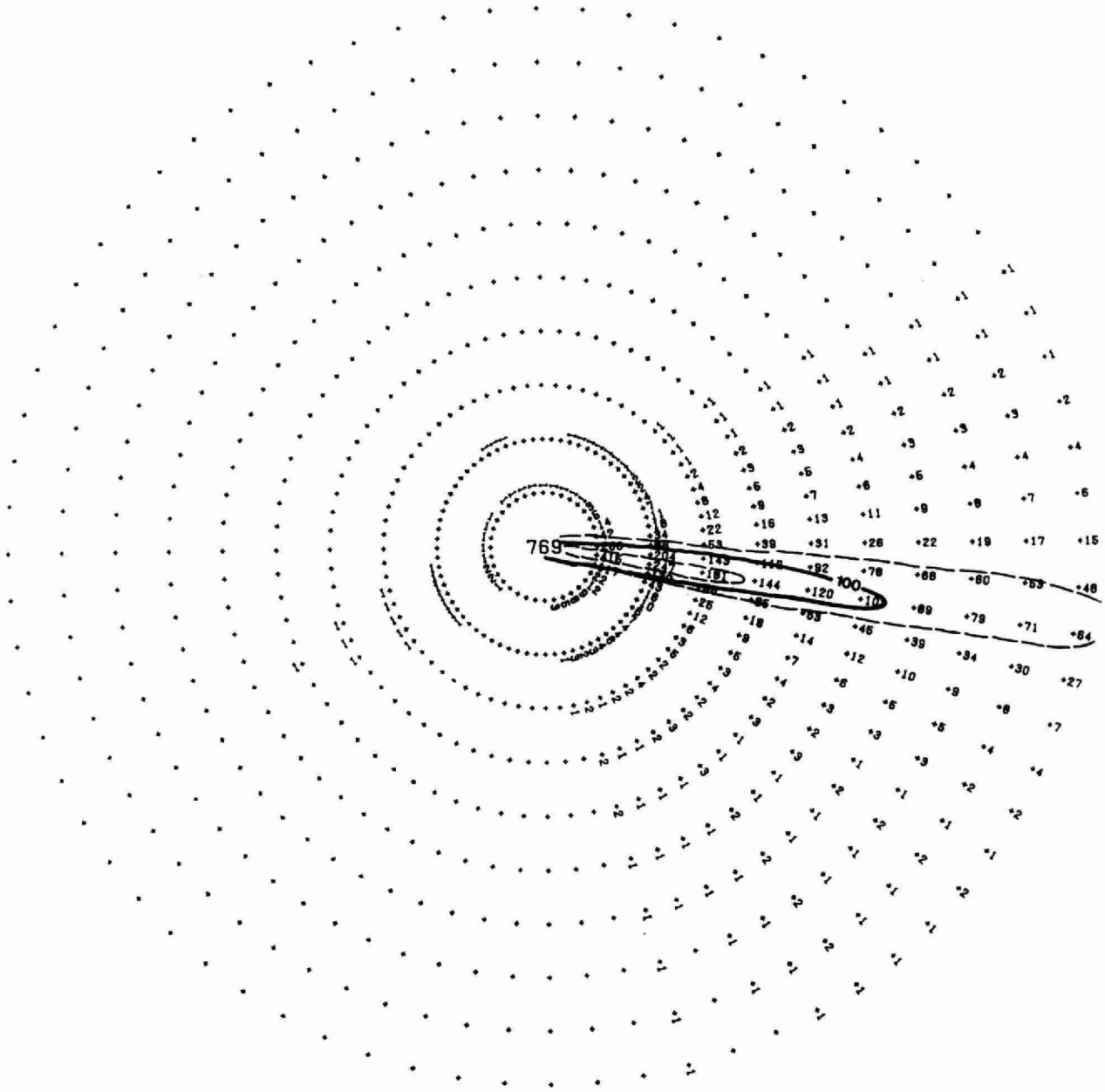

Figure 1.12 Extent of the 100 Concentration Contour

*** CURRENT ADVECTION DIAGRAM ***

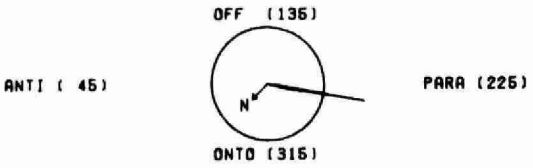

THE IRREGULAR CONTOUR CIRCUMSCRIBES THE ESTIMATED MAXIMUM ADVECTION OF THE SECTOR CURRENT SUMS.

THE ABOVE CIRCLE REPRESENTS THE OUTER 20.0 KM RADIUS CIRCLE OF THE MAIN PLOT.

*** CURRENT HISTOGRAM ***
(137 EVENTS. 5.0° SECTORS)

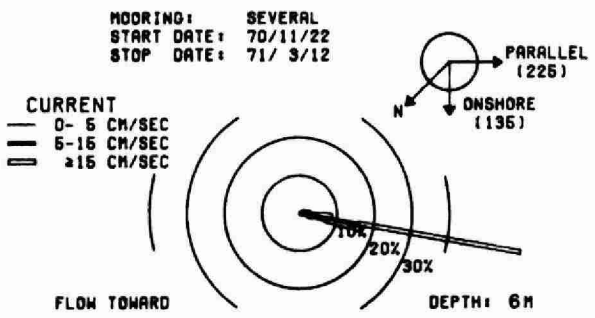

*** AVERAGE CONCENTRATION FIELD ***
(BASED ON CURRENT SPEED-DIRECTION HISTOGRAM)

CONSERVED (WINTER). MEAN LAKEVIEW FIELD.
SPEED > 15 CM/SEC. SHORE PARALLEL.

CM MOORING:	SEVERAL	START DATE:	70/11/22
CM DEPTH:	6.0 M.	STOP DATE:	71/ 3/12

DIFFUSIVITY:	1200.0	CM**2/SEC.
DISCHARGE RATE:	2100.0	L/SEC.
DISCHARGE SPEED:	48.0	CM/SEC.
DENSITY ANOMALY:	1.6	PPT.
SOURCE DILUTION:	13.0	(TO 1.0)
CURRENT SPEED:	15.7	CM/SEC.
DIFFUSION LAYER:	1.3	M THICK.
DIFFUSER DEPTH:	9.6	M.
DIFFUSER WIDTH:	200.0	M.
DIFFUSER ANGLE:	135.0	DEGREES.
SHORELINE ANGLE:	225.0	DEGREES.
DIFFUSER-SHORE:	90.0	DEGREES.
DISTANCE-SHORE:	1.3	KM.

- THE CONCENTRATIONS ARE SCALED BY 10**4
- THE DIFFUSIVITY INCREASES AS THE 4/3 POWER OF THE SCALE OF THE DIFFUSION FIELD.

OUTER RADIUS:	20.0	KM.
ANGULAR INCREMENT:	5.0	DEGREES.
RADIAL INCREMENT:	2000.0	METRES.
CURRENT HISTOGRAM:	137.0	EVENTS
SECTOR INCREMENT:	5.0	DEGREES.
SPEED INCREMENT:	1.0	CM/SEC.

Figure 1.13 Contours of the Mean Concentration Field

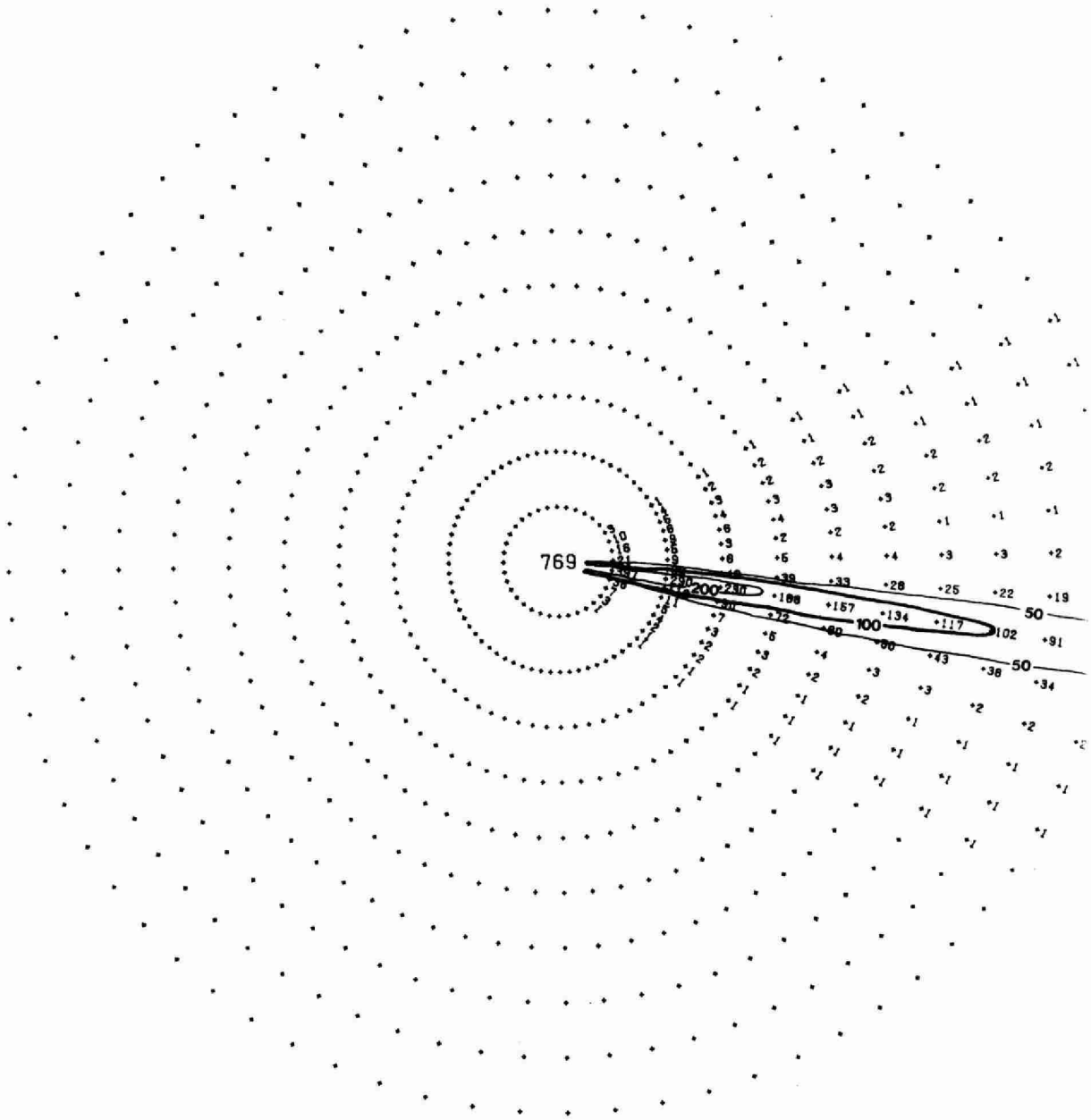

Figure 1.13 Contours of the Mean Concentration Field

*** CURRENT ADVECTION DIAGRAM ***

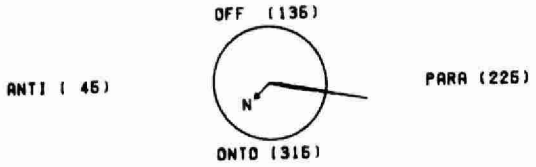

THE IRREGULAR CONTOUR CIRCUMSCRIBES THE ESTIMATED MAXIMUM ADVECTION OF THE SECTOR CURRENT SUMS.

THE ABOVE CIRCLE REPRESENTS THE OUTER 20.0 KM RADIUS CIRCLE OF THE MAIN PLOT.

*** CURRENT HISTOGRAM ***
(137 EVENTS. 5.0° SECTORS)

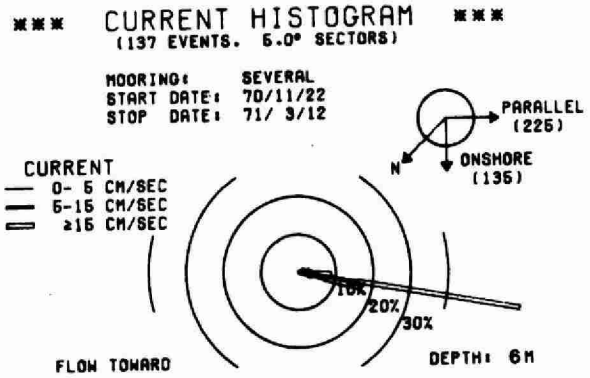

*** AVERAGE CONCENTRATION FIELD ***
(BASED ON CURRENT SPEED-DIRECTION HISTOGRAM)

CONSERVED (WINTER). 0.01 CONTOUR RANGE.
LAKEVIEW MIN. MEAN. MAX. (> 15 CM/S, P)

CM MOORING: SEVERAL — START DATE: 70/11/22
CM DEPTH: 6.0 M. — STOP DATE: 71/ 3/12

DIFFUSIVITY:	1200.0	CM**2/SEC.
DISCHARGE RATE:	2100.0	L/SEC.
DISCHARGE SPEED:	40.0	CM/SEC.
DENSITY ANOMALY:	1.6	PPT.
SOURCE DILUTION:	13.0	(TO 1.0)
CURRENT SPEED:	15.7	CM/SEC.
DIFFUSION LAYER:	1.3	M THICK.
DIFFUSER DEPTH:	9.5	M.
DIFFUSER WIDTH:	200.0	M.
DIFFUSER ANGLE:	135.0	DEGREES.
SHORELINE ANGLE:	225.0	DEGREES.
DIFFUSER-SHORE:	90.0	DEGREES.
DISTANCE-SHORE:	1.3	KM.

- THE CONCENTRATIONS ARE SCALED BY 10**4
- THE DIFFUSIVITY INCREASES AS THE 4/3 POWER OF THE SCALE OF THE DIFFUSION FIELD.

OUTER RADIUS:	20.0	KM.
ANGULAR INCREMENT:	5.0	DEGREES.
RADIAL INCREMENT:	2000.0	METRES.
CURRENT HISTOGRAM:	137.0	EVENTS
SECTOR INCREMENT:	5.0	DEGREES.
SPEED INCREMENT:	1.0	CM/SEC.

Figure 1.14 Extent of the 100 Concentration Contour

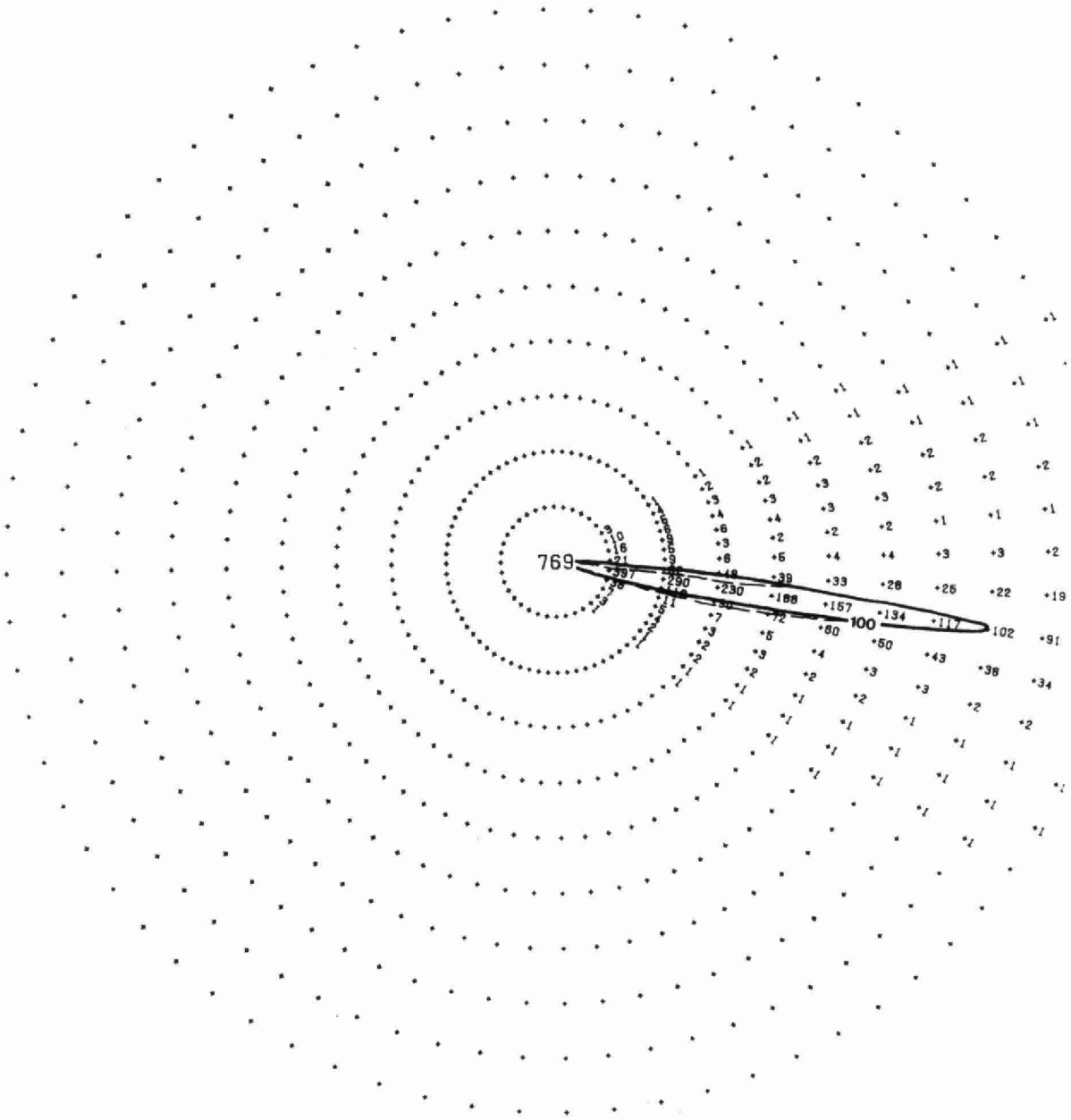

Figure 1.14 Extent of the 100 Concentration Contour

*** CURRENT ADVECTION DIAGRAM ***

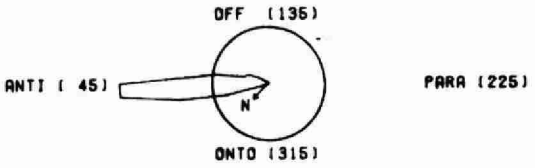

THE IRREGULAR CONTOUR CIRCUMSCRIBES THE ESTIMATED MAXIMUM ADVECTION OF THE SECTOR CURRENT SUMS.

THE ABOVE CIRCLE REPRESENTS THE OUTER 6.0 KM RADIUS CIRCLE OF THE MAIN PLOT.

*** CURRENT HISTOGRAM ***
(240 EVENTS. 5.0° SECTORS)

MOORING: SEVERAL
START DATE: 70/11/11
STOP DATE: 71/ 4/11

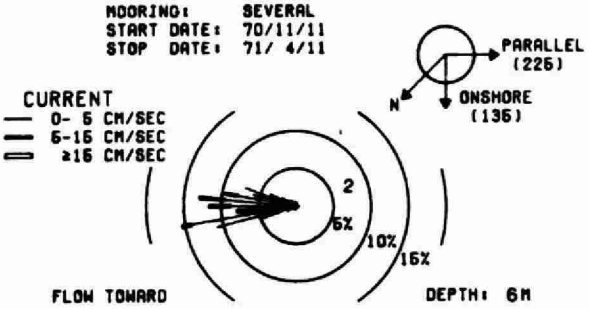

*** AVERAGE CONCENTRATION FIELD ***
(BASED ON CURRENT SPEED-DIRECTION HISTOGRAM)

CONSERVED (WINTER). MEAN LAKEVIEW FIELD.
SPEED 0-5 CM/SEC. SHORE ANTIPARALLEL.

CM MOORING:	SEVERAL	START DATE:	70/11/11
CM DEPTH:	6.0 M.	STOP DATE:	71/ 4/11

DIFFUSIVITY:	1200.0	CM**2/SEC.
DISCHARGE RATE:	2100.0	L/SEC.
DISCHARGE SPEED:	48.0	CM/SEC.
DENSITY ANOMALY:	1.5	PPT.
SOURCE DILUTION:	13.0	(TO 1.0)
CURRENT SPEED:	3.3	CM/SEC.
DIFFUSION LAYER:	4.6	M THICK.
DIFFUSER DEPTH:	9.5	M.
DIFFUSER WIDTH:	200.0	M.
DIFFUSER ANGLE:	135.0	DEGREES.
SHORELINE ANGLE:	225.0	DEGREES.
DIFFUSER-SHORE:	90.0	DEGREES.
DISTANCE-SHORE:	1.3	KM.

* THE CONCENTRATIONS ARE SCALED BY 10**4
* THE DIFFUSIVITY INCREASES AS THE 4/3 POWER OF THE SCALE OF THE DIFFUSION FIELD.

OUTER RADIUS:	6.0	KM.
ANGULAR INCREMENT:	5.0	DEGREES.
RADIAL INCREMENT:	500.0	METRES.
CURRENT HISTOGRAM:	240.0	EVENTS
SECTOR INCREMENT:	5.0	DEGREES.
SPEED INCREMENT:	1.0	CM/SEC.

Figure 1.15 Contours of the Mean Concentration Field

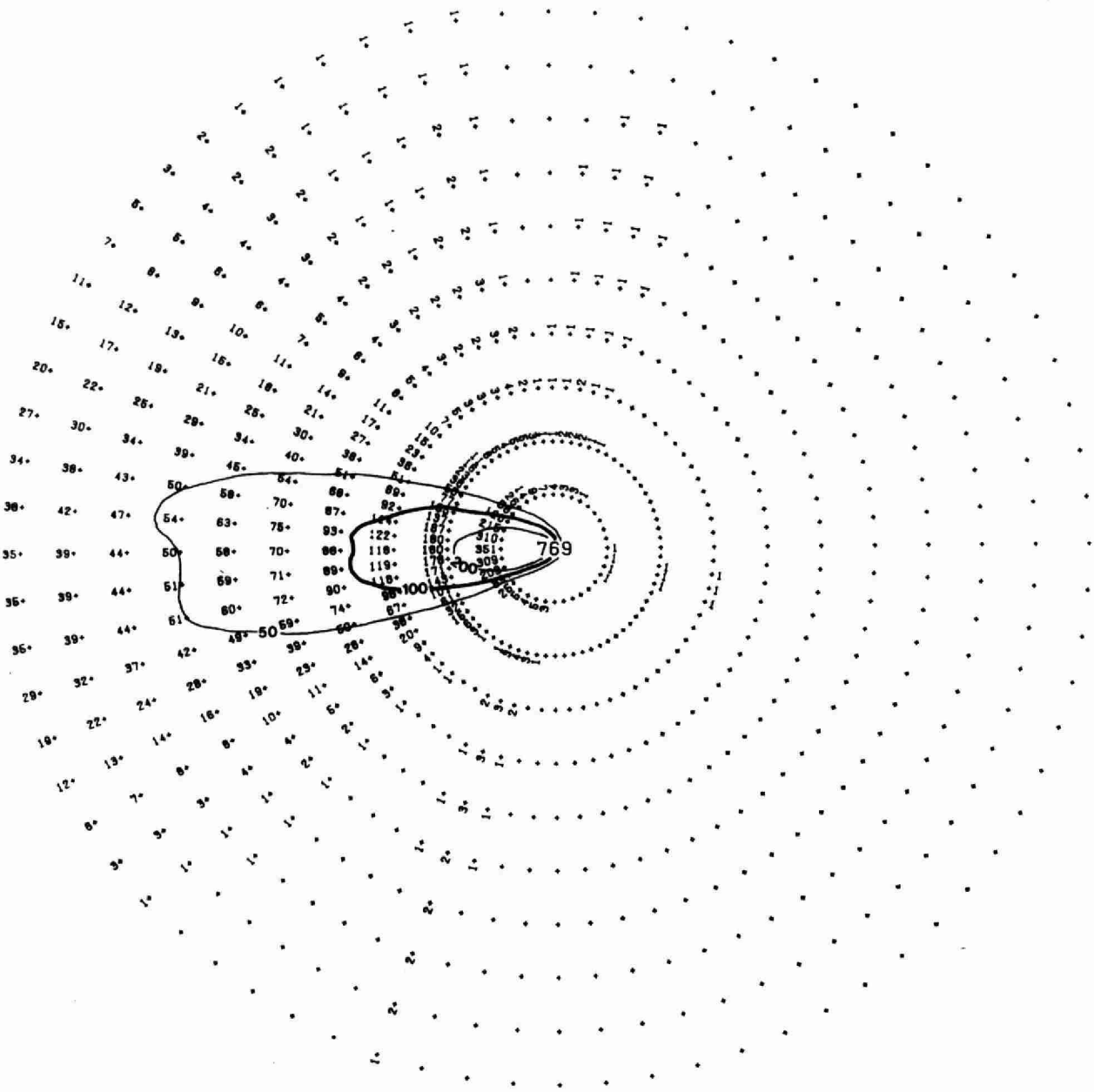

Figure 1.15 Contours of the Mean Concentration Field

*** CURRENT ADVECTION DIAGRAM ***

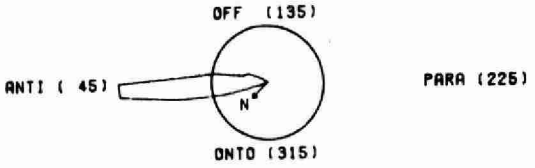

THE IRREGULAR CONTOUR CIRCUMSCRIBES THE ESTIMATED MAXIMUM ADVECTION OF THE SECTOR CURRENT SUMS.

THE ABOVE CIRCLE REPRESENTS THE OUTER 5.0 KM RADIUS CIRCLE OF THE MAIN PLOT.

*** CURRENT HISTOGRAM ***
(240 EVENTS. 5.0° SECTORS)

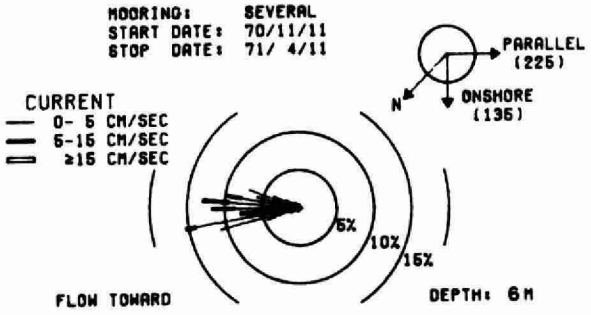

*** AVERAGE CONCENTRATION FIELD ***
(BASED ON CURRENT SPEED-DIRECTION HISTOGRAM)

CONSERVED (WINTER). 0.01 CONTOUR RANGE.
LAKEVIEW MIN. MEAN. MAX. (0-5 CM/S. AP)

CM MOORING: SEVERAL START DATE: 70/11/11
CM DEPTH: 6.0 M. STOP DATE: 71/ 4/11

DIFFUSIVITY:	1200.0	CM**2/SEC.
DISCHARGE RATE:	- 2100.0	L/SEC.
DISCHARGE SPEED:	48.0	CM/SEC.
DENSITY ANOMALY:	1.5	PPT.
SOURCE DILUTION:	13.0	(TO 1.0)
CURRENT SPEED:	3.3	CM/SEC.
DIFFUSION LAYER:	4.6	M THICK.
DIFFUSER DEPTH:	9.5	M.
DIFFUSER WIDTH:	200.0	M.
DIFFUSER ANGLE:	135.0	DEGREES.
SHORELINE ANGLE:	225.0	DEGREES.
DIFFUSER-SHORE:	90.0	DEGREES.
DISTANCE-SHORE:	1.3	KM.

- THE CONCENTRATIONS ARE SCALED BY 10**4
- THE DIFFUSIVITY INCREASES AS THE 4/3 POWER OF THE SCALE OF THE DIFFUSION FIELD.

OUTER RADIUS:	5.0	KM.
ANGULAR INCREMENT:	5.0	DEGREES.
RADIAL INCREMENT:	500.0	METRES.
CURRENT HISTOGRAM:	240.0	EVENTS
SECTOR INCREMENT:	5.0	DEGREES.
SPEED INCREMENT:	1.0	CM/SEC.

Figure 1.16 Extent of the 100 Concentration Contour

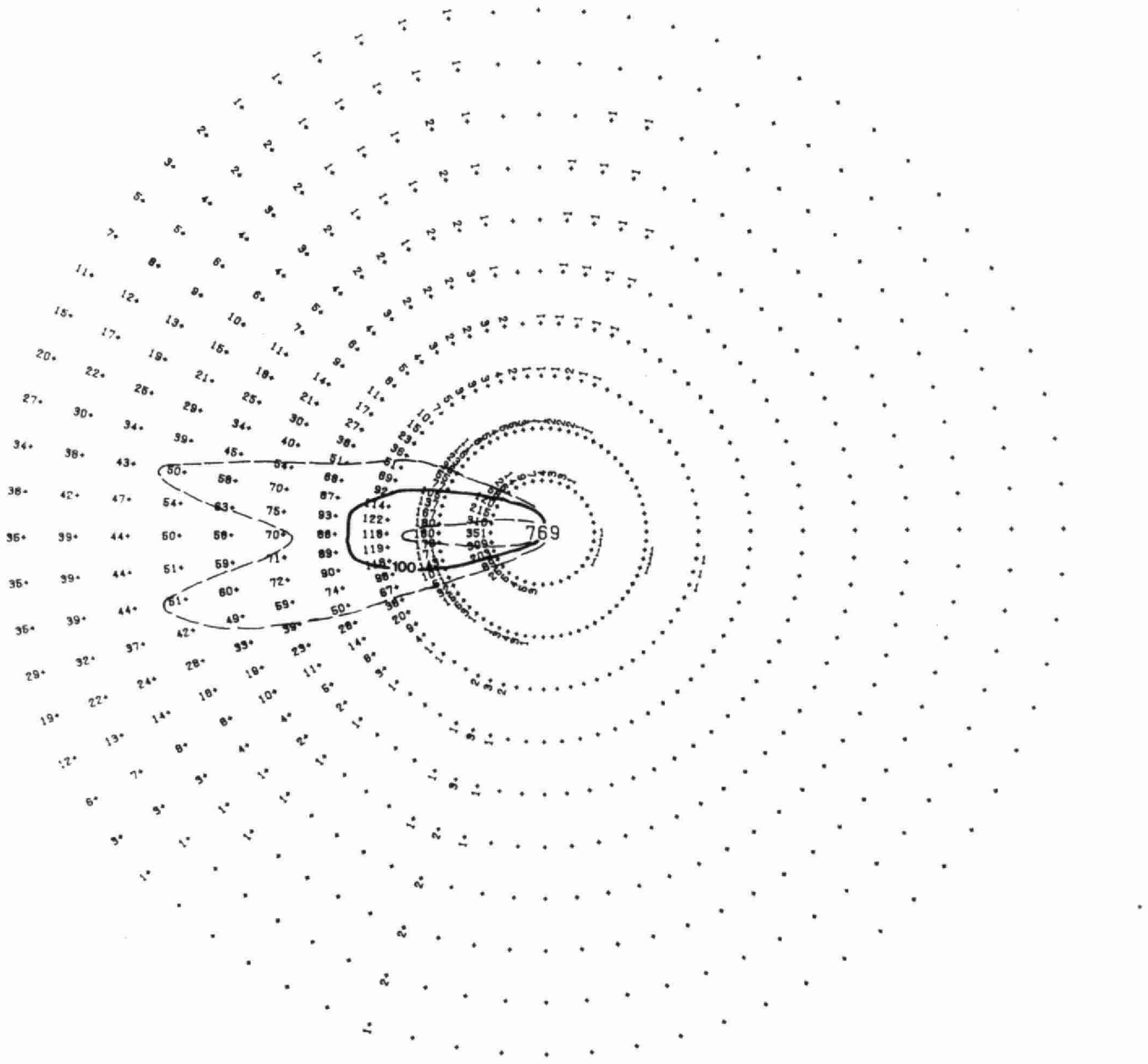

Figure 1.16 Extent of the 100 Concentration Contour

*** CURRENT ADVECTION DIAGRAM ***

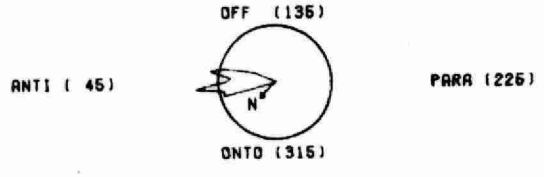

THE IRREGULAR CONTOUR CIRCUMSCRIBES THE ESTIMATED MAXIMUM ADVECTION OF THE SECTOR CURRENT SUMS.

THE ABOVE CIRCLE REPRESENTS THE OUTER 10.0 KM RADIUS CIRCLE OF THE MAIN PLOT.

*** CURRENT HISTOGRAM ***
(336 EVENTS. 5.0° SECTORS)

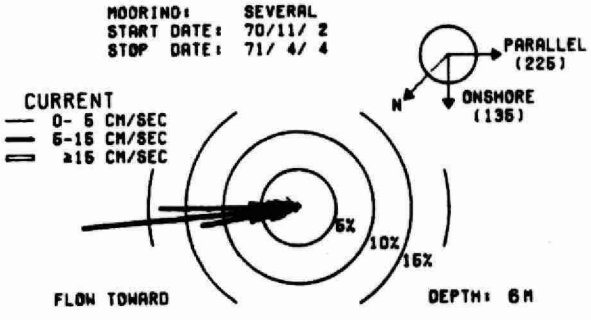

*** AVERAGE CONCENTRATION FIELD ***
(BASED ON CURRENT SPEED-DIRECTION HISTOGRAM)

CONSERVED (WINTER). MEAN LAKEVIEW FIELD.
SPEED 5-15 CM/SEC. SHORE ANTIPARALLEL.

CM MOORING:	SEVERAL	START DATE:	70/11/ 2
CM DEPTH:	6.0 M.	STOP DATE:	71/ 4/ 4

DIFFUSIVITY:	1200.0	CM**2/SEC.
DISCHARGE RATE:	2100.0	L/SEC.
DISCHARGE SPEED:	48.0	CM/SEC.
DENSITY ANOMALY:	1.5	PPT.
SOURCE DILUTION:	13.0	(TO 1.0)
CURRENT SPEED:	6.8	CM/SEC.
DIFFUSION LAYER:	2.6	M THICK.
DIFFUSER DEPTH:	9.5	M.
DIFFUSER WIDTH:	200.0	M.
DIFFUSER ANGLE:	135.0	DEGREES.
SHORELINE ANGLE:	225.0	DEGREES.
DIFFUSER-SHORE:	90.0	DEGREES.
DISTANCE-SHORE:	1.3	KM.

* THE CONCENTRATIONS ARE SCALED BY 10**4
* THE DIFFUSIVITY INCREASES AS THE 4/3 POWER OF THE SCALE OF THE DIFFUSION FIELD.

OUTER RADIUS:	10.0	KM.
ANGULAR INCREMENT:	5.0	DEGREES.
RADIAL INCREMENT:	1000.0	METRES.
CURRENT HISTOGRAM:	336.0	EVENTS
SECTOR INCREMENT:	5.0	DEGREES.
SPEED INCREMENT:	1.0	CM/SEC.

Figure 1.17 Contours of the Mean Concentration Field

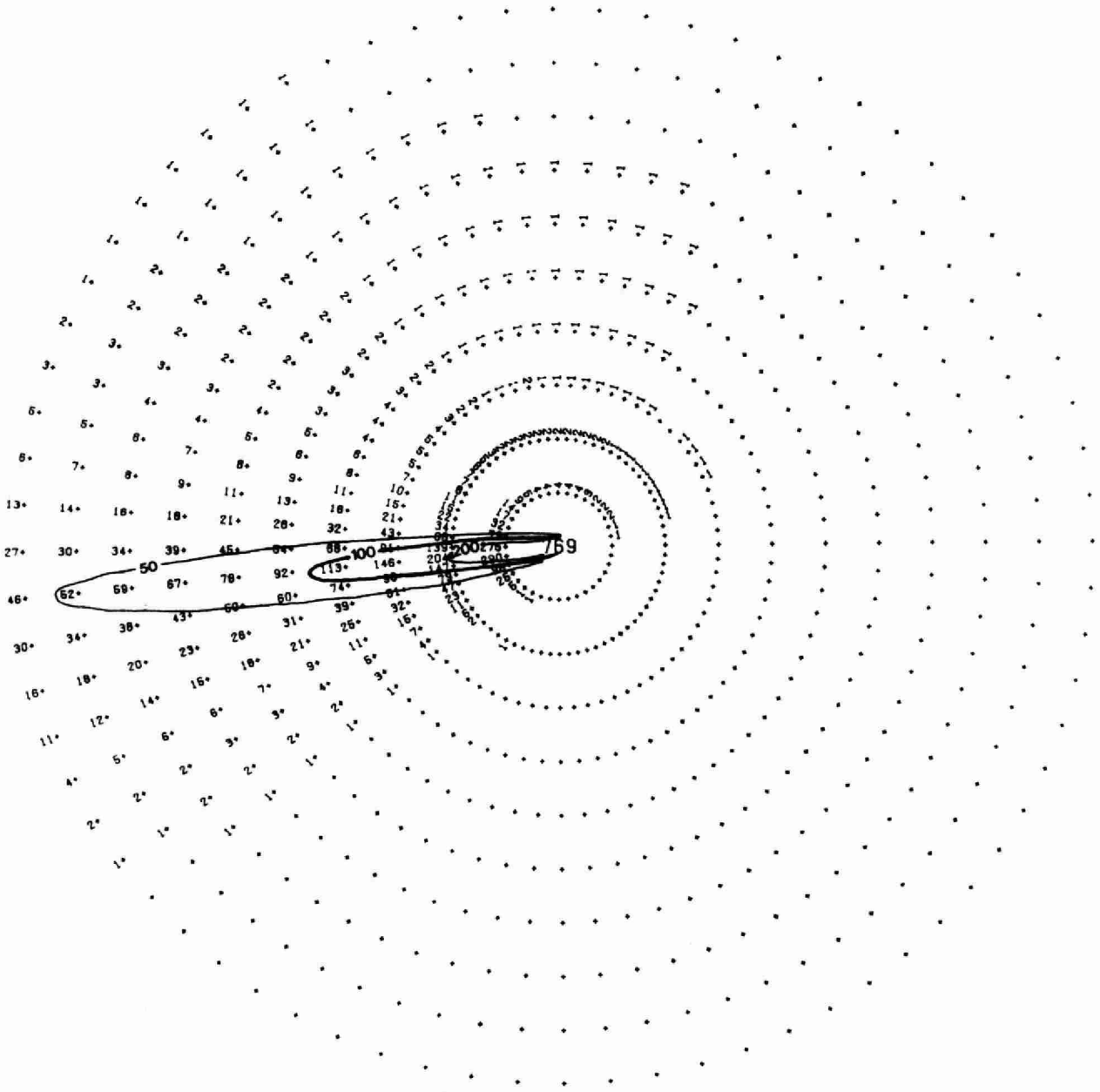

Figure 1.17 Contours of the Mean Concentration Field

*** CURRENT ADVECTION DIAGRAM ***

THE IRREGULAR CONTOUR CIRCUMSCRIBES THE ESTIMATED MAXIMUM ADVECTION OF THE SECTOR CURRENT SUMS.

THE ABOVE CIRCLE REPRESENTS THE OUTER 10.00 KM RADIUS CIRCLE OF THE MAIN PLOT.

*** CURRENT HISTOGRAM ***
(336 EVENTS. 5.0° SECTORS)

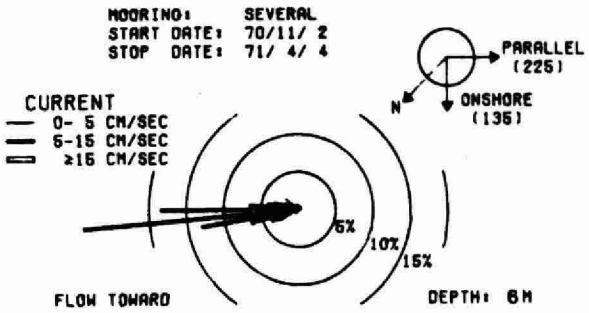

*** AVERAGE CONCENTRATION FIELD ***
(BASED ON CURRENT SPEED-DIRECTION HISTOGRAM)

CONSERVED (WINTER). 0.01 CONTOUR RANGE.
LAKEVIEW MIN. MEAN. MAX. (5-15 CM/S. AP)

CM MOORING:	SEVERAL	START DATE: 70/11/ 2
CM DEPTH:	6.0 M.	STOP DATE: 71/ 4/ 4

DIFFUSIVITY:	1200.0	CM**2/SEC.
DISCHARGE RATE:	2100.0	L/SEC.
DISCHARGE SPEED:	48.0	CM/SEC.
DENSITY ANOMALY:	1.6	PPT.
SOURCE DILUTION:	13.0	(TO 1.0)
CURRENT SPEED:	6.8	CM/SEC.
DIFFUSION LAYER:	2.6	M THICK.
DIFFUSER DEPTH:	9.5	M.
DIFFUSER WIDTH:	200.0	M.
DIFFUSER ANGLE:	135.0	DEGREES.
SHORELINE ANGLE:	225.0	DEGREES.
DIFFUSER-SHORE:	90.0	DEGREES.
DISTANCE-SHORE:	1.3	KM.

- THE CONCENTRATIONS ARE SCALED BY 10**4
- THE DIFFUSIVITY INCREASES AS THE 4/3 POWER OF THE SCALE OF THE DIFFUSION FIELD.

OUTER RADIUS:	10.00	KM.
ANGULAR INCREMENT:	5.0	DEGREES.
RADIAL INCREMENT:	1000.0	METRES.
CURRENT HISTOGRAM:	336.0	EVENTS
SECTOR INCREMENT:	5.0	DEGREES.
SPEED INCREMENT:	1.0	CM/SEC.

Figure 1.18 Extent of the 100 Concentration Contour

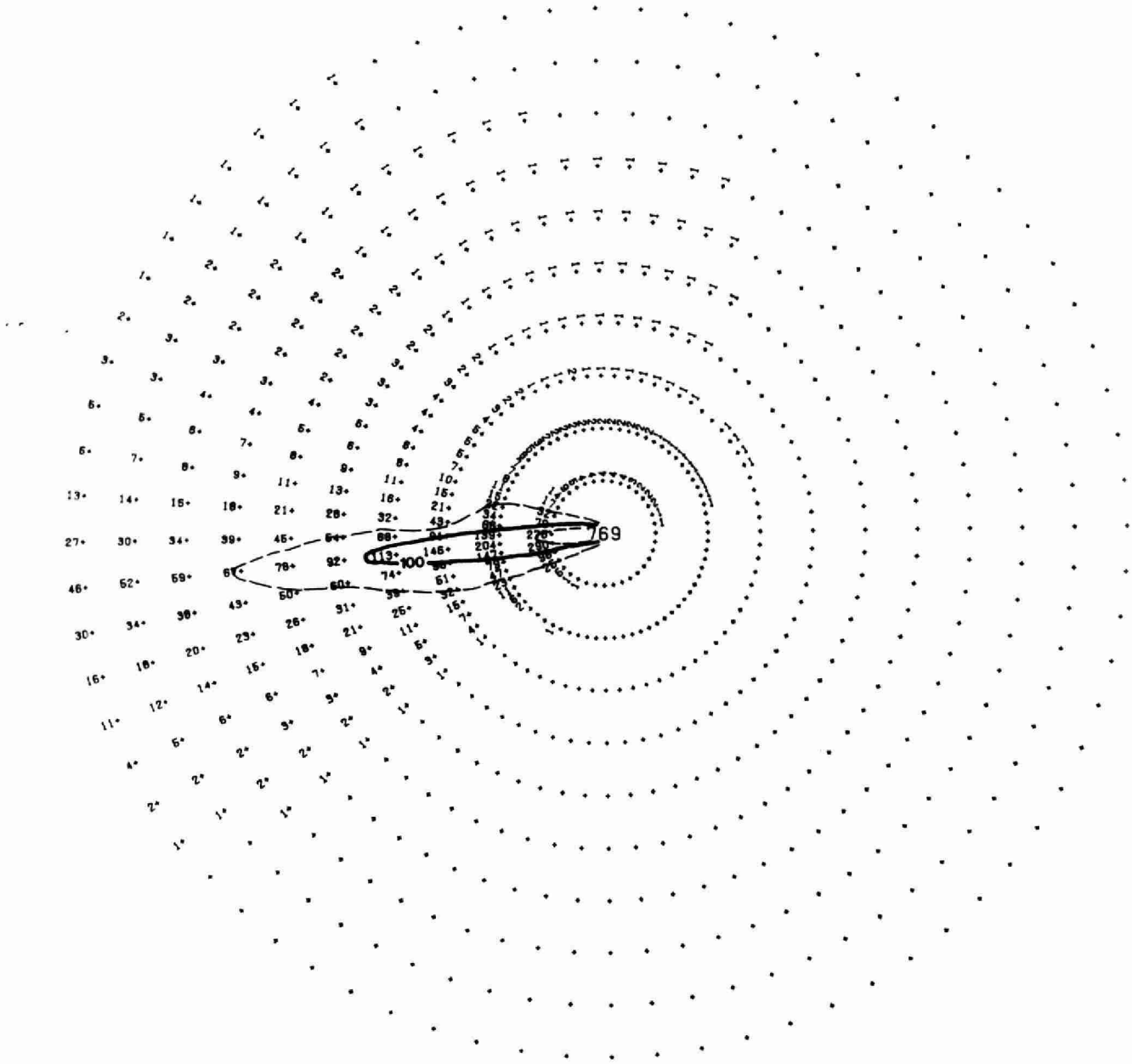

Figure 1.18 Extent of the 100 Concentration Contour

*** CURRENT ADVECTION DIAGRAM ***

THE IRREGULAR CONTOUR CIRCUMSCRIBES THE ESTIMATED MAXIMUM ADVECTION OF THE SECTOR CURRENT SUMS.

THE ABOVE CIRCLE REPRESENTS THE OUTER 20.0 KM RADIUS CIRCLE OF THE MAIN PLOT.

*** CURRENT HISTOGRAM ***
(95 EVENTS. 5.0° SECTORS)

MOORING: 71-00C-008
START DATE: 71/ 2/21
STOP DATE: 71/ 3/11

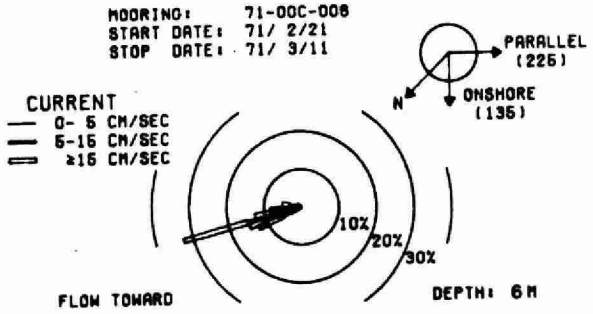

*** AVERAGE CONCENTRATION FIELD ***
(BASED ON CURRENT SPEED-DIRECTION HISTOGRAM)

CONSERVED (WINTER). MEAN LAKEVIEW FIELD.
SPEED > 15 CM/SEC. SHORE ANTIPARALLEL.

CM MOORING:	71-00C-008	START DATE:	71/ 2/21
CM DEPTH:	6.0 M.	STOP DATE:	71/ 3/11

DIFFUSIVITY:	1200.0	CM**2/SEC.
DISCHARGE RATE:	2100.0	L/SEC.
DISCHARGE SPEED:	48.0	CM/SEC.
DENSITY ANOMALY:	1.5	PPT.
SOURCE DILUTION:	13.0	(TO 1.0)
CURRENT SPEED:	14.4	CM/SEC.
DIFFUSION LAYER:	1.4	M THICK.
DIFFUSER DEPTH:	9.5	M.
DIFFUSER WIDTH:	200.0	M.
DIFFUSER ANGLE:	135.0	DEGREES.
SHORELINE ANGLE:	225.0	DEGREES.
DIFFUSER-SHORE:	90.0	DEGREES.
DISTANCE-SHORE:	1.9	KM.

* THE CONCENTRATIONS ARE SCALED BY 10**4
* THE DIFFUSIVITY INCREASES AS THE 4/3 POWER OF THE SCALE OF THE DIFFUSION FIELD.

OUTER RADIUS:	20.0	KM.
ANGULAR INCREMENT:	5.0	DEGREES.
RADIAL INCREMENT:	2000.0	METRES.
CURRENT HISTOGRAM:	95.0	EVENTS
SECTOR INCREMENT:	5.0	DEGREES.
SPEED INCREMENT:	1.0	CM/SEC.

Figure 1.19 Contours of the Mean Concentration Field

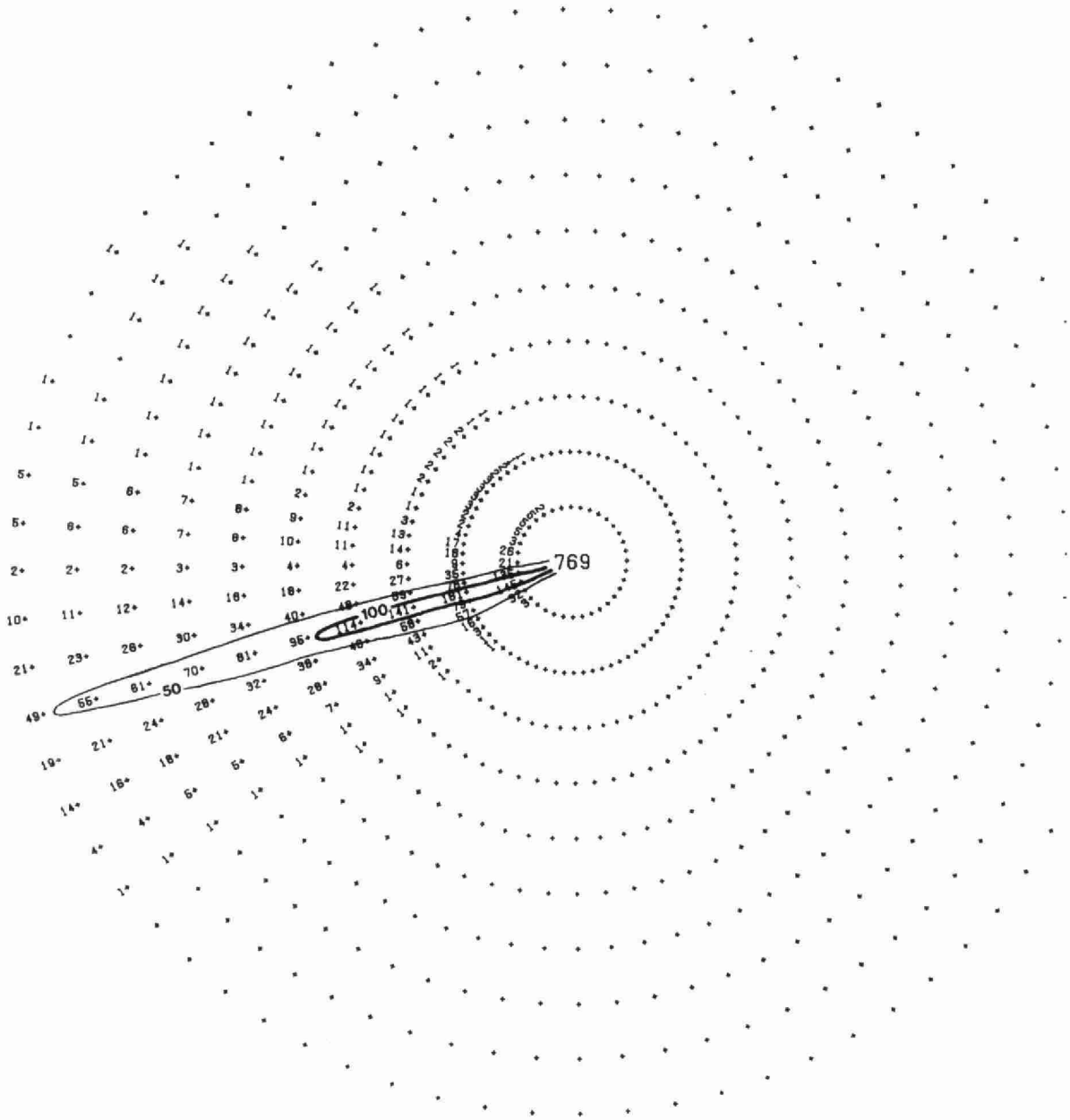

Figure 1.19 Contours of the Mean Concentration Field

*** CURRENT ADVECTION DIAGRAM ***

THE IRREGULAR CONTOUR CIRCUMSCRIBES THE ESTIMATED MAXIMUM ADVECTION OF THE SECTOR CURRENT SUMS.

THE ABOVE CIRCLE REPRESENTS THE OUTER 20.0 KM RADIUS CIRCLE OF THE MAIN PLOT.

*** CURRENT HISTOGRAM ***
(95 EVENTS. 5.0° SECTORS)

MOORING: 71-00C-006
START DATE: 71/ 2/21
STOP DATE: 71/ 3/11

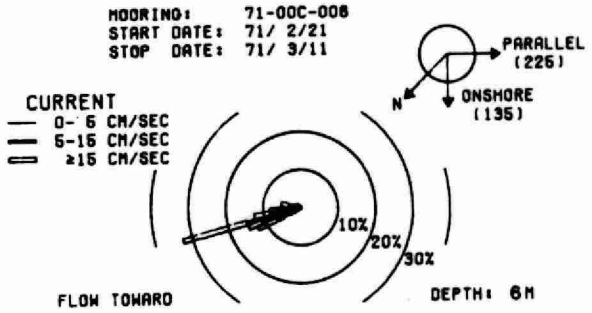

*** AVERAGE CONCENTRATION FIELD ***
(BASED ON CURRENT SPEED-DIRECTION HISTOGRAM)

CONSERVED (WINTER). 0.01 CONTOUR RANGE.
LAKEVIEW MIN. MEAN. MAX. (> 15 CM/S. AP)

CM MOORING:	71-00C-006		START DATE:	71/ 2/21
CM DEPTH:	6.0	M.	STOP DATE:	71/ 3/11

DIFFUSIVITY:	1200.0	CM**2/SEC.
DISCHARGE RATE:	2100.0	L/SEC.
DISCHARGE SPEED:	48.0	CM/SEC.
DENSITY ANOMALY:	1.5	PPT.
SOURCE DILUTION:	13.0	(TO 1.0)
CURRENT SPEED:	14.4	CM/SEC.
DIFFUSION LAYER:	1.4	M THICK.
DIFFUSER DEPTH:	9.6	M.
DIFFUSER WIDTH:	200.0	M.
DIFFUSER ANGLE:	135.0	DEGREES.
SHORELINE ANGLE:	225.0	DEGREES.
DIFFUSER-SHORE:	90.0	DEGREES.
DISTANCE-SHORE:	1.3	KM.

* THE CONCENTRATIONS ARE SCALED BY 10**4
* THE DIFFUSIVITY INCREASES AS THE 4/3 POWER OF THE SCALE OF THE DIFFUSION FIELD.

OUTER RADIUS:	20.0	KM.
ANGULAR INCREMENT:	5.0	DEGREES.
RADIAL INCREMENT:	2000.0	METRES.
CURRENT HISTOGRAM:	95.0	EVENTS
SECTOR INCREMENT:	5.0	DEGREES.
SPEED INCREMENT:	1.0	CM/SEC.

Figure 1.20 Extent of the 100 Concentration Contour

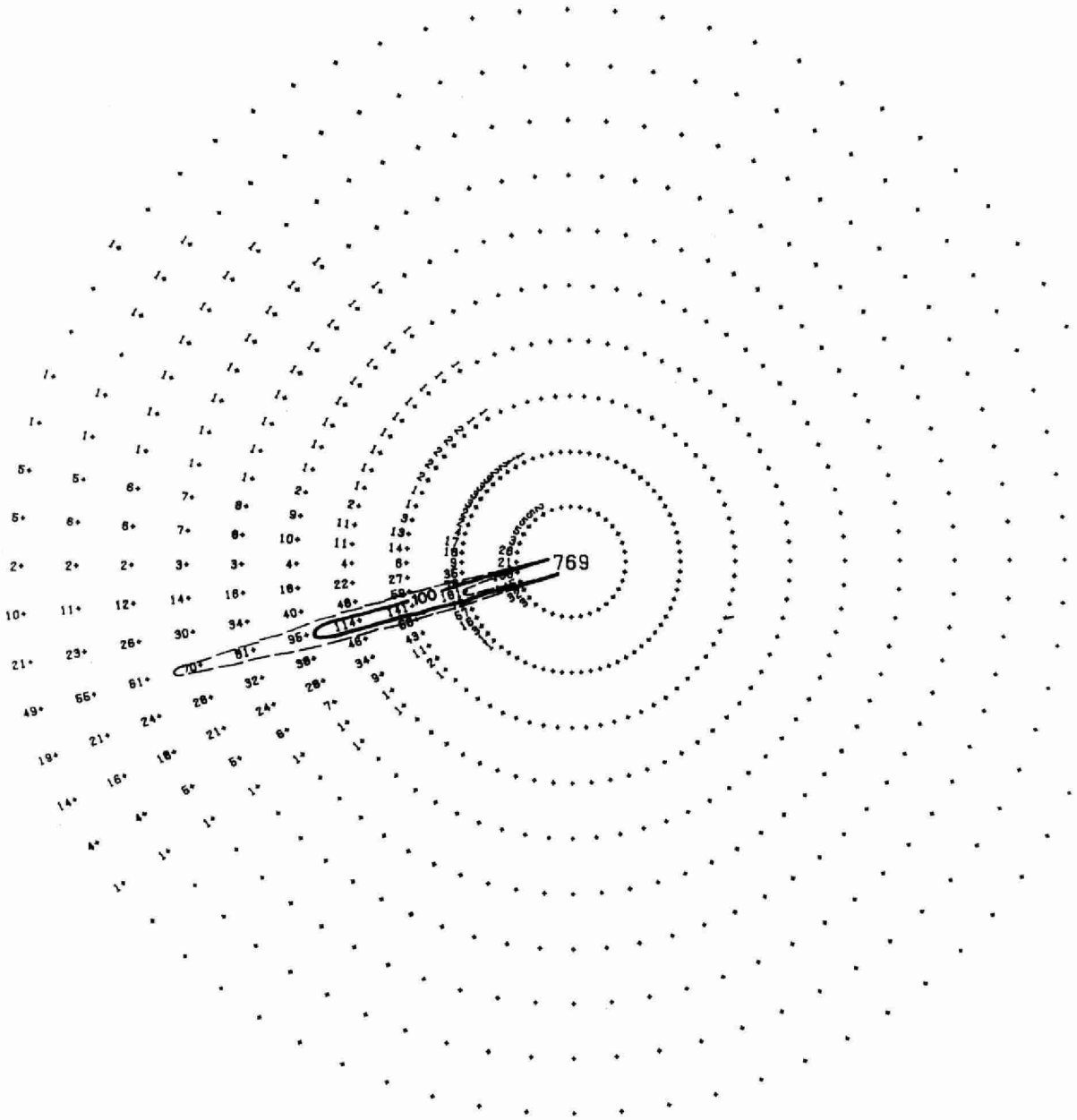

Figure 1.20 Extent of the 100 Concentration Contour

LAKEVIEW

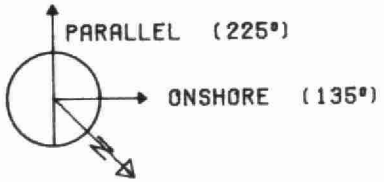

DATE: MAY 1970
LAKE ONTARIO

CURRENT VECTORS (6 HOUR AVERAGE) 0 10 CM/SEC

MOORING: 70-00C-006
DEPTH: 6 M
1.3 KM FROM SHORE

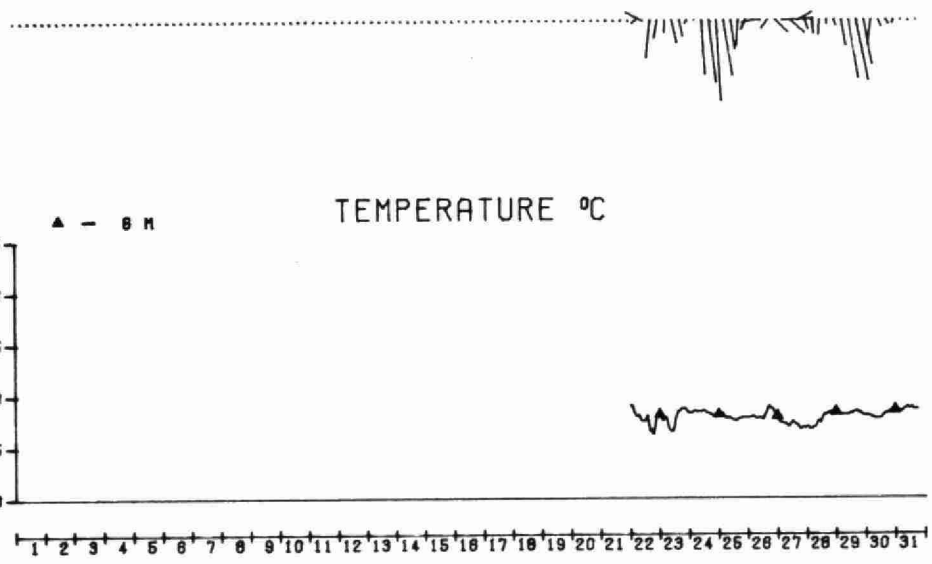

MONTHLY CURRENT SUMMARY
(234 EVENTS. 45.0° SECTORS)

MOORING: 70-00C-006
START DATE: 70/ 5/22
STOP DATE: 70/ 5/31

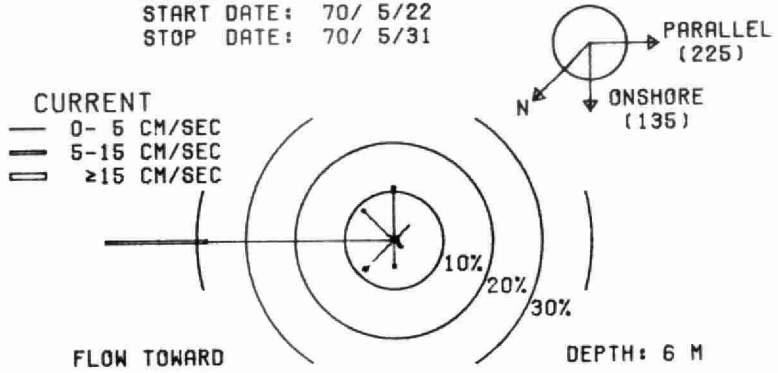

Figure 1.21

LAKEVIEW

DATE: JUNE 1970
LAKE ONTARIO

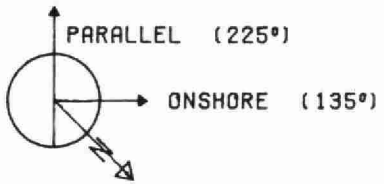

CURRENT VECTORS (6 HOUR AVERAGE) 0 10 CM/SEC

MOORING: 70-00C-006
DEPTH: 6 M
1.3 KM FROM SHORE

TEMPERATURE °C

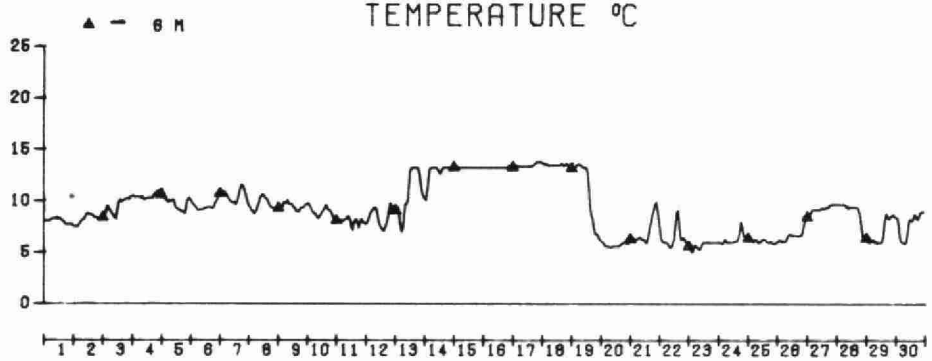

MONTHLY CURRENT SUMMARY
(718 EVENTS, 45.0° SECTORS)

MOORING: 70-00C-006
START DATE: 70/ 6/ 1
STOP DATE: 70/ 6/30

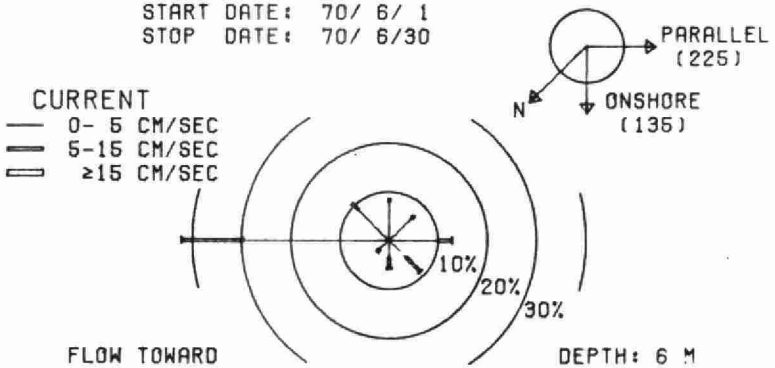

Figure 1.22

LAKEVIEW

DATE: JULY 1970

LAKE ONTARIO

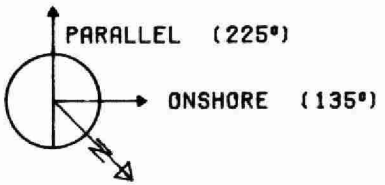

CURRENT VECTORS (6 HOUR AVERAGE) 0 10 CM/SEC

MOORING: 70-00C-006
DEPTH: 6 M
1.3 KM FROM SHORE

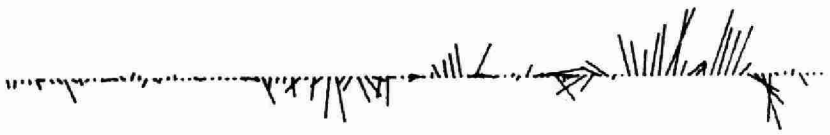

TEMPERATURE °C

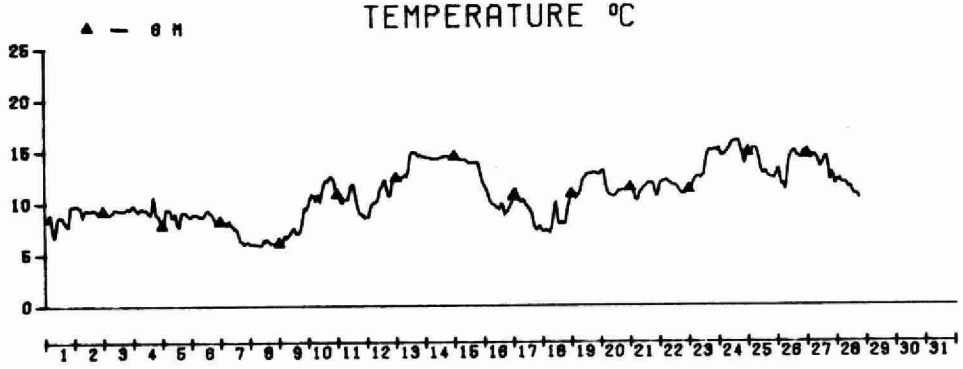

MONTHLY CURRENT SUMMARY
(665 EVENTS, 45.0° SECTORS)

MOORING: 70-00C-006
START DATE: 70/ 7/ 1
STOP DATE: 70/ 7/28

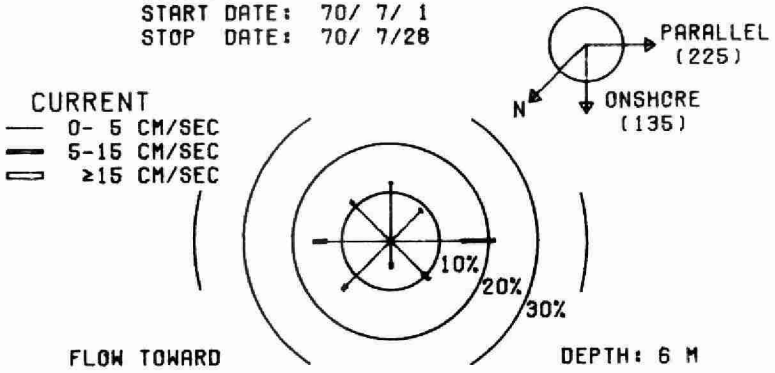

Figure 1.23

LAKEVIEW

DATE: AUG 1970
LAKE ONTARIO

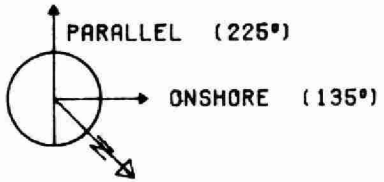

CURRENT VECTORS (6 HOUR AVERAGE) 0 10 CM/SEC

MOORING: 70-00C-006
DEPTH: 6 M
1.3 KM FROM SHORE

TEMPERATURE °C

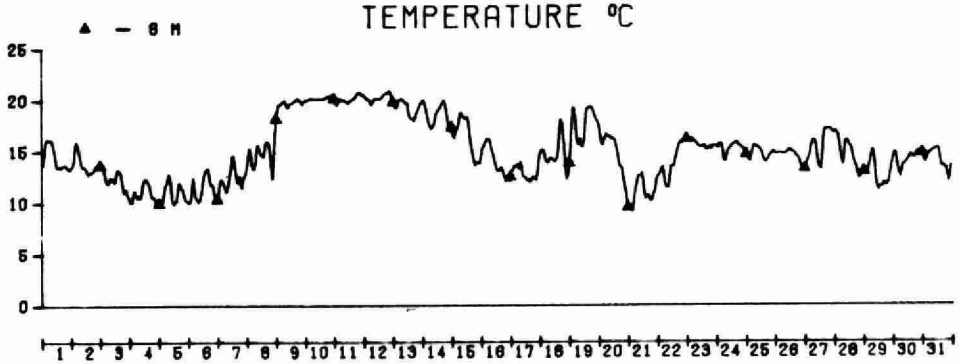

MONTHLY CURRENT SUMMARY
(743 EVENTS, 45.0° SECTORS)

MOORING: 70-00C-006
START DATE: 70/ 8/ 1
STOP DATE: 70/ 8/31

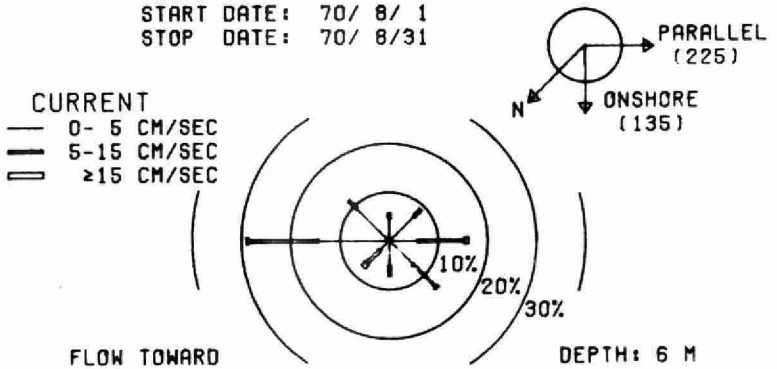

Figure 1.24

LAKEVIEW

DATE: SEPT 1970
LAKE ONTARIO

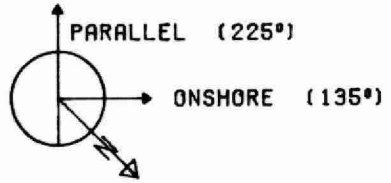

CURRENT VECTORS (6 HOUR AVERAGE) 0 10 CM/SEC

MOORING: 70-00C-006
DEPTH: 6 M
1.3 KM FROM SHORE

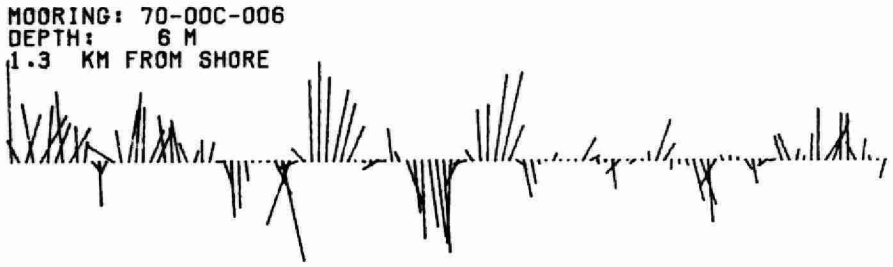

TEMPERATURE °C

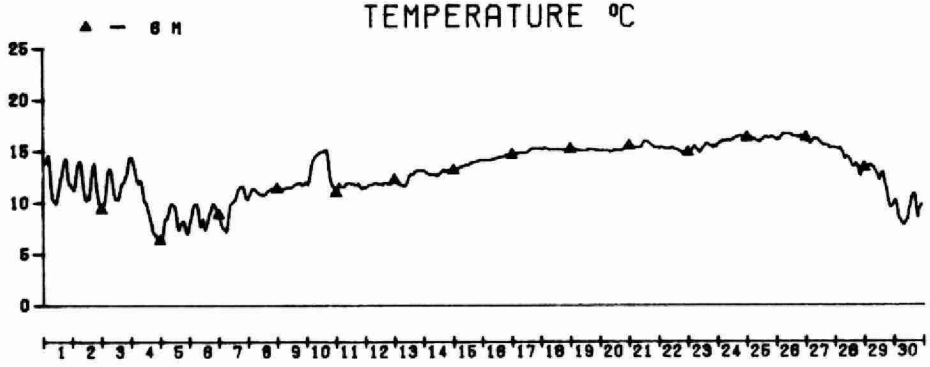

MONTHLY CURRENT SUMMARY
(718 EVENTS, 45.0° SECTORS)

MOORING: 70-00C-006
START DATE: 70/ 9/ 1
STOP DATE: 70/ 9/30

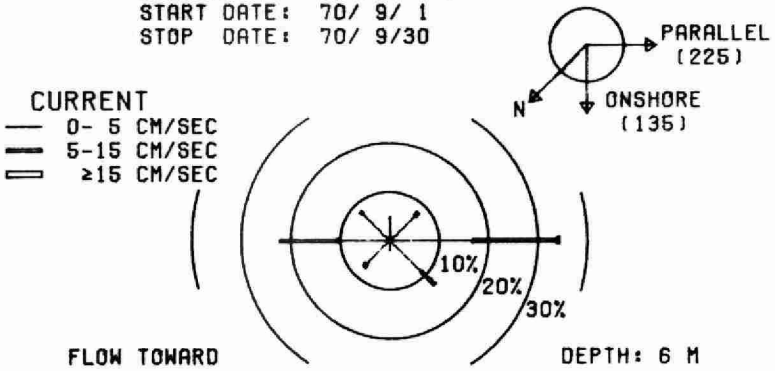

Figure 1.25

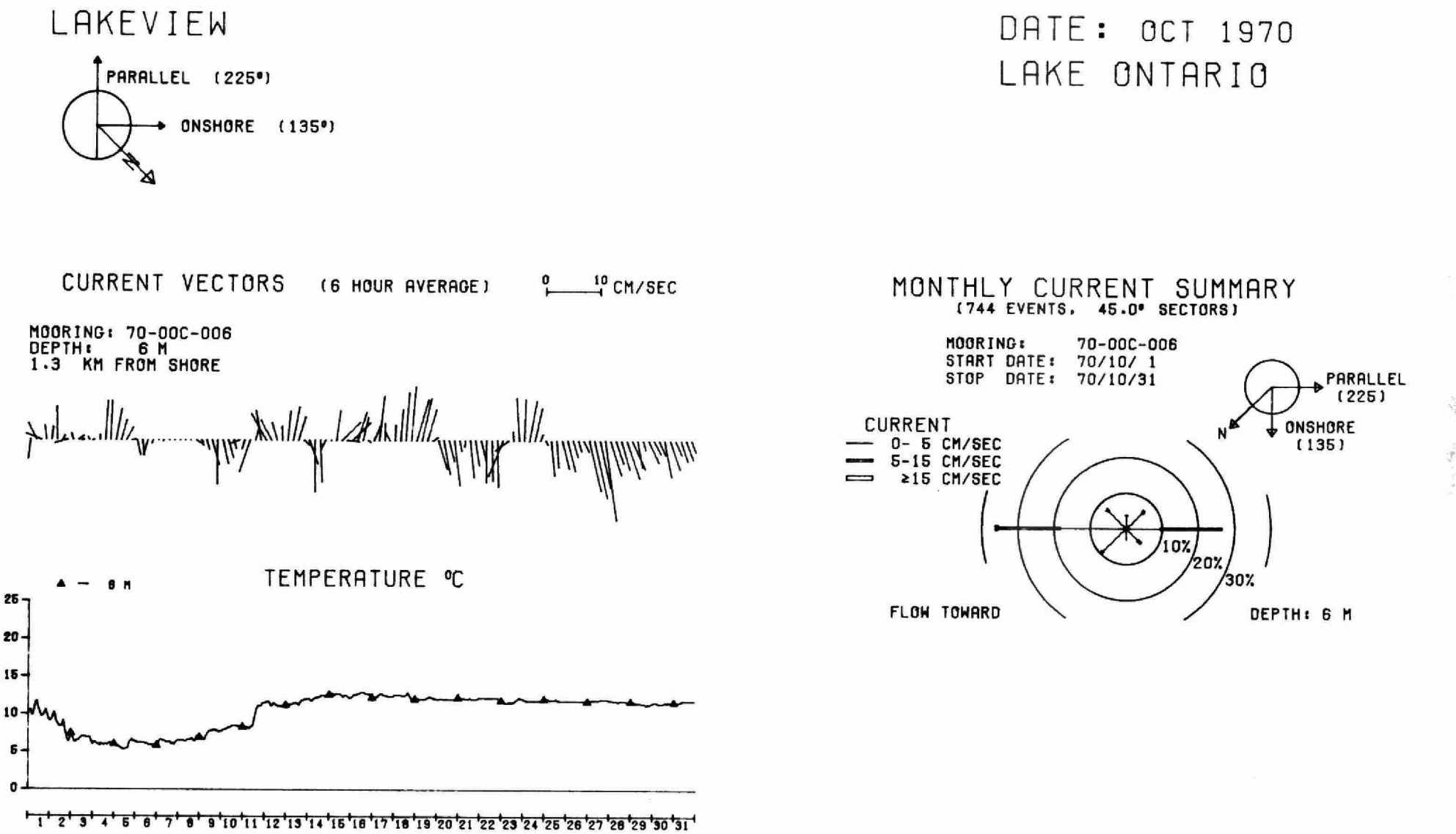
LAKEVIEW
PARALLEL (225°)
ONSHORE (135°)
DATE: OCT 1970
LAKE ONTARIO
CURRENT VECTORS (6 HOUR AVERAGE)
0 10 CM/SEC
MOORING: 70-00C-006
DEPTH: 6 M
1.3 KM FROM SHORE
▲ — 6 M
TEMPERATURE °C
25
20
15
10
5
0
1 2 3 4 5 6 7 8 9 10 11 12 13 14 15 16 17 18 19 20 21 22 23 24 25 26 27 28 29 30 31
MONTHLY CURRENT SUMMARY
(744 EVENTS, 45.0° SECTORS)
MOORING: 70-00C-006
START DATE: 70/10/ 1
STOP DATE: 70/10/31
CURRENT
0- 5 CM/SEC
5-15 CM/SEC
≥15 CM/SEC
PARALLEL (225)
ONSHORE (135)
N
10%
20%
30%
FLOW TOWARD
DEPTH: 6 M

Figure 1.26

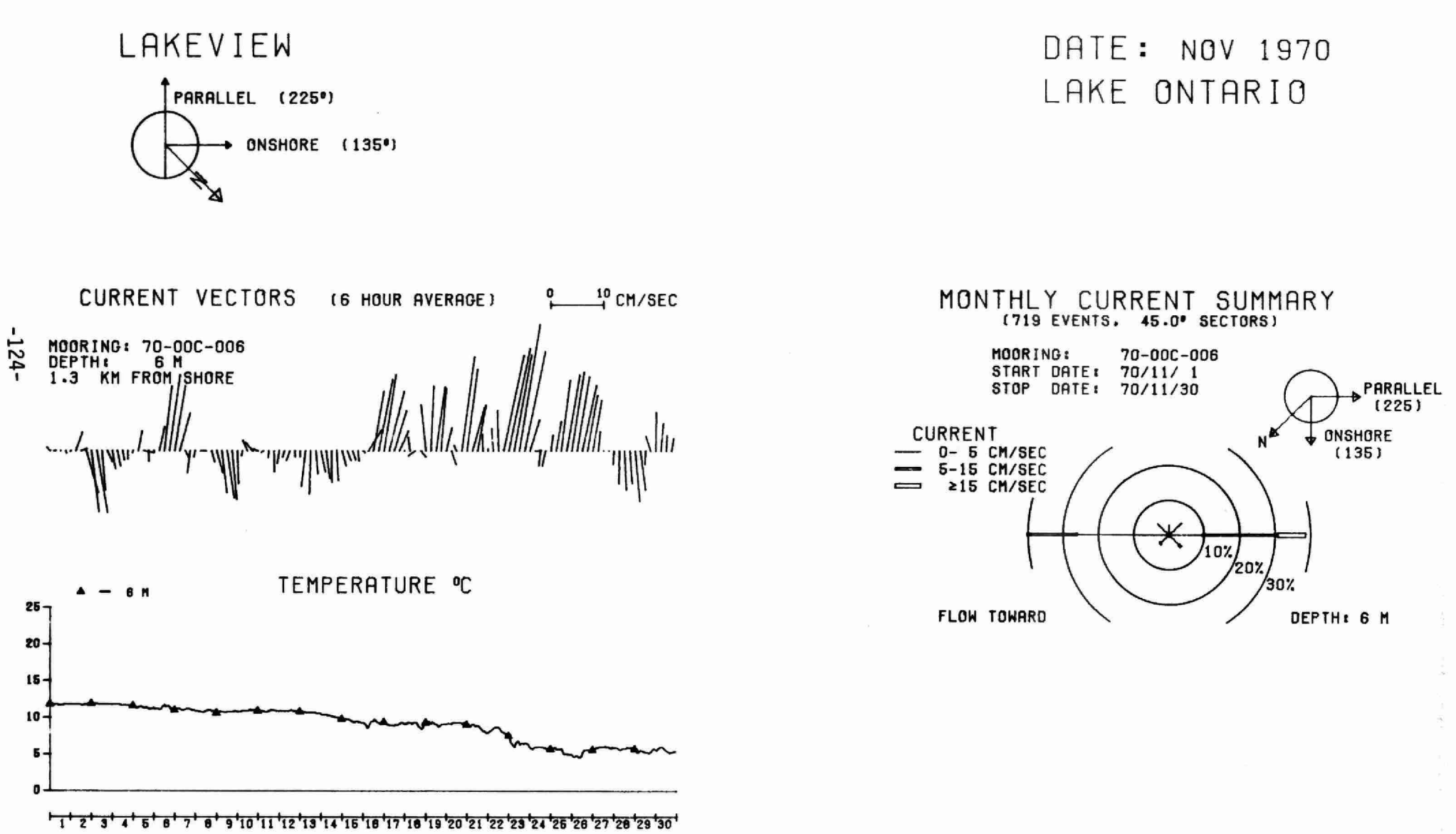
LAKEVIEW
PARALLEL (225°)
ONSHORE (135°)
DATE: NOV 1970
LAKE ONTARIO
CURRENT VECTORS (6 HOUR AVERAGE)
0 10 CM/SEC
-124-
MOORING: 70-00C-006
DEPTH: 6 M
1.3 KM FROM SHORE
TEMPERATURE °C
▲ — 6 M
25
20
15
10
5
0
1 2 3 4 5 6 7 8 9 10 11 12 13 14 15 16 17 18 19 20 21 22 23 24 25 26 27 28 29 30
MONTHLY CURRENT SUMMARY
(719 EVENTS, 45.0° SECTORS)
MOORING: 70-00C-006
START DATE: 70/11/ 1
STOP DATE: 70/11/30
CURRENT
0- 5 CM/SEC
5-15 CM/SEC
≥15 CM/SEC
PARALLEL
(225)
N
ONSHORE
(135)
10%
20%
30%
FLOW TOWARD
DEPTH: 6 M

Figure 1.27

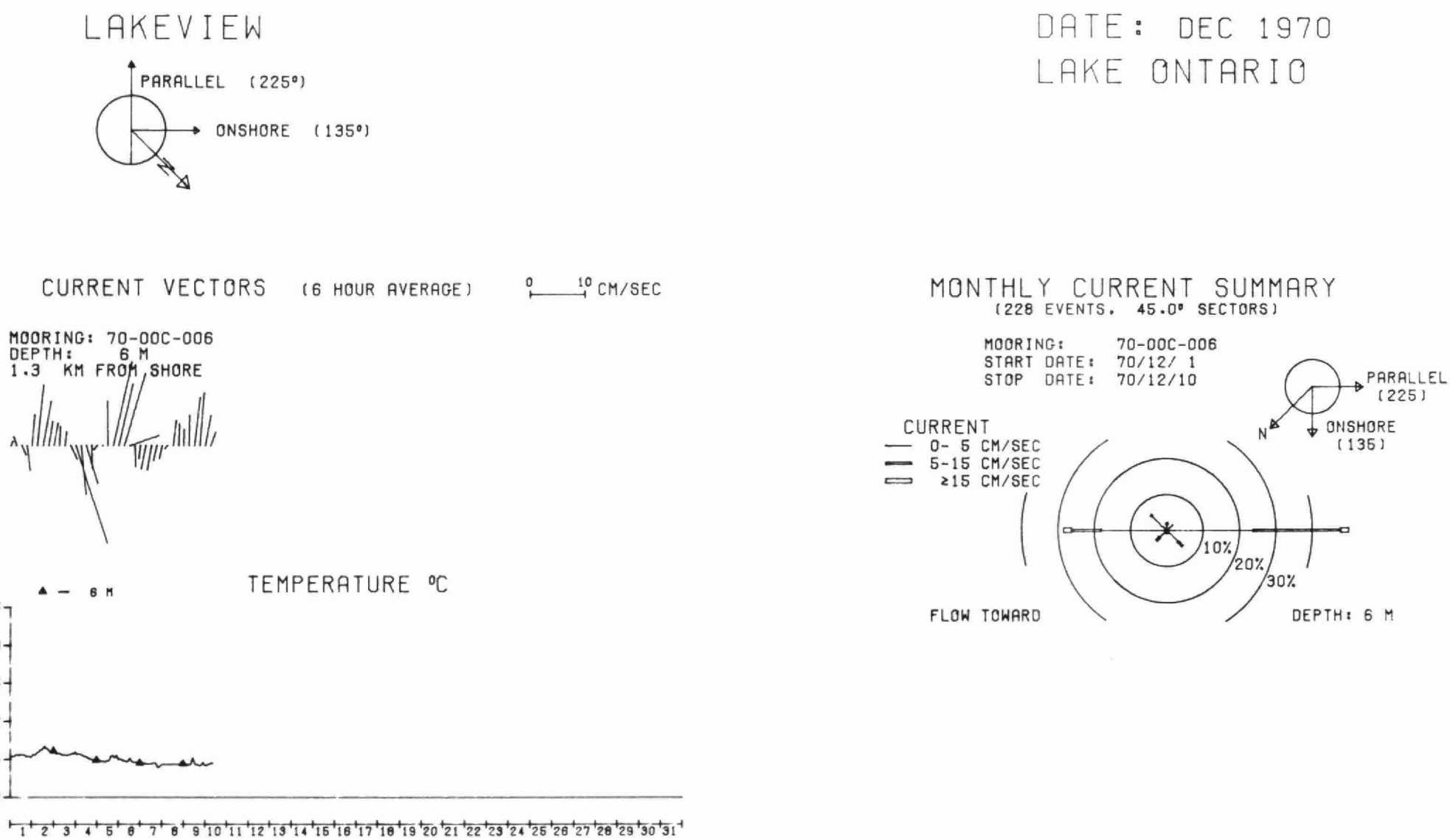
LAKEVIEW
PARALLEL (225°)
ONSHORE (135°)
DATE: DEC 1970
LAKE ONTARIO
CURRENT VECTORS (6 HOUR AVERAGE)
0 10 CM/SEC
MOORING: 70-00C-006
DEPTH: 6 M
1.3 KM FROM SHORE
MONTHLY CURRENT SUMMARY
(228 EVENTS. 45.0° SECTORS)
MOORING: 70-00C-006
START DATE: 70/12/ 1
STOP DATE: 70/12/10
PARALLEL (225)
ONSHORE (135)
N
CURRENT
0- 5 CM/SEC
5-15 CM/SEC
≥15 CM/SEC
10%
20%
30%
FLOW TOWARD
DEPTH: 6 M
TEMPERATURE °C
6 M
25
20
15
10
5
0
1 2 3 4 5 6 7 8 9 10 11 12 13 14 15 16 17 18 19 20 21 22 23 24 25 26 27 28 29 30 31

Figure 1.28

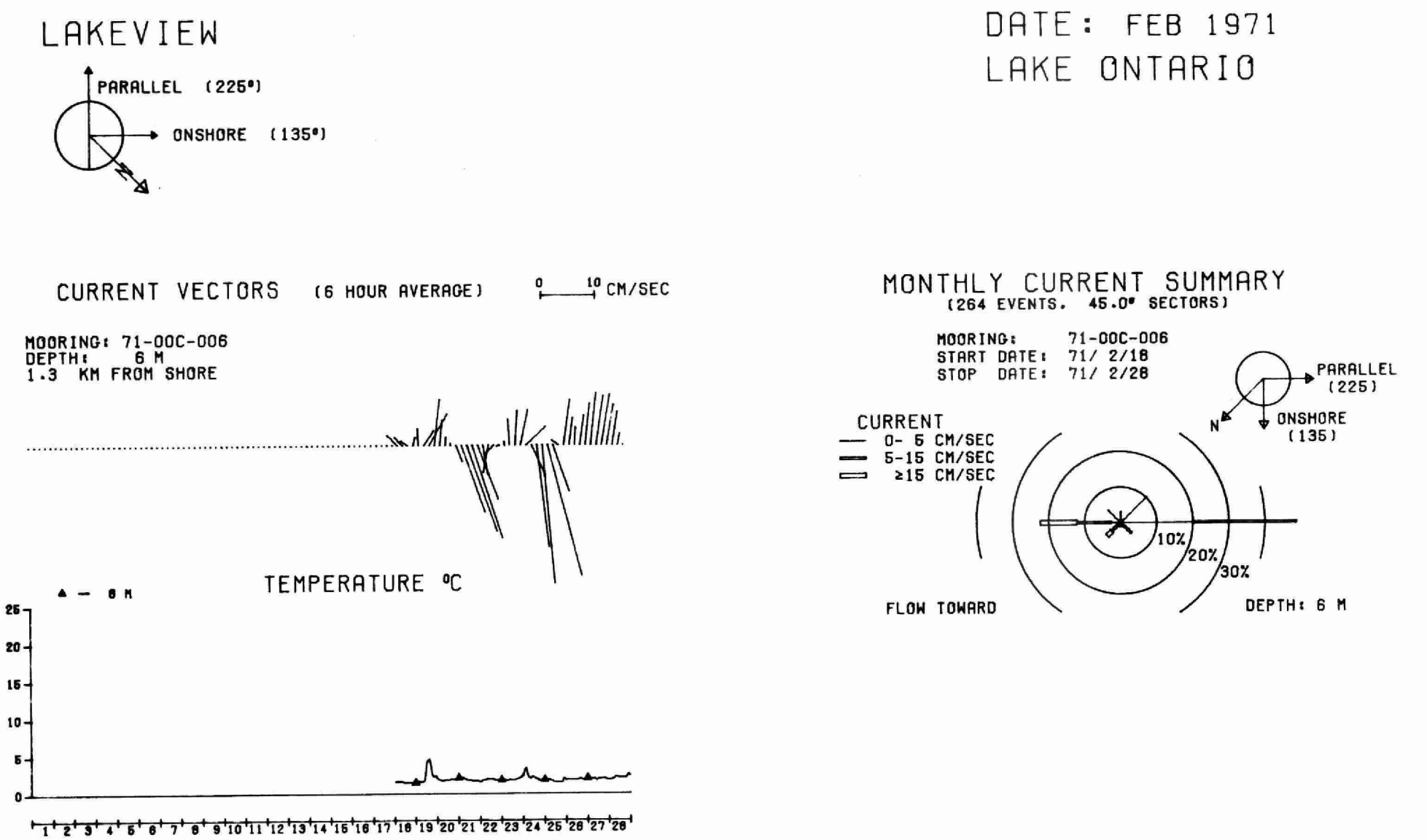
LAKEVIEW
PARALLEL (225°)
ONSHORE (135°)
DATE: FEB 1971
LAKE ONTARIO
CURRENT VECTORS (6 HOUR AVERAGE)
0 10 CM/SEC
MOORING: 71-00C-006
DEPTH: 6 M
1.3 KM FROM SHORE
TEMPERATURE °C
▲ — 6 M
25
20
15
10
5
0
1 2 3 4 5 6 7 8 9 10 11 12 13 14 15 16 17 18 19 20 21 22 23 24 25 26 27 28
MONTHLY CURRENT SUMMARY
(264 EVENTS. 45.0° SECTORS)
MOORING: 71-00C-006
START DATE: 71/ 2/18
STOP DATE: 71/ 2/28
CURRENT
0- 5 CM/SEC
5-15 CM/SEC
≥15 CM/SEC
PARALLEL
(225)
N
ONSHORE
(135)
10%
20%
30%
FLOW TOWARD
DEPTH: 6 M

Figure 1.29

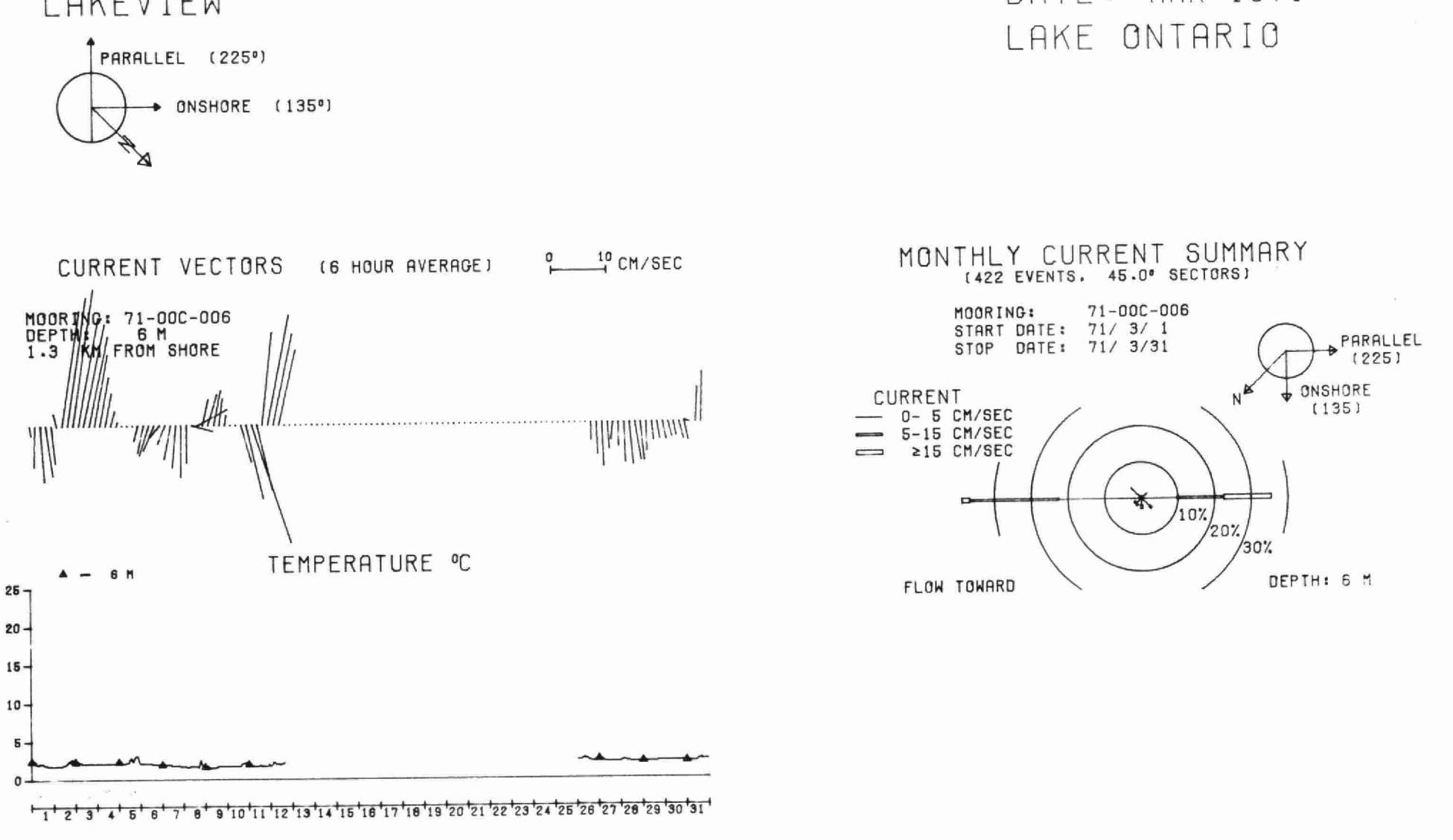
LAKEVIEW
PARALLEL (225°)
ONSHORE (135°)
DATE: MAR 1971
LAKE ONTARIO
CURRENT VECTORS (6 HOUR AVERAGE)
0 10 CM/SEC
MOORING: 71-00C-006
DEPTH: 6 M
1.3 KM FROM SHORE
TEMPERATURE °C
▲ — 6 M
25
20
15
10
5
0
1 2 3 4 5 6 7 8 9 10 11 12 13 14 15 16 17 18 19 20 21 22 23 24 25 26 27 28 29 30 31
MONTHLY CURRENT SUMMARY
(422 EVENTS. 45.0° SECTORS)
MOORING: 71-00C-006
START DATE: 71/ 3/ 1
STOP DATE: 71/ 3/31
PARALLEL (225)
ONSHORE (135)
N
CURRENT
0- 5 CM/SEC
5-15 CM/SEC
≥15 CM/SEC
10%
20%
30%
FLOW TOWARD
DEPTH: 6 M

Figure 1.30

LAKEVIEW

DATE: APR 1971
LAKE ONTARIO

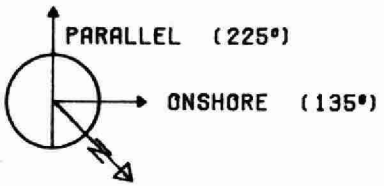

CURRENT VECTORS (6 HOUR AVERAGE) 0 10 CM/SEC

MOORING: 71-00C-006
DEPTH: 6 M
1.3 KM FROM SHORE

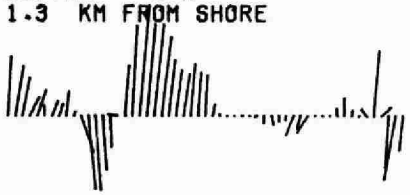

TEMPERATURE °C

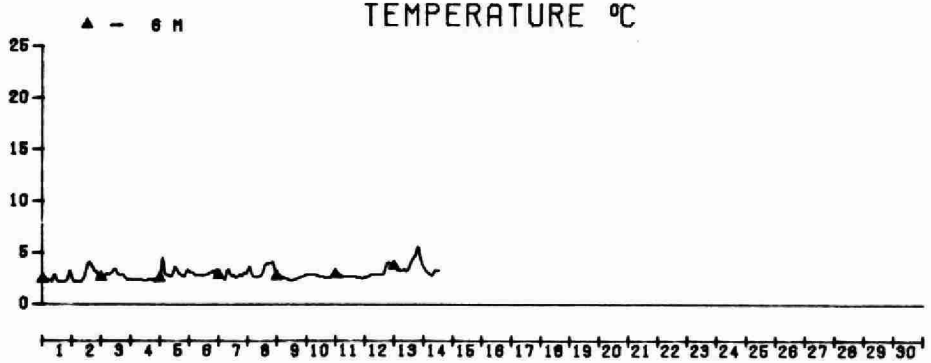

MONTHLY CURRENT SUMMARY
(325 EVENTS. 45.0° SECTORS)

MOORING: 71-00C-006
START DATE: 71/ 4/ 1
STOP DATE: 71/ 4/14

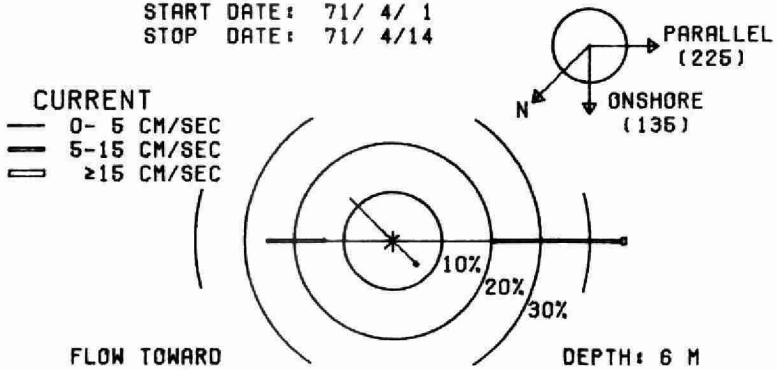

Figure 1.31

NOTES


9693600000819 6